EFFECTS OF ABLATION ON THE PITCHING MOMENT DERIVATIVES OF CONES IN HYPERSONIC FLOW

FLUIDYNE ENGINEERING CORPORATION

EFFECTS OF ABLATION ON THE PITCHING MOMENT DERIVATIVES OF CONES IN HYPERSONIC FLOW

by

Shukry K. Ibrahim

FluiDyne Engineering Corporation
5900 Olson Memorial Highway
Minneapolis, Minnesota 55422
Report 0414-4-4-67

This work is being supported by the

Advanced Research Projects Agency
Ballistic Missile Defense Office
Pentration Aids Branch

and technically administered by the

Fluid Dynamics Branch
Office of Naval Research

Order Number ARPA No. 576
Contract Nonr-4624(00)

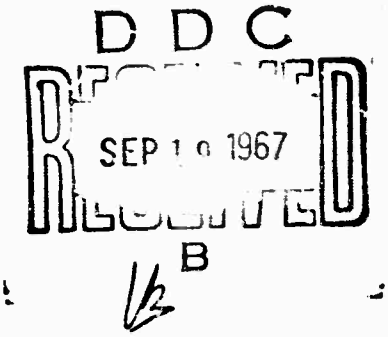

109

FOREWORD

The work described in this report was carried out as part of a program to investigate the effects of mass transfer on the stability of re-entry type vehicles. In addition to the theoretical analysis reported here, an experimental investigation was conducted in the FluiDyne Hypersonic Wind Tunnel at a nominal Mach number of 11. It involved free oscillation tests with ablating and blowing models using a specially-designed, sting-mounted air bearing with the necessary control and recording apparatus. The overall program was supported by the Advanced Research Projects Agency, Ballistic Missile Defense Office, Penetration Aids Branch, and was technically administered by the Fluid Dynamics Branch of the Office of Naval Research. The author wishes to acknowledge the essential contribution of Dr. James S. Holdhusen, the co-author of an earlier report on the subject which laid the foundation for the present work.

TABLE OF CONTENTS

EFFECTS OF ABLATION ON THE PITCHING MOMENT DERIVATIVES OF CONES IN HYPERSONIC FLOW

Shukry K. Ibrahim

FluiDyne Engineering Corporation
Minneapolis, Minnesota

ABSTRACT

This work presents a method of calculating the static and dynamic pitching moment derivatives at hypersonic speeds for pointed or slightly blunted cones performing small-amplitude, single-degree-of-freedom oscillations about an arbitrary pivotal axis, taking into account the effects of ablation or blowing over all or specified portions of the cone surface. The study is motivated by the need for detailed understanding of the large destabilizing changes in the pitching oscillations sometimes observed on re-entry vehicle test flights by developing analytic expressions which describe the role and relative importance of the relevant parameters.

An early report on the subject[1] with a limited distribution was presented in April 1966. Significant improvements have since been made to the earlier paper in that the effects of skin friction, as modified by ablation or blowing, on the static and dynamic pitching moment derivatives are now included. Other refinements include the

choice of a body coordinate system centered at the cone apex, or virtual apex for blunted cones, leading to a more unified approach to the effects of nose bluntness and the relaxation of certain geometric restrictions.

The analysis is restricted to considerations of rigid body motions at low values of the reduced frequency parameter, $\frac{\omega d}{2U_\infty}$, and quasi-steady conditions are postulated. The formulation adopted is sufficiently general and permits a great deal of latitude in the choice of parameters that apply to specific cases. The primary independent quantities, other than the cone angle, nose bluntness and center of gravity location are the distribution, intensity and phase-shift of the ablation or blowing rate. In the analysis, the ablation gases leaving the body are assumed to produce the following two-fold effect:

1) a deflection of the external flow which produces a change in the local static pressure coefficient readily calculated by the Newtonian flow theory and

2) a change in the local skin-friction coefficient.

These inviscid and viscous effects are treated separately, and their individual contributions to the static and dynamic derivatives are calculated so that they may be compared with, and later added to, the static and dynamic derivatives without ablation. The resulting expressions conform to the observed sign and order of magnitude of experimental observations. Under certain restrictions clearly delineated, a very simple relation, involving only the reduced frequency parameter and the phase-shift

angle, is shown to exist between the dynamic and static moment derivatives due to ablation.

Illustrative examples showing detailed calculation procedures and typical results for three different ablation configurations under both laminar and turbulent boundary layer conditions are presented.

1. INTRODUCTION AND LITERATURE REVIEW

It is known that ablation may produce order-of-magnitude changes in the dynamic pitching derivatives of cones in hypersonic flow. Such changes have been observed both in free flight and in wind tunnel tests[2] with ablation. In examining the dynamic stability of an ablating hypersonic vehicle, one is faced with very complex aero-thermo-chemical phenomena involving unsteady heat and mass transfer processes, multi-component boundary layer effects, different mechanisms of decomposition of the ablating material, and finally, changes in shape and mass distribution resulting from the removal of ablated material.

Any analysis of reasonably wide application entails, of necessity, a number of simplifications dictated either by the underlying assumptions of the theories involved or by the desire to reduce the necessary computational work. The latter restrictions may be relaxed at the expense of additional computational labor but the former are intrinsic to the nature of the theoretical approach adopted.

From the fundamental viewpoint, the present analysis uses the classical concepts of dynamic stability theory such as those of stability derivatives and the principle of superposition implying the assumption of linearity. It also rests on the assumptions of the Newtonian flow theory and of quasi-steady flow conditions.

From the practical computational viewpoint, a number of simplifying assumptions are made in the interest

of clarity and simplicity. Only the primary effects taking place in the ablating region are considered and secondary effects as might be induced on the body upstream or downstream of the ablating region are ignored. The convective heat transfer rate is assumed to be dominant so that radiation effects may be ignored. Possible changes in shape or mass distribution resulting from ablation are also ignored, and the dynamic stability effects of ablation on the small, spherical nose cap are neglected. In principle, there are no difficulties in relaxing any or all of these simplifying assumptions.

The open literature treating specifically the complex interactions between the phenomena of ablation and the vehicle dynamic stability characteristics is quite limited and of very recent vintage[1-6]. By contrast, the literature on some of the underlying problem areas is quite extensive and only a representative number of references in the areas of high speed heat and mass transfer[7-20], stability characteristics at hypersonic speeds[21-25], ablation processes and material properties[26-37] are listed here.

2. PITCHING MOMENT DERIVATIVES FOR NONABLATING CONES

2.1 Geometric Considerations

The cone geometry is illustrated in Figure 1. The origin of the cylindrical coordinate system (x, r, φ) is taken at the apex of the cone. For blunted cones, the origin is taken at the virtual apex as shown.

The significance of the symbols L, L_o, L_1, x_o, r_N, r_B, and θ is illustrated in Figure 1. The nose bluntness ratio is defined by:

$$\xi = \frac{r_N}{r_B} \quad .$$

The following relations apply to a right circular cone with a spherical nose cap:

$$r = x\tan\theta \ , \ r_B = L\tan\theta \ , \ d = 2L\tan\theta$$

$$L_1 = \frac{r_N(1-\sin^2\theta)}{\sin\theta} \ , \ \xi = \frac{r_N}{r_B} = \frac{L_1}{L}\sec\theta \qquad (1)$$

2.2 Local Pressure Coefficient Without Ablation, $C_p(o)$

The local pressure coefficient for hypersonic flow for a cone is based on Newton's simple impact theory (valid for $M \to \infty$) to be modified by a correction factor η given in Truitt[38] by the expression

$$\eta = 1 + \frac{\gamma-1}{\gamma+1}\left(\frac{1}{4} + \frac{\gamma+1}{4(\gamma-1)\ M_\infty{}^2\Delta^2}\right) \qquad (2)$$

where γ is the ratio of specific heats
M_∞ is the free stream Mach number
and Δ represents the angle between the tangent to the local surface and the free stream direction.

Under these conditions, the local pressure coefficient is given by:

$$C_p(o) = 2\Delta^2\eta \quad . \qquad (3)$$

The local deflection angle, Δ, is expressed in terms of the cone angle θ and the local effective angle of attack, α_e, composed of the instantaneous angle of attack and the angle induced by the pitching velocity q:

$$\alpha_e = \alpha + \frac{q(x-x_o)}{U_\infty} \quad .$$

Introducing the dimensionless quantities:

$$\bar{x} = \frac{x}{L}\ ,\ \bar{x}_o = \frac{x_o}{L}\ ,\ \bar{L}_1 = \frac{L_1}{L}$$

then $$\alpha_e = \alpha + \frac{qL}{U_\infty}(\bar{x}-\bar{x}_o) = \alpha + \frac{qd}{2U_\infty}\left(\frac{\bar{x}-\bar{x}_o}{\tan\theta}\right) \quad . \qquad (4)$$

Following the earlier analysis[1], we use

$$\Delta = \theta - \alpha_e \sin\varphi \qquad (5)$$

and obtain for the pressure coefficient with no ablation using Eqs. (3) and (5):

$$C_p(o) = 2\eta(\theta - \alpha_e \sin\varphi)^2 \quad . \tag{6}$$

2.3 Pitching Moment Coefficient and Derivatives for Nonablating Cone Surface

The differential pitching moment coefficient about the pivotal axis located at x_o for a nonablating conical element at x is given by

$$dC_M(o,c) = \frac{2}{A_B d}\int_{\varphi=-\pi/2}^{\varphi=\pi/2}\left[r\sin\theta + (x-x_o)\cos\theta\right]C_p(o)\sin\varphi\, dS \tag{7}$$

where the cone base area A_B and base diameter d are used for reference. Noting that $A_B = \pi r_B^2$, $d = 2r_B$ and that the element of area dS on the cone surface is given by $dS = \frac{r\,d\varphi\,dx}{\cos\theta} = \frac{x\sin\theta\, d\varphi\, dx}{\cos^2\theta}$, then by substitution from Eq. (1) and introducing the dimensionless quantities $\bar{x}$, $\bar{x}_o$, and $\bar{L}_1$, there is obtained from Eq. (7):

$$dC_M(o,c) = \frac{1}{\pi\tan^2\theta}\int_{-\pi/2}^{\pi/2}(\bar{x}^2\sec^2\theta - \bar{x}\bar{x}_o)\, C_p(o)\sin\varphi\, d\varphi\, d\bar{x} \quad .$$

The moment coefficient $C_M(o,c)$, contributed by the nonablating cone surface, requires an integration with respect to $\bar{x}$ from the shoulder of the cone near the nose, i.e., $\bar{x} = \bar{L}_1$ to the cone base, $\bar{x} = 1$.

$$C_M(o,c) = \frac{1}{\pi \tan^2\theta} \int_{\bar{L}_1}^{1} \int_{-\pi/2}^{\pi/2} (\bar{x}^2 \sec^2\theta - \bar{x}\bar{x}_o)\, C_p(o) \sin\varphi \, d\varphi \, d\bar{x} \quad (8)$$

Thus, the moment coefficient depends on the geometrical quantities θ, $\bar{L}_1$, and $\bar{x}_o$ and on the distribution of the pressure coefficient with respect to the variables φ and $\bar{x}$. The nose bluntness ratio, ξ, does not appear explicitly in Eq. (8) but its effect is incorporated in the lower limit of integration, $\bar{L}_1$.

It should be pointed out that, except for pointed cones, the numerical values of $\bar{x}_o$, as defined in the present and in the previous report[1] will be different for the same geometrical configuration and axial location so that the calculated moment coefficients and their derivatives cannot be strictly compared with $\bar{x}_o$ as the independent variable.

By substitution from Eq. (6) into Eq. (8), there follows:

$$C_M(o,c) = \frac{2\eta}{\pi \tan^2\theta} \int_{\bar{L}_1}^{1} \int_{-\pi/2}^{\pi/2} (\bar{x}^2 \sec^2\theta - \bar{x}\bar{x}_o)(\theta - \alpha_e \sin\varphi)^2 \sin\varphi \, d\varphi \, d\bar{x} \quad (9)$$

The expansion of Eq. (9) yield terms involving $\sin\varphi$ and its powers up to $\sin^3\varphi$. Since the integrals of the odd powers of $\sin\varphi$ with limits $\varphi = -\pi/2$ and $+\pi/2$ will vanish and since

$$\int_{-\pi/2}^{\pi/2} \sin^2\varphi \, d\varphi = \frac{\pi}{2} \quad .$$

Then, after integration of Eq. (9) with respect to φ and substitution for α_e from Eq. (4), there is obtained for the moment coefficient without ablation

$$C_M(o,c) = -\frac{2\eta\,\theta}{\tan^2\theta}\,\alpha\int_{\bar{L}_1}^{1}(\bar{x}^2\sec^2\theta - \bar{x}\bar{x}_o)d\bar{x} -$$

$$\frac{2\eta\,\theta}{\tan^3\theta}\,\frac{qd}{2U_\infty}\int_{\bar{L}_1}^{1}(\bar{x}^2\sec^2\theta - \bar{x}\bar{x}_o)(\bar{x}-\bar{x}_o)d\bar{x} \quad . \qquad (10)$$

After carrying out the integrations with respect to $\bar{x}$, taking appropriate derivatives and using the abbreviations:

$$C_1 = \left(\frac{1-\bar{L}_1^3}{3}\right)\sec^2\theta - \left(\frac{1-\bar{L}_1^2}{2}\right)\bar{x}_o \qquad (11)$$

and

$$C_2 = \left(\frac{1-\bar{L}_1^4}{4}\right)\sec^2\theta - \left(\frac{1-\bar{L}_1^3}{3}\right)(\sec^2\theta + 1)\bar{x}_o + \left(\frac{1-\bar{L}_1^2}{2}\right)\bar{x}_o^2 \qquad (12)$$

There is obtained for the pitching moment derivatives:

$$C_{M_\alpha}(o,c) = -\frac{2\eta\theta}{\tan^2\theta}\,C_1 \qquad (13)$$

and

$$C_{M_q}(o,c) = -\frac{2\eta\theta}{\tan^3\theta}\,C_2 \quad . \qquad (14)$$

It is observed that, for a given problem, C_1 and C_2 are constant coefficients, specified by purely geometric factors, namely, the cone angle θ, the pivotal axis location

$\bar{x}_o$ and the nose bluntness which controls $\bar{L}_1$. C_1 is linear and C_2 is quadratic in $\bar{x}_o$. For the special case of a pointed cone, $\bar{L}_1 = 0$ and the coefficients C_1 and C_2 become, respectively:

$$C_1' = \frac{1}{3}\sec^2\theta - \frac{1}{2}\bar{x}_o$$

and

$$C_2' = \frac{1}{4}\sec^2\theta - \frac{1}{3}(\sec^2\theta + 1)\bar{x}_o + \frac{1}{2}\bar{x}_o^2 \quad .$$

Figures 2 and 3 illustrate the variation of C_1 and C_2 with pivotal axis location, $\bar{x}_o$, for a 10° half-angle cone for different values of the bluntness ratio, ξ. Figures 4 and 5 present the nonablating static and dynamic pitching moment derivatives produced by the conical surface and given by Eqs. (13) and (14).

2.4 Pitching Moment Derivatives of Spherical Nose Cap

The pitching moment derivatives contributed by the spherical nose cap are readily calculated by means of the Newtonian Impact Theory. From Eq. (9) of Reference 39 but with the cone base area and base diameter as reference area and reference length, respectively, the pitching moment derivatives about $\bar{x}_o$, contributed by the spherical nose are expressed by

$$C_{M_\alpha}(o,N) = \frac{\xi \cos^4\theta}{2\tan\theta}(\bar{x}_o - \bar{L}_o - \xi\tan\theta) \qquad (15)$$

and

$$C_{M_q}(o,N) = -\frac{\xi^2 \cos^4\theta}{\tan^2\theta}\,(\bar{x}_o - \bar{L}_o - \xi\tan\theta)^2 \quad . \qquad (16)$$

These contributions to the static and dynamic pitching moment derivatives for a bluntness ratio $\xi = .2$ are illustrated in Figures 4 and 5.

2.5 Pitching Moment Derivatives of Blunted Cones Without Ablation

The resultant static and dynamic pitching moment derivatives for the nonablating spherically blunted cone are calculated from Eqs. (13), (14), (15), and (16) by addition, so that

$$C_{M_\alpha}(o) = C_{M_\alpha}(o,c) + C_{M_\alpha}(o,N) = -\frac{2\eta\theta}{\tan^2\theta}\,C_1 + \frac{\xi^2\cos^4\theta}{2\tan\theta}\,(\bar{x}_o - \bar{L}_o - \xi\tan\theta) \qquad (17)$$

and

$$C_{M_q}(o) = C_{M_q}(o,c) + C_{M_q}(o,N) = -\frac{2\eta\theta}{\tan^3\theta}\,C_2 - \frac{\xi^2\cos^4\theta}{\tan^2\theta}\,(\bar{x}_o - \bar{L}_o - \xi\tan\theta)^2 \quad . \qquad (18)$$

The calculated resultant values for a 10° half-angle cone with a bluntness ratio $\xi = .2$ are illustrated in Figures 4 and 5.

3. CHANGES IN PITCHING MOMENT DERIVATIVES DUE TO ABLATION

3.1 General Considerations

The general approach will be to calculate the convective heat transfer rate on the local element of conical surface by suitable transformation of flat plate data at angle of attack, choosing the latter to correspond with the local flow inclination. The local rate of mass transfer of ablation gases into the boundary layer may then be calculated. Either one of the following procedures may be adopted.

A. To calculate the heat transfer rates by means of accepted calculation procedures assuming no ablation and then apply the concept of an "effective heat of ablation," H_{eff}, to account for the thermal cooling properties of the ablator and ambient flow conditions,

or

B. To calculate the heat transfer rates taking into account the alleviation resulting from the ablating process and then to determine the local rate of mass transfer from the known thermal properties of the ablating surface material.

The first method was adopted and led to a simple analysis. It should be stressed that the effective heat of ablation is not a material property of the ablator exclusively but depends on the flow characteristics as well.

In turn, the local mass release at the surface is assumed to produce a two-fold effect:

1) a local incremental deflection in the flow which contributes an increment to the local pressure coefficient, designated by $C_p(\beta)$, and readily calculated by a simple Newtonian analysis,

and

2) a change in the local boundary layer velocity profile, more specifically a reduction of the normal derivative of the velocity at the wall surface and a consequent reduction of the local skin friction coefficient.

The inviscid and viscous effects are treated separately and their respective contributions to the pitching moment coefficient, designated by $C_M(\beta)$ and $C_M(f)$ are calculated independently and later added to the pitching moment coefficient without ablation, $C_M(o)$, to yield the resultant pitching moment C_M.

3.2 Heat Transfer Rates on Cone Surface Element

Simplified expressions for the rate of convective heat transfer to a flat plate at angle of attack, α, under re-entry conditions, have been presented in Reference 40. For the laminar boundary layer case, the following expression is given:

$$\frac{\dot{q}_\ell \, x^{.5}}{\sigma^{.5}\left(\frac{U_\infty}{1000}\right)^3\left(1-\frac{h_w}{h_s}\right)} = \frac{.3068}{\left(\frac{\gamma-1}{\gamma}\right)^{.25}} \frac{\sin\alpha\,(\cos\alpha)^{.5}}{\left[.186 + .5\,\frac{h_w}{h_s} + .314(\sin\alpha)^2\right]^{.25}} \qquad (19)$$

where

$\dot{q}_\ell$ = convective heating rate for laminar flow ($BTU/ft^2 sec$)
x = coordinate distance along the surface (ft)
σ = altitude density ratio , $\frac{\rho_\infty}{\rho_{S.L.}}$
U_∞ = free stream velocity (ft/sec)
h = enthalpy
γ = ratio of specific heats
w,s = subscripts to designate the wall and stagnation values, respectively.

For small values of α , such that

$$\sin \alpha \approx \alpha \quad \text{and} \quad \cos \alpha \approx 1$$

it is shown in Appendix B that one may use the approximation

$$\frac{\sin \alpha \, (\cos \alpha)^{.5}}{\left[.186 + .5 \frac{h_w}{h_s} + .314(\sin \alpha)^2\right]^{.25}} \approx \frac{\alpha}{\left[.186 + .5 \frac{h_w}{h_s}\right]^{.25}} \qquad (20)$$

The heat transfer rate, $\dot{q}(F.P.)$, on the flat plate may be converted to that on the cone, $\dot{q}(c)$ at the same distance x by means of the Mangler transformation. For the laminar boundary layer case:

$$\dot{q}_\ell(c) = \sqrt{3}\, \dot{q}_\ell(F.P.) \quad . \qquad (21)$$

It should be pointed out that, for the cone, the flow conditions must be those at the edge of the boundary

layer, designated by subscript e, and not the free stream conditions indicated by subscript ∞. The distance, s, along the conical surface for a point with coordinate x is given by $s = x/\cos\theta = L\bar{x}/\cos\theta$. The instantaneous local inclination, Δ, of the flow which corresponds to the angle α of the flat place is given by Eq. (5).

By virtue of Eqs. (19), (20), (21), and (5), there is obtained for the local heat transfer rate on the conical surface under laminar flow conditions:

$$\dot{q}_\ell(c) = \sqrt{3}\,\sigma^{.5}\left(\frac{U_e}{1000}\right)^3\left(1 - \frac{h_w}{h_s}\right)\frac{.3068}{\left(\frac{\gamma-1}{\gamma}\right)^{.25}}\,\frac{L^{-.5}(\cos\theta)^{.5}}{\left[.186 + .5\,\frac{h_w}{h_s}\right]^{.25}}\,\Delta\bar{x}^{-.5} =$$

$$C_\ell\,\Delta(L\bar{x})^{-.5} \qquad (22)$$

where the coefficient C_ℓ is given by

$$C_\ell = \sqrt{3}\,\sigma^{.5}\left(\frac{U_e}{1000}\right)^3\left(1 - \frac{h_w}{h_s}\right)\frac{.3068}{\left(\frac{\gamma-1}{\gamma}\right)^{.25}}\,\frac{(\cos\theta)^{.5}}{\left[.186 + .5\,\frac{h_w}{h_s}\right]^{.25}} \qquad (23)$$

It is determined by the geometric configuration and the flow characteristics.

The local heat transfer rate on the conical surface under turbulent boundary layer conditions may be calculated along similar lines. Reference 40 gives the simplified heating equation for the flat plate at angle of attack for the turbulent case as

$$\frac{\dot{q}_t \, x^{.2}}{\sigma^{.8}\left(\frac{U_\infty}{1000}\right)^3\left(1 - \frac{h_w}{h_s}\right)} = \frac{3.711}{\left(\frac{\gamma-1}{\gamma}\right)^{.7}} \frac{(\sin\alpha)^{1.6}(\cos\alpha)^{.8}}{\left[.197 + .5\frac{h_w}{h_s} + .303(\sin\alpha)^2\right]^{.7}} \tag{24}$$

It is shown in Appendix B that, for small values of α, one may use the approximation:

$$\frac{(\sin\alpha)^{1.6}(\cos\alpha)^{.8}}{\left[.197 + .5\frac{h_w}{h_s} + .303(\sin\alpha)^2\right]^{.7}} \approx \frac{\alpha^{1.6}}{\left[.197 + .5\frac{h_w}{h_s}\right]^{.7}} \tag{25}$$

The Mangler relationship for this case yields

$$\dot{q}_t(c) = 1.14\ \dot{q}_t \text{ (F.P.)} \quad . \tag{26}$$

Following the same procedure as before, there is obtained for the local heat transfer rate on the conical surface under turbulent boundary layer conditions:

$$\dot{q}_t(c) = 1.14\,\sigma^{.8}\left(\frac{U_e}{1000}\right)^3\left(1 - \frac{h_w}{h_s}\right)\frac{3.711}{\left(\frac{\gamma-1}{\gamma}\right)^{.7}}\frac{L^{-.2}(\cos\theta)^{.2}}{\left[.197 + .5\frac{h_w}{h_s}\right]^{.7}}\Delta^{1.6}\bar{x}^{-.2}$$

$$= C_t\,\Delta^{1.6}(L\bar{x})^{-.2} \tag{27}$$

where

$$C_t = 1.14\,\sigma^{.8}\left(\frac{U_e}{1000}\right)^3\left(1 - \frac{h_w}{h_s}\right)\frac{3.711}{\left(\frac{\gamma-1}{\gamma}\right)^{.7}}\frac{(\cos\theta)^{.2}}{\left[.197 + .5\frac{h_w}{h_s}\right]^{.7}} \tag{28}$$

In order to unify the analysis of the laminar and turbulent cases and generalize the approach (to encompass other ablation or blowing configurations), it is convenient to adopt the general formulation

$$\dot{q}(c) = C\,\Delta^m (L\bar{x})^p \tag{29}$$

where the coefficient C represents an intensity factor
the exponent m indicates the angular dependence
and the exponent p denotes the x-wise variation of the heat transfer rate.

In general m is positive but p is negative; the special case $p = 0$ implies no direct x-wise dependence of the heat transfer along the surface.

For the laminar case:

$$C = C_\ell \ , \ m = 1 \ , \text{ and } p = -.5$$

and for the turbulent case

$$C = C_t \ , \ m = 1.6 \ , \text{ and } p = -.2 \ .$$

3.3 Mass Transfer and Flow Deflection due to Ablation

We introduce the dimensionless mass injection parameters:

$$F_e = \frac{\rho_w v_w}{\rho_e U_e} \tag{30}$$

and

$$F_\infty = \frac{\rho_w v_w}{\rho_\infty U_\infty} \tag{31}$$

where v represents the normal velocity
U represents the tangential velocity
ρ represents the density

and the subscripts w, e, and ∞ indicate conditions at the wall, edge of the boundary layer, and the free stream, respectively. Applying the concept of the effective heat of ablation, H_{eff}, we write

$$\dot{q}(c) = \dot{m}_w \times H_{eff} = (\rho_w v_w) \times H_{eff} \quad .$$

By virtue of Eq. (29), there is obtained

$$\dot{m}_w = \frac{C\,\Delta^m (L\bar{x})^p}{H_{eff}}$$

Therefore
$$F_e = \frac{C\,\Delta^m (L\bar{x})^p}{H_{eff}(\rho_e U_e)} \tag{32}$$

and

$$F_\infty = \frac{C\,\Delta^m (L\bar{x})^p}{H_{eff}(\rho_\infty U_\infty)} \tag{33}$$

It is to be noted that

$$F_e = \frac{\rho_\infty U_\infty}{\rho_e U_e} F_\infty = bF_\infty \tag{34}$$

where b is used to designate the quantity $\frac{\rho_\infty U_\infty}{\rho_e U_e}$ which may be considered a constant quantity for any given problem being a function of the free stream Mach number, M_∞ and the cone angle.

The additional local flow deflection due to ablation mass transfer is designated by β . From the work of Mann[41], Thyson and Schurmann[42] and others, one may write to a satisfactory approximation

$$\beta = \frac{v_e}{U_e} = F_e + \frac{d\delta^*}{dx} \tag{35}$$

where δ^* designates the displacement thickness of the boundary layer with ablation or blowing. It is fair to assume, following Danberg, Winckler and Chang[19] and also Ericsson and Reding[6] that the rate of increase of the displacement thickness with distance is linearly related to the mass injection parameter so that

$$\beta = a\, F_e \quad . \tag{36}$$

Experimental evidence regarding the proportionality factor, a , indicates its dependence on the flow characteristics, more specifically on the wall temperature and flow Mach number and may range between 6 and 16.≠ For example, Danberg[18] obtained a value of 8.5 for turbulent flow on a flat plate at M = 6.7 in air and Studerus[43] obtained a value of 6.2 for turbulent flow over a cone in air at Mach 10.

By virtue of Eqs. (33), (34), and (36), there is obtained:

$$B = \frac{a\, b\, C\, \Delta^m (L\bar{x})^p}{H_{eff}\, (\rho_\infty U_\infty)} \quad . \tag{37}$$

≠ The author is indebted to Messrs. M. L. Roberts and J. B. Arnaiz for information and references about the proportionality factor, a , and its range of variation. This information was given in prepared comments on the author's earlier paper.

The quantity, $K_1 = \frac{abCL^p}{H_{eff}\rho_\infty U_\infty}$, is a constant for a particular configuration and with this abbreviation, the expression for the deflection angle due to ablation becomes

$$\beta = K_1 \Delta^m \bar{x}^p \quad . \tag{38}$$

One final consideration remains to be introduced, namely, that of possible phase-shifts between the instantaneous local flow characteristics at the surface and the consequent mass release due to ablation; there may also be phase-shifts between the local mass release and the ensuing flow deflection. In this analysis, the combined effects of thermal diffusivity and viscous lag are assumed to produce a time shift, Δt, considered to be constant over the full oscillation cycle so that the angular phase-shift, designated by λ will be given by

$$\lambda = \frac{2\pi \Delta t}{T} \text{ radians} \tag{39}$$

where T is the period of oscillation.

The determination of the actual phase-shift for a particular problem requires a separate analysis which may involve consideration of unsteady boundary layer and temperature change, thermal diffusivity properties, etc. Such an analysis goes beyond the scope of this work. Here, average phase-shifts involving either a lag or a lead with respect to the angle of oscillation are assumed and their possible effects on the stability derivatives are examined.

The expression for the angle β taking account of a phase-shift angle λ with respect to the oscillation angle α becomes:

$$\beta = K_1 \Delta^m \bar{x}^p e^{i\lambda} \quad . \tag{40}$$

For an actual re-entry vehicle following a specified trajectory, the vehicle speed as well as the ambient atmospheric conditions, e.g., pressure, density, etc., will continuously change. However, it is convenient and quite adequate for the purpose of calculating the dynamic stability characteristics to assume that the re-entry cone is moving at some representative velocity and altitude conditions while undergoing small-amplitude, low-frequency, essentially sinusoidal oscillations about the zero angle. Such are also the conditions simulated in the free oscillation wind tunnel tests. In terms of an initial displacement angle α_o and oscillation frequency ω, the angle α and pitching velocity q are expressed by:

$$\alpha = \alpha_o e^{i\omega t} \quad , \quad q = \dot{\alpha} = i\omega\alpha_o e^{i\omega t} = i\omega\alpha \quad . \tag{41}$$

Eq. (6) for the pressure coefficient without ablation may be written in the abbreviated form:

$$C_p(o) = 2\eta\theta^2 y^2 \tag{42}$$

where $y = 1 - \dfrac{\alpha_e \sin\varphi}{\theta}$.

Noting that $\Delta = \theta y$, Eq. (40) becomes

$$\beta = K_1 \theta^m y^m \bar{x}^p e^{i\lambda} \quad . \tag{43}$$

The Newtonian pressure coefficient with ablation may be expressed by

$$C_p = 2\eta (\theta y + \beta)^2 \quad . \tag{44}$$

Therefore, the pressure coefficient contributed by ablation, $C_p(\beta)$, may be written as

$$C_p(\beta) = C_p - C_p(o) \quad .$$

By virtue of Eqs. (42), (43), and (44), one obtains

$$C_p(\beta) = 4\eta\, K_1 \theta^{m+1} y^{m+1} \bar{x}^{-p} e^{i\lambda} + 2\eta\, K_1^2 \theta^{2m} y^{2m} \bar{x}^{-2p} e^{2i\lambda} \quad . \qquad (45)$$

For $\left| \frac{\alpha_e \sin\varphi}{\theta} \right| < 1$, the binomial series expansion yields:

$$y^m = \left(1 - \frac{\alpha_e \sin\varphi}{\theta}\right)^m = \sum_{n=0}^{\infty} (-1)^n \binom{m}{n} \left(\frac{\alpha_e \sin\varphi}{\theta}\right)^n \quad .$$

When this is applied to Eq. (45) there is obtained for the pressure coefficient contributed by ablation

$$C_p(\beta) = 4\eta\, K_1\, \theta^{m+1}\, \bar{x}^{-p} e^{i\lambda} \sum_{n=0}^{\infty} (-1)^n \binom{m+1}{n} \left(\frac{\alpha_e \sin\varphi}{\theta}\right)^n$$

$$+ 2\eta\, K_1^2 \theta^{2m}\, \bar{x}^{-2p}\, e^{2i\lambda} \sum_{n=0}^{\infty} (-1)^n \binom{2m}{n} \left(\frac{\alpha_e \sin\varphi}{\theta}\right)^n \quad . \qquad (46)$$

3.4 Pitching Moment Due to Ablation Mass Transfer

The expression for the pitching moment coefficient contributed by ablation takes the same form as Eq. (8) but with $C_p(\beta)$ in the place of $C_p(o)$ and with the appropriate limits for the $\bar{x}$-integration. In other words

$$C_M(\beta) = \frac{1}{\pi \tan^2\theta} \int_{\bar{x}_1}^{\bar{x}_2} \int_{-\pi/2}^{\pi/2} (\bar{x}^2 \sec^2\theta - \bar{x}\,\bar{x}_o) C_p(\beta) \sin\varphi \, d\varphi \, d\bar{x} \quad . \quad (47)$$

Consider first the integration with respect to φ :

$$\int_{-\pi/2}^{\pi/2} (\sin\varphi)^{n+1} d\varphi = \frac{\sin^n\varphi \cos\varphi}{n+1} \Big|_{-\pi/2}^{\pi/2} + \frac{n}{n+1} \int_{-\pi/2}^{\pi/2} \sin^{n-1}\varphi \, d\varphi \quad .$$

The first term on the right-hand side vanishes for the integration limits $-\pi/2$ and $+\pi/2$ and the second term vanishes only for even values of n ; for odd values, one gets:

$$\frac{\pi}{2} \text{ for } n = 1 \; ; \; \frac{3}{8}\pi \text{ for } n = 3 \text{ and } \frac{5}{16}\pi \text{ for } n = 5 \quad .$$

After summation to $n = 5$ and integration with respect to φ , one obtains:

$$I_1 = \int_{-\pi/2}^{\pi/2} C_p(\beta) \sin\varphi \, d\varphi = 4\eta \, K_1 \theta^{m+1} \bar{x}^p e^{i\lambda} \Big[-(m+1)\frac{\pi}{2}\frac{\alpha_e}{\theta} -$$

$$\binom{m+1}{3} \frac{3}{8}\pi \left(\frac{\alpha_e}{\theta}\right)^3 - \binom{m+1}{5} \frac{5}{16}\pi \left(\frac{\alpha_e}{\theta}\right)^5 \ldots \Big] +$$

$$2\eta \, K_1^2 \theta^{2m} \bar{x}^{2p} e^{2i\lambda} \Big[-2m\frac{\pi}{2}\left(\frac{\alpha_e}{\theta}\right) - \binom{2m}{3} \frac{3}{8}\pi \left(\frac{\alpha_e}{\theta}\right)^3 -$$

$$\binom{2m}{5} \frac{5}{16}\pi \left(\frac{\alpha_e}{\theta}\right)^5 \ldots \Big] \quad . \quad (48)$$

3.4.1 Laminar Boundary Layer

For the laminar case, $m = 1$ and only the binomial coefficients $(m + 1)$ and $2m$ will remain in Eq. (48) so that

$$I_{1\ell} = -4\eta\pi\, K_{1\ell}\bar{x}^{p}\, e^{i\lambda}\alpha_e - 2\eta\pi\, K_{1\ell}^{2}\,\theta\,\bar{x}^{2p}\, e^{2i\lambda}\alpha_e \qquad (49)$$

where the subscript ℓ has been used to indicate laminar values. By substitution from Eqs. (4) and (49) into Eq. (47) there is obtained:

$$C_M(\beta,\ell) = -\frac{4\eta\, K_{1\ell}\theta e^{i\lambda}}{\tan^2\theta}\int_{\bar{x}_1}^{\bar{x}_2}\left(\bar{x}^{2+p}\sec^2\theta - \bar{x}^{1+p}\bar{x}_o\right)\left(\alpha + \frac{qd}{2U\tan\theta}(\bar{x}-\bar{x}_o)\right)d\bar{x}$$

$$-\frac{2\eta\, K_{1\ell}^{2}\theta e^{2i\lambda}}{\tan^2\theta}\int_{\bar{x}_1}^{\bar{x}_2}\left(\bar{x}^{2+2p}\sec^2\theta - \bar{x}^{1+2p}\bar{x}_o\right)\left(\alpha + \frac{qd}{2U\tan\theta}(\bar{x}-\bar{x}_o)\right)d\bar{x} \quad . (50)$$

Let $$C_3 = \left(\frac{\bar{x}_2^{3+p} - \bar{x}_1^{3+p}}{3+p}\right)\sec^2\theta - \left(\frac{\bar{x}_2^{2+p} - \bar{x}_1^{2+p}}{2+p}\right)\bar{x}_o \qquad (51)$$

$$C_4 = \left(\frac{\bar{x}_2^{3+2p} - \bar{x}_1^{3+2p}}{3+2p}\right)\sec^2\theta - \left(\frac{\bar{x}_2^{2+2p} - \bar{x}_1^{2+2p}}{2+2p}\right)\bar{x}_o \qquad (52)$$

$$C_5 = \left(\frac{\bar{x}_2^{4+p} - \bar{x}_1^{4+p}}{4+p}\right)\sec^2\theta - \left(\frac{\bar{x}_2^{3+p} - \bar{x}_1^{3+p}}{3+p}\right)(\sec^2\theta+1)\bar{x}_o + \left(\frac{\bar{x}_2^{2+p} - \bar{x}_1^{2+p}}{2+p}\right)\bar{x}_o^{2} \qquad (53)$$

$$\text{and } C_6 = \left(\frac{\bar{x}_2^{4+2p} - \bar{x}_1^{4+2p}}{4+2p}\right)\sec^2\theta - \left(\frac{\bar{x}_2^{3+2p} - \bar{x}_1^{3+2p}}{3+2p}\right)(\sec^2\theta+1)\bar{x}_o + \left(\frac{\bar{x}_2^{2+2p} - \bar{x}_1^{2+2p}}{2+2p}\right)\bar{x}_o^2 \quad . \tag{54}$$

These four coefficients, constant for any given configuration, are specified by purely geometric conditions, namely, the cone angle θ, pivotal axis location $\bar{x}_o$, the coordinates $\bar{x}_1$ and $\bar{x}_2$ which specify the ablation region and the exponent p which controls the x-dependence of the ablation distribution.

After carrying out the integrations in Eq. (50) and introducing the coefficients C_3, C_4, C_5 and C_6 there is obtained:

$$C_M(\beta,\ell) = -\frac{4\eta K_1 \ell^3 e^{i\lambda}}{\tan^2\theta}\left(\alpha C_3 + \frac{qd}{2U\tan\theta} C_5\right) - \frac{2\eta K_1 \ell^2 \theta e^{2i\lambda}}{\tan^2\theta}\left(\alpha C_4 + \frac{qd}{2U\tan\theta} C_6\right) \quad . \tag{55}$$

After using the relations

$$e^{i\lambda} = \cos\lambda + i\sin\lambda \ , \ e^{2i\lambda} = \cos 2\lambda + i \sin 2\lambda \text{ and } q = i\omega\alpha$$

In Eq. (55) and separating the real and imaginary parts, there follows

$$C_M(\beta,\ell) = -\frac{4\eta K_1 \ell^\theta}{\tan^2\theta}\left[\alpha\left(C_3\cos\lambda - \frac{\omega d}{2U\tan\theta}C_5\sin\lambda\right) + \right.$$

$$\left. \frac{i\alpha\omega d}{2U\tan\theta}\left(C_5\cos\lambda + \frac{2U\tan\theta}{\omega d}C_3\sin\lambda\right)\right]$$

$$-\frac{2\eta K_1 \ell^{2\theta}}{\tan^2\theta}\left[\alpha\left(C_4\cos 2\lambda - \frac{\omega d}{2U\tan\theta}C_6\sin 2\lambda\right) + \right.$$

$$\left. \frac{i\alpha\omega d}{2U\tan\theta}\left(C_6\cos 2\lambda + \frac{2U}{\omega d\tan\theta}C_4\sin 2\lambda\right)\right] \quad . \qquad (56)$$

The pitching moment derivatives are readily obtained from Eq. (56) by appropriate differentiation giving

$$C_{M_\alpha}(\beta,\ell) = -\frac{4\eta K_1 \ell^\theta}{\tan^2\theta}\left(C_3\cos\lambda - \frac{\omega d}{2U\tan\theta}C_5\sin\lambda\right)$$

$$-\frac{2\eta K_1 \ell^{2\theta}}{\tan^2\theta}\left(C_4\cos 2\lambda - \frac{\omega d}{2U\tan\theta}C_6\sin 2\lambda\right) \qquad (57)$$

and

$$C_{M_q}(\beta,\ell) = \frac{\partial C_M(\beta,\ell)}{\partial\left(\frac{qd}{2U}\right)} = -\frac{4\eta K_1 \ell^\theta}{\tan^2\theta}\left(\frac{2U}{\omega d}\right)\left(C_3\sin\lambda + \frac{\omega d}{2U}\frac{C_5\cos\lambda}{\tan\theta}\right)$$

$$-\frac{2\eta K_1 \ell^{2\theta}}{\tan^2\theta}\left(\frac{2U}{\omega d}\right)\left(C_4\sin 2\lambda + \frac{\omega d}{2U}\frac{C_6\cos 2\lambda}{\tan\theta}\right) \quad . \qquad (58)$$

Eqs. (57) and (58) express the static and dynamic pitching moment derivatives produced by ablation for the general

laminar boundary layer case in terms of the aerothermodynamic quantities η and $K_{1\ell}$, the geometric coefficients C_3, C_4, C_5, C_6, and cone angle θ, the reduced frequency, $\frac{\omega d}{2U}$, and the phase-shift angle, λ.

3.4.2 Turbulent Boundary Layer

For the turbulent boundary layer case, $m = 1.6$. The binomial coefficients of Eq. (48), when evaluated, give:

$$(m+1) = 2.6 \; ; \quad \binom{m+1}{3} = .416 \; ; \quad \binom{m+1}{5} = -.0112$$

$$2m = 3.2 \; ; \quad \binom{2m}{3} = 1.408 \; ; \quad \binom{2m}{5} = -.0113 \quad .$$

By substitution of these values in Eq. (48) and noting that, for $\left|\frac{\alpha_e}{\theta}\right| < 1$, the terms involving $\left(\frac{\alpha_e}{\theta}\right)^5$ may be neglected with respect to the other terms, there is then obtained

$$I_{1t} = \int_{-\pi/2}^{\pi/2} C_p(\beta)\sin\varphi \, d\varphi = -5.2\eta\pi \, K_{1t}\theta^{1.6} \bar{x}^{p} e^{i\lambda\alpha_e}\left(1 + .12\left(\frac{\alpha_e}{\theta}\right)^2\right)$$

$$- 3.2\eta\pi \, K_{1t}{}^2\theta^{2.2} \bar{x}^{2p} e^{2i\lambda\alpha_e}\left(1 + .33\left(\frac{\alpha_e}{\theta}\right)^2\right) \qquad (59)$$

where the subscript t is now used to designate the turbulent boundary layer conditions. By substitution from Eq. (59) into Eq. (47), the expression for the pitching moment coefficient produced by ablation becomes:

$$C_M(\beta,t) = -\frac{5.2\eta\, K_{1t}\theta^{1.6}\, e^{i\lambda}}{\tan^2\theta}\int_{\bar{x}_1}^{\bar{x}_2}\left(\bar{x}^{2+p}\sec^2\theta-\bar{x}^{1+p}\bar{x}_o\right)\alpha_e\left[1+.12\left(\frac{\alpha_e}{\theta}\right)^2\right]d\bar{x}$$

$$-\frac{3.2\eta\, K_{1t}^2\theta^{2.2}\, e^{2i\lambda}}{\tan^2\theta}\int_{\bar{x}_1}^{\bar{x}_2}\left(\bar{x}^{2+2p}\sec^2\theta-\bar{x}^{1+2p}\bar{x}_o\right)\alpha_e\left[1+.33\left(\frac{\alpha_e}{\theta}\right)^2\right]d\bar{x} \qquad (60)$$

Eq. (60) reveals that, unlike the laminar case, the moment coefficient for the turbulent case is non-linear in α_e. For small values of $\frac{\alpha_e}{\theta}$, say $\left|\frac{\alpha_e}{\theta}\right| < \frac{1}{2}$ the contribution of the non-linear terms will be very small and has been neglected here. Under these conditions, there is obtained, after introducing the expression for α_e of Eq. (4) and the coefficients C_3, C_4, C_5, C_6 given earlier and carrying out the integration with respect to $\bar{x}$:

$$C_M(\beta,t) = -\frac{5.2\eta\, K_{1t}\theta^{1.6}e^{i\lambda}}{\tan^2\theta}\left(\alpha\, C_3+\frac{qd}{2U\tan\theta}\, C_5\right)$$

$$-\frac{3.2\eta\, K_{1t}^2\theta^{2.2}e^{2i\lambda}}{\tan^2\theta}\left(\alpha\, C_4+\frac{qd}{2U\tan\theta}\, C_6\right) \qquad . \qquad (61)$$

After introducing the complex trigonometric expressions for $e^{i\lambda}$ and $e^{2i\lambda}$ and using $q = i\omega\alpha$ into Eq. (61) and separating the real and imaginary parts, there follows:

$$C_{M_\alpha}(\beta,t) = -\frac{5.2\eta K_{1t}\theta^{1.6}}{\tan^2\theta}\left[\alpha\left(C_3\cos\lambda - \frac{\omega d}{2U\tan\theta}C_5\sin\lambda\right) + \frac{i\omega\alpha d}{2U\tan\theta}\left(C_5\cos\lambda + \frac{2U\tan\theta}{\omega d}C_3\sin\lambda\right)\right]$$

$$-\frac{3.2\eta K_{1t}^2\theta^{2.2}}{\tan^2\theta}\left[\alpha\left(C_4\cos 2\lambda - \frac{\omega d}{2U\tan\theta}C_6\sin 2\lambda\right) + \frac{i\omega\alpha d}{2U\tan\theta}\left(C_6\cos 2\lambda + \frac{2U\tan\theta}{\omega d}C_4\sin 2\lambda\right)\right] \quad . \qquad (62)$$

The pitching moment derivatives are obtained from Eq. (62) by appropriate differentiation. Thus

$$C_{M_\alpha}(\beta,t) = -\frac{5.2\eta K_{1t}\theta^{1.6}}{\tan^2\theta}\left(C_3\cos\lambda - \frac{\omega d}{2U\tan\theta}C_5\sin\lambda\right) - \frac{3.2\eta K_{1t}^2\theta^{2.2}}{\tan^2\theta}\left(C_4\cos 2\lambda - \frac{\omega d}{2U}\cdot\frac{C_6\sin 2\lambda}{\tan\theta}\right) \qquad (63)$$

and

$$C_{M_q}(\beta,t) = -\frac{5.2\eta K_{1t}\theta^{1.6}}{\tan^2\theta}\left(\frac{2U}{\omega d}\right)\left(C_3\sin\lambda + \frac{\omega d}{2U}\frac{C_5\cos\lambda}{\tan\theta}\right) - \frac{3.2\eta K_{1t}^2\theta^{2.2}}{\tan^2\theta}\left(\frac{2U}{\omega d}\right)\left(C_4\sin 2\lambda + \frac{\omega d}{2U}\frac{C_6\cos 2\lambda}{\tan\theta}\right) \quad . \qquad (64)$$

Eqs. (63) and (64) express the static and dynamic pitching moment derivatives for the general turbulent boundary

layer case with the additional assumption of negligibly small nonlinear terms in α_e. They are similar, in form, to the corresponding equations for the laminar case, i.e., Eqs. (57) and (58). For the same geometric configuration, the pitching derivatives will differ in magnitude for the two cases on account of the differences in the values of $K_{1\ell}$ and K_{1t}, the constant multiplying factors, the exponents of θ and the coefficients C_3, C_4, C_5, and C_6.

3.4.3 Relations Between the Dynamic and Static Ablation Derivatives

It is useful to examine the relationship between the dynamic and the static pitching derivatives produced by ablation. The values of $C_{M_q}(\beta)/C_{M_\alpha}(\beta)$ may be calculated by dividing Eq. (58) by Eq. (57) for the laminar case and Eq. (64) by Eq. (63) for the turbulent case. The resulting expressions for the general case are somewhat unwieldy. However, under rather realistic conditions when K_1 is small (say, of order 10^{-1}) and the reduced frequency $\frac{\omega d}{2U}$ is low (say, of order 10^{-3}) then the terms in K_1^2 produce a relatively negligible contribution and the relations may be approximated as follows:

For the laminar case:

$$C_{M_\alpha}(\beta,\ell) \approx -\frac{4\eta K_{1\ell}\theta}{\tan^2\theta} C_3 \cos\lambda \qquad (65)$$

and

$$C_{M_q}(\beta,\ell) \approx -\frac{4\eta K_{1\ell}\theta}{\tan^2\theta} \left(\frac{2U}{\omega d}\right)\left(C_3 \sin\lambda + \frac{\omega d}{2U}\frac{C_5 \cos\lambda}{\tan\theta}\right) \quad . \qquad (66)$$

In a similar way, for the turbulent case

$$C_{M_\alpha}(\beta,t) \approx -\frac{5.2\eta\, K_{1t}\theta^{1.6}}{\tan^2\theta} C_3 \cos\lambda \qquad (67)$$

and

$$C_{M_q}(\beta,t) \approx -\frac{5.2\eta\, K_{1t}\theta^{1.6}}{\tan^2\theta}\left(\frac{2U}{\omega d}\right)\left(C_3\sin\lambda + \frac{\omega d}{2U}\frac{C_5\cos\lambda}{\tan\theta}\right) . \qquad (68)$$

Then, for both the laminar and turbulent cases:

$$\frac{C_{M_q}(\beta)}{C_{M_\alpha}(\beta)} \approx \frac{2U}{\omega d}\tan\lambda + \frac{C_5}{C_3\tan\theta} \quad . \qquad (69)$$

If, in addition, the following inequality applies

$$\left|\frac{2U}{\omega d}\tan\lambda\right| \gg \left|\frac{C_5}{C_3\tan\theta}\right|$$

then, a very simple relationship between the dynamic and the static pitching derivatives is obtained, namely

$$\frac{C_{M_q}(\beta)}{C_{M_\alpha}(\beta)} \approx \frac{2U}{\omega d}\tan\lambda \quad . \qquad (70)$$

Eq. (70) illustrates a characteristic effect of the phase-shift angle λ. For a phase lag ($\lambda < 0$) with $0 < |\lambda| < \frac{\pi}{2}$, the effect of ablation on the dynamic derivative will be of opposite sign to that on the static derivative. It also shows that the quantity $\frac{2U}{\omega d}$, the inverse of the reduced frequency, acts as an "amplification factor" for the dynamic derivative with respect to the static one.

3.4.4 Relations Between the Ablating and Nonablating Pitching Moment Derivatives

It is of interest to relate, parametrically, the static and dynamic pitching moment derivatives contributed by ablation to the corresponding values without ablation. Attention will be restricted to the special cases given by Eqs. (65 - 68). The small contributions of the spherical nose to $C_{M_\alpha}(o)$ and $C_{M_q}(o)$ will not be considered. From Eqs. (65) and (13) one obtains, for the laminar case:

$$\frac{C_{M_\alpha}(\beta,\ell)}{C_{M_\alpha}(o)} = 2 \quad K_{1\ell}\cos\lambda\,\frac{C_3}{C_1} \quad . \qquad (71)$$

For the turbulent case, Eqs. (67) and (13) yield

$$\frac{C_{M_\alpha}(\beta,t)}{C_{M_\alpha}(o)} = 2.6 \quad K_{1t}\theta^{.6}\cos\lambda\,\frac{C_3}{C_1} \quad . \qquad (72)$$

Equations (71) and (72) illustrate the relative importance of the different factors contributing to the fractional static pitching moment derivatives, namely, the quantity K_1, the geometric coefficients C_3 and C_1, the cone angle θ and $\cos\lambda$. For small phase-shifts, of the order of ± 10 degrees, $\cos\lambda \approx 1$ so that the fractional static moment derivative is insensitive to phase-shifts as regards both magnitude and direction. Further, since $\frac{C_3}{C_1}$ may be positive or negative depending on the ablation

and cone geometries, the ablation contribution to C_{M_α}, namely, $C_{M_\alpha}(\beta)$ may be stabilizing or destabilizing.

Turning our attention to the fractional dynamic pitching derivatives, then Eqs. (66) and (14) give

$$\frac{C_{M_q}(\beta,\ell)}{C_{M_q}(o)} = 2\, K_{1\ell}\tan\theta\left(\frac{2U}{\omega d}\right)\left(\sin\lambda\,\frac{C_3}{C_2} + \frac{\omega d}{2U}\,\frac{\cos\lambda}{\tan\theta}\,\frac{C_5}{C_2}\right) \qquad (73)$$

Eqs. (68) and (14) yield for the turbulent case:

$$\frac{C_{M_q}(\beta,t)}{C_{M_q}(o)} = 2.6\, K_{1t}\theta^{.6}\tan\theta\left(\frac{2U}{\omega d}\right)\left(\sin\lambda\,\frac{C_3}{C_2} + \frac{\omega d}{2U}\,\frac{\cos\lambda}{\tan\theta}\,\frac{C_5}{C_2}\right) \qquad (74)$$

Eqs. (73) and (74) show that the fractional dynamic pitching moment derivative depends, as before, on the quantity K_1 and also on θ, $\sin\lambda$, $\cos\lambda$, $\frac{2U}{\omega d}$, and the ratios $\frac{C_3}{C_2}$ and $\frac{C_5}{C_2}$.

If the quantities involving $\frac{\omega d}{2U}$ in Eqs. (73) and (74) are negligibly small, relative to the other term and if we note that K_1, θ, $\frac{2U}{\omega d}$, and C_2 are nonnegative, it becomes apparent that the dynamic derivative due to ablation, $C_{M_q}(\beta)$, will be of the same polarity as $C_{M_q}(o)$, i.e., damping whenever $C_3\sin\lambda$ is positive.

Therefore, positive values of C_3 coupled with phase lead or negative values of C_3 coupled with phase lag will

produce the same result, namely, an increased damping. On the other hand, when C_3 and $\sin\lambda$ are of opposite sign, the dynamic effect of ablation will be destabilizing.

3.5 Effect of Ablation on the Local Friction Coefficient

The gases generated as a result of ablation and injected into the boundary layer may produce a significantly large change of the local skin friction coefficient. This, in turn, produces a corresponding change in the pitching moment coefficient and the pitching moment derivatives, designated here by $C_M(f)$, $C_{M_\alpha}(f)$, and $C_{M_q}(f)$.

The dependence of the local skin friction coefficient on ablation or blowing will involve the local mass transfer parameter as well as other flow characteristics such as the wall to free stream temperature ratio and the mol cular weight ratio of the free stream and vaporized gases.

Li and Gross[11] have proposed the following expression for a compressible, laminar boundary layer with blowing or suction

$$\frac{C_f}{C_{f_o}} = 1 + A\left(\frac{T_w}{T_o}\right)K \qquad (75)$$

where C_f and C_{f_o} are the skin friction coefficients with and without blowing, respectively;
A is a positive quantity, fixed for a given fluid;
T_w and T_o denote the uniform wall temperature and the free stream stagnation temperature, respectively;

and K is a nondimensional mass transfer parameter such that $K < 0$ for blowing and $K > 0$ for suction.

Gross, Hartnett, Masson and Gazley[12] have examined the available analyses of the binary, laminar boundary layer and concluded that, for engineering design calculations, the skin friction, in the presence of mass transfer cooling with a foreign gas, may be approximated quite well by the expression

$$\frac{C_f}{C_{f_o}} = 1 - 2.08 \left(\frac{m_a}{m_c}\right)^{1/3} F_e \sqrt{\frac{Re_x}{C^*}} \qquad (76)$$

where $\frac{m_a}{m_c}$ represents the ratio of the molecular weights for air and the coolant gas;

F_e is the nondimensional mass transfer parameter;

Re_x is the local Reynolds number

and C^* is the Chapman-Rubesin parameter, calculated at the reference temperature.

For the turbulent boundary layer case, Danberg, Winkler and Chang[18] obtained experimental results for the effects of air transpiration and wall temperature on skin friction on a flat plate at a Mach number of 6.7 indicating a strong dependence of the skin friction coefficient on mass transfer even for the relatively low mass transfer coefficients, $F_e = .0025$. Tests encompassing the following range of parameters

$$0 \le F_e \le .0025 \; ; \quad 0 \le \frac{2F_e}{C_{f_o}} < 4 \; ; \quad 1 \ge \frac{C_f}{C_{f_o}} > .2$$

yielded the following simple expression:

$$\frac{C_f}{C_{f_o}} = 1 - .22 \frac{2F_e}{C_{f_o}} \quad . \tag{77}$$

Equations (75), (76), and (77) are all of the generalized type:

$$\frac{C_f}{C_{f_o}} = 1 - \varkappa F_e \tag{78}$$

where the nondimensional factor $\varkappa$ is determined by the relevant parameters of the problem at hand. It replaces the quantity $A\left(\frac{T_w}{T_o}\right)$ of Eq. (75), the more general quantity

$$2.08\left(\frac{m_a}{m_c}\right)^{1/3}\sqrt{\frac{Re_x}{C^*}}$$

of E (76) or the quantity $\frac{.44}{C_{f_o}}$ of Eq. (77) for the turbulent boundary layer case.

If one refers to Figure 1 and focuses attention on the elemental normal and axial forces due to friction, $dN(f)$ and $dX(f)$, respectively, acting on an element of surface, dS, on the cone, one may write

$$dN(f) = q_e C_f \sin\theta \sin\varphi \, dS$$

and

$$dX(f) = q_e C_f \cos\theta \, dS$$

where $q_e = 1/2 \, \rho_e U_e^2$.

3.6 Pitching Moment Derivatives Due to Changes in Skin Friction

The elemental pitching moment, $dM(f)$, about the pivotal axis at x_o can be expressed by

$$dM(f) = dX(f)\, r \sin\varphi - dN(f)\,(x-x_o) \quad . \tag{79}$$

Noting that $r = x\tan\theta$ and $dS = \frac{r\,d\varphi dx}{\cos\theta} = \frac{x\sin\theta\, d\varphi dx}{\cos^2\theta}$

then, by substituting for $dX(f)$, $dN(f)$, r and dS in Eq. (75) and simplifying, there is obtained

$$dM(f) = q_e \tan^2\theta\, C_f x x_o \sin\varphi\, d\varphi dx \quad .$$

The corresponding pitching moment due to friction, $M(f)$, is obtained by integration over the cone surface

$$M(f) = 2\int_{L_1}^{L}\int_{-\pi/2}^{\pi/2} dM(f)\, d\varphi dx = 2q_e\tan^2\theta\int_{L_1}^{L}\int_{-\pi/2}^{\pi/2} C_f \sin\varphi\, x x_o\, d\varphi dx \tag{80}$$

When we introduce, as before, the nondimensional quantities $\bar{x}$, $\bar{x}_o$, $\bar{L}_1$, use the cone base area A_B and base diameter d as reference area and moment arm, respectively, and refer the moment coefficient to the free stream dynamic pressure, $q_\infty = 1/2\ \rho_\infty U_\infty^2$, then the moment coefficient due to friction will be given by

$$C_M(f) = \frac{M(f)}{q_\infty A_B d} = \frac{q_e}{q_\infty \pi\tan\theta}\int_{\bar{L}_1}^{1}\int_{-\pi/2}^{\pi/2} C_f\, \bar{x}\bar{x}_o \sin\varphi\, d\varphi d\bar{x} \quad . \tag{81}$$

By virtue of Eq. (81), the pitching moment coefficient due to friction can be calculated once the functional relation between the local skin friction coefficient, C_f, and the variables φ and x is known. Equation (78) permits the contribution to the local skin friction due to ablation, designated here by ΔC_f to be written as follows:

$$\Delta C_f = C_f - C_{f_o} = - \varkappa F_e C_{f_o} \quad . \tag{82}$$

The corresponding pitching moment coefficient, $C_M(f)$ may be obtained by means of Eq. (81) but with ΔC_f instead of C_f and with the limits of integration of $\bar{x}$ determined by the ablation region. Hence

$$C_M(f) = - \frac{q_e}{q_\infty \pi \tan\theta} \int_{\bar{x}_1}^{\bar{x}_2} \int_{-\pi/2}^{\pi/2} \varkappa F_e C_{f_o} \bar{x}\, \bar{x}_o \sin\varphi \, d\varphi \, d\bar{x} \quad . \tag{83}$$

In Eq. (83), $\varkappa$ and C_{f_o} are independent of the angle φ so that one may write

$$C_M(f) = - \frac{q_e}{q_\infty \pi \tan\theta} \int_{\bar{x}_1}^{\bar{x}_2} \varkappa C_{f_o} \bar{x}\, \bar{x}_o \int_{-\pi/2}^{\pi/2} F_e \sin\varphi \, d\varphi \, d\bar{x} \quad . \tag{84}$$

If we use for F_e the expression obtained from Eqs. (36) and (40), namely

$$F_e = \frac{K_1 \theta^m y^m \bar{x}^p e^{i\lambda}}{a}$$

then, Eq. (84) becomes

$$C_M(f) = - \frac{q_e K_1 \theta^m e^{i\lambda}}{a q_\infty \pi \tan\theta} \int_{\bar{x}_1}^{\bar{x}_2} \varkappa C_{f_o} \bar{x}^{1+p} \bar{x}_o \int_{-\pi/2}^{\pi/2} y^m \sin\varphi \, d\varphi \, d\bar{x} \quad . \tag{85}$$

We restrict consideration to the case $\left|\frac{\alpha_e \sin\varphi}{\theta}\right| < 1$ and use the binomial series expansion

$$y^m = \left(1 - \frac{\alpha_e \sin\varphi}{\theta}\right)^m = \sum_{n=0}^{\infty} (-1)^n \binom{m}{n} \left(\frac{\alpha_e \sin\varphi}{\theta}\right)^n \quad .$$

Considering first the last integral in Eq. (85):

$$I_2 = \int_{-\pi/2}^{\pi/2} \sum_{n=0}^{\infty} (-1)^n \binom{m}{n} \left(\frac{\alpha_e}{\theta}\right)^n (\sin\varphi)^{n+1} \, d\varphi \quad .$$

It will vanish for zero and even values of n while for odd values, it yields

$$I_2 = -\pi \frac{\pi}{2} \frac{\alpha_e}{\theta} - \binom{m}{3} \frac{3}{8}\pi \left(\frac{\alpha_e}{\theta}\right)^3 - \binom{m}{5} \frac{5}{16}\pi \left(\frac{\alpha_e}{\theta}\right)^5 - \ldots$$

By substitution into Eq. (85) there is obtained the following general expression for the pitching moment contribution due to friction

$$C_M(f) = -\frac{q_e}{q_\infty} \frac{K_1 \theta^m e^{i\lambda}}{a \tan\theta} \int_{\bar{x}_1}^{\bar{x}_2} \pi \, C_{f_o} \bar{x}^{1+p} \bar{x}_c \left[-\frac{m}{2} \frac{\alpha_e}{\theta} - \binom{m}{3} \frac{3}{8} \left(\frac{\alpha_e}{\theta}\right)^3 - \binom{m}{5} \left(\frac{5}{16}\right) \left(\frac{\alpha_e}{\theta}\right)^5 \right] d\bar{x} \quad . \tag{86}$$

3.6.1 Laminar Case

For the laminar boundary layer case, $m = 1$ and only the first term inside the square brackets remains so that

$$C_M(f,\ell) = \frac{q_e K_{1\ell} e^{i\lambda}}{2q_\infty a \tan\theta} \int_{\bar{x}_1}^{\bar{x}_2} \varkappa_\ell C_{f_{o,\ell}} \bar{x}^{1+p} \bar{x}_o \alpha_e d\bar{x} \quad . \tag{87}$$

If one uses for $\varkappa_\ell$ the very general expression, derived from Eqs. (76) and (78), namely

$$\varkappa_\ell = 2.08 \left(\frac{m_a}{m_c}\right)^{1/3} \frac{\sqrt{Re_x}}{\sqrt{C^*}} \tag{88}$$

and, for $C_{f_{o,\ell}}$ the general expression given in Reference 44 modified to apply to the case of the cone, i.e.,

$$C_{f_{o,\ell}} = \sqrt{3} \times \frac{.644}{\sqrt{Re_x}} \left(\frac{T^*}{T_e}\right)^{\frac{1+\epsilon}{2}} \tag{89}$$

where the subscripts $*$ and e denote the reference temperature and gas temperature at the edge of the boundary layer, respectively, and ϵ denotes the exponent in viscosity power-law relationships. Then, by combining Eqs. (88) and (89), it is apparent that the product $\varkappa_\ell C_{f_{o,\ell}}$ will not involve the local Reynolds' number and may therefore be taken outside the integral sign. Therefore, after using Eq. (4) for α_e and the abbreviation, $K_{2\ell} = \varkappa_\ell C_{f_{o,\ell}}$, Eq. (87) becomes:

$$C_M(f,\ell) = \frac{q_e}{q_\infty} \frac{K_{1\ell} K_{2\ell}\, e^{i\lambda}}{2a \tan\theta} \int_{\bar{x}_1}^{\bar{x}_2} \bar{x}^{1+p} \bar{x}_o \left[\alpha + \frac{qd(\bar{x}-\bar{x}_o)}{2U \tan\theta}\right] d\bar{x} \quad . \tag{90}$$

$$\text{Let} \quad C_7 = \left(\frac{\bar{x}_2^{2+p} - \bar{x}_1^{2+p}}{2+p}\right)\bar{x}_o \tag{91}$$

and

$$C_8 = \left(\frac{\bar{x}_2^{3+p} - \bar{x}_1^{3+p}}{3+p}\right)\bar{x}_o - \left(\frac{\bar{x}_2^{2+p} - \bar{x}_1^{2+p}}{2+p}\right)\bar{x}_o^2 \quad . \tag{92}$$

These two coefficients are determined by purely geometric conditions and are therefore constant for a given configuration.

After integration of Eq. (90) and the introduction of the coefficients C_7 and C_8, there is obtained

$$C_M(f,\ell) = \frac{q_e}{q_\infty}\frac{K_{1\ell}K_{2\ell}}{2a\tan\theta}\, e^{i\lambda}\left[\alpha\, C_7 + \frac{qd}{2U\tan\theta}\, C_8\right] \quad . \tag{93}$$

After using the relations $e^{i\lambda} = \cos\lambda + i\sin\lambda$ and $q = i\omega\alpha$ in Eq. (93) and separating the real and imaginary parts, the following expression is obtained for the moment coefficient:

$$C_M(f,\ell) = \frac{q_e}{q_\infty}\frac{K_{1\ell}K_{2\ell}}{2a\tan\theta}\left[\alpha\left(C_7\cos\lambda - \frac{\omega d}{2U\tan\theta}\, C_8 \sin\lambda\right) + \right.$$

$$\left. + \frac{qd}{2U}\left(\frac{C_8\cos\lambda}{\tan\theta} + \frac{2U}{\omega d}\, C_7 \sin\lambda\right)\right] \quad . \tag{94}$$

The pitching moment derivatives due to the frictional effects of ablation readily follow from Eq. (94) by appropriate differentiation

$$C_{M_\alpha}(f,\ell) = \frac{q_e}{q_\infty}\frac{K_{1\ell}K_{2\ell}}{2a\tan\theta}\left(C_7\cos\lambda - \frac{\omega d}{2U}\frac{C_8\sin\lambda}{\tan\theta}\right) \qquad (95)$$

and

$$C_{M_q}(f,\ell) = \frac{q_e}{q_\infty}\frac{K_{1\ell}K_{2\ell}}{2a\tan\theta}\left(\frac{2U}{\omega d}\right)\left[C_7\sin\lambda + \frac{\omega d}{2U}\frac{C_8\cos\lambda}{\tan\theta}\right] \quad . \qquad (96)$$

3.6.2 Turbulent Case

For the turbulent boundary layer case, m = 1.6 and the binomial coefficients in Eq. (86) give

$$m = 1.6 \; ; \quad \binom{m}{3} = -.064 \; ; \quad \text{and} \quad \binom{m}{5} = -.0108$$

By substitution of these values into Eq. (86) there is obtained

$$C_M(f,t) = -\frac{q_e}{q_\infty}\frac{K_{1t}\theta^{.6}e^{i\lambda}}{a\tan\theta}\int_{\bar{x}_1}^{\bar{x}_2} K_{2t}\bar{x}^{1+p}\bar{x}_o\left[-.8\,\alpha_e + .024\left(\frac{\alpha_e}{\theta}\right)^2 + .003\left(\frac{\alpha_e}{\theta}\right)^4\right]d\bar{x} \quad . \qquad (97)$$

Unlike the laminar case, the moment coefficient produced by turbulent friction is not linear in α_e. However, for $\left|\frac{\alpha_e}{\theta}\right| < 1$, the nonlinear terms are quite small so that only the first term inside the square bracket of Eq. (97) need be retained. Noting also that the quantity K_{2t} is independent of $\bar{x}$, then after simplification and integration of Eq. (97) and the introduction of the coefficients C_7 and C_8, there is obtained:

$$C_M(f,t) = .8 \frac{q_e}{q_\infty} \frac{K_{1t}K_{2t}\theta^{.6}}{a \tan\theta} e^{i\lambda}\left[\alpha C_7 + \frac{qd}{2U\tan\theta} C_8\right] . \quad (98)$$

Following the procedure described earlier to resolve Eq. (94) into its real and imaginary parts yields the following expression for the turbulent, frictional pitching moment coefficients:

$$C_M(f,t) = .8 \frac{q_e}{q_\infty} \frac{K_{1t}K_{2t}\theta^{.6}}{a \tan\theta} \left[\alpha\left(C_7 \cos\lambda - \frac{\omega d}{2U} \frac{C_8 \sin\lambda}{\tan\theta}\right) + \right.$$

$$\left. + \frac{qd}{2U}\left(\frac{C_8 \cos\lambda}{\tan\theta} + \frac{2U}{\omega d} C_7 \sin\lambda\right)\right] . \quad (99)$$

The corresponding pitching moment derivatives will be

$$C_{M_\alpha}(f,t) = .8 \frac{q_e}{q_\infty} \frac{K_{1t}K_{2t}\theta^{.6}}{a \tan\theta}\left(C_7 \cos\lambda - \frac{\omega d}{2U} \frac{C_8 \sin\lambda}{\tan\theta}\right) \quad (100)$$

and

$$C_{M_q}(f,t) = \frac{.8\, q_e K_{1t}K_{2t}\theta^{.6}}{a\, q_\infty \tan\theta} \left(\frac{2U}{\omega d}\right)\left[C_7 \sin\lambda + \frac{\omega d}{2U} \frac{C_8 \cos\lambda}{\tan\theta}\right] . \quad (101)$$

3.6.3 Relation Between the Dynamic and Static Frictional Pitching Moment Derivatives

The relation between the dynamic and the static derivatives contributed by frictional effects may be calculated from Eqs. (96) and (95) for the laminar case and Eqs. (101) and (100) for the turbulent case. In general, the following inequality holds:

$$\left|\frac{\omega d}{2U\tan\theta} C_8 \sin\lambda\right| << \left|C_7 \cos\lambda\right| .$$

Therefore, Eqs. (96) and (95) and also Eqs. (101) and (100) yield

$$\frac{C_{M_q}(f)}{C_{M_\alpha}(f)} = \frac{2U}{\omega d}\tan\lambda + \frac{C_8}{C_7\tan\theta} \quad . \tag{102}$$

Eq. (102) is valid for both the laminar and turbulent cases; it is similar, in form, to Eq. (69) but with $\frac{C_8}{C_7}$ replacing $\frac{C_5}{C_3}$.

With the further restriction that

$$\left|\frac{2U}{\omega d}\tan\lambda\right| \gg \left|\frac{C_8}{C_7\tan\theta}\right| \quad .$$

Then, the very simple relationship between the dynamic and the static pitching derivatives found to apply to the inviscid effect is also valid, namely,

$$\frac{C_{M_q}(f)}{C_{M_\alpha}(f)} \approx \frac{2U}{\omega d}\tan\lambda \quad . \tag{103}$$

4. AVERAGE HEAT AND MASS TRANSFER RATES

In Section 3, explicit expressions were given for the local heat transfer on the cone surface, $\dot{q}(c)$, for both the laminar and turbulent boundary layer conditions. Through the concept of the effective heat of ablation, H_{eff}, the corresponding local rates of mass ablation, $\dot{m}_w$ are readily calculated:

$$\dot{m}_w = \frac{\dot{q}(c)}{H_{eff}} \quad .$$

In order to calculate the overall rates of heat transfer and mass ablation, $\dot{Q}(c)$ and $\dot{M}_w$, respectively, it is only necessary to integrate the local values over the ablating surface on the cone. Therefore

$$\dot{Q}(c) = \int_S \dot{q}(c)dS = 2\int_{x_1}^{x_2}\int_{-\pi/2}^{\pi/2} \frac{\dot{q}(c)x \sin\theta \, d\varphi \, dx}{\cos^2\theta} \qquad (104)$$

and

$$\dot{M}_w = \int_S \dot{m}_w dS = 2\int_{x_1}^{x_2}\int_{-\pi/2}^{\pi/2} \frac{\dot{q}(c)x \sin\theta \, d\varphi \, dx}{H_{eff} \cos^2\theta} \quad . \qquad (105)$$

By substituting the general expression for $\dot{q}(c)$ given by Eq. (29) and introducing nondimensional quantities as before, there is obtained:

$$\dot{Q}(c) = \frac{2L^{2+p}C \sin\theta}{\cos^2\theta} \int_{\bar{x}_1}^{\bar{x}_2}\int_{-\pi/2}^{\pi/2} \Delta^m \bar{x}^{1+p} \, d\varphi \, d\bar{x} \quad . \qquad (106)$$

Noting that $\Delta^m = \theta^m y^m$ where, as before $y = 1 - \frac{\alpha_\epsilon \sin\varphi}{\theta}$ then, using the binomial series expansion, there is obtained from Eq. (104):

$$\dot{Q}(c) = \frac{2L^{2+p}C\ \theta^m \sin\theta}{\cos^2\theta} \int_{\bar{x}_1}^{\bar{x}_2}\int_{-\pi/2}^{\pi/2} \sum_{n=0}^{\infty} (-1)^n \binom{m}{n} \bar{x}^{1+p} \left(\frac{\alpha_e}{\theta}\right)^n (\sin\varphi)^n \cdot d\varphi d\bar{x} \tag{107}$$

The integrals involving odd powers of $\sin\varphi$ will vanish for the present limits of φ and the expansion of Eq. (107) yields:

$$\dot{Q}(c) = \frac{2L^{2+p}C\ \theta^m \sin\theta}{\cos^2\theta} \int_{\bar{x}_1}^{\bar{x}_2} \bar{x}^{1+p} \left[\pi + \binom{m}{2}\left(\frac{\alpha_e}{\theta}\right)^2 \frac{\pi}{2} + \binom{m}{4}\left(\frac{\alpha_e}{\theta}\right)^4 \frac{5}{16}\pi \cdots\right] d\bar{x} \tag{108}$$

4.1 Laminar Boundary Layer

For the laminar case, $m = 1$ and Eq. (108) is readily integrated and yields

$$\dot{Q}_\ell(c) = \frac{2L^{2+p}C_\ell\theta \sin\theta}{\cos^2\theta} \cdot \int_{\bar{x}_1}^{\bar{x}_2} \bar{x}^{1+p}\, \pi\, d\bar{x}$$

$$= \frac{2\pi\, L^{2+p}C_\ell\theta \sin\theta}{\cos^2\theta} \left(\frac{\bar{x}_2^{2+p} - \bar{x}_1^{2+p}}{2+p}\right)$$

$$= \frac{2\pi\, L^{2+p}C_\ell\theta \sin\theta}{\cos^2\theta} \frac{C_7}{\bar{x}_o} \quad . \tag{109}$$

The overall rate of mass ablation will be given by the expression

$$\dot{M}_{w,\ell} = \frac{\dot{Q}_\ell(c)}{H_{eff}} = \frac{2\pi\, L^{2+p} C_{\ell 6} \sin\theta}{H_{eff}\ \cos^2\theta}\ \frac{C_7}{\bar{x}_o} \quad . \tag{110}$$

4.2 Turbulent Boundary Layer

For the turbulent boundary layer case, $m = 1.6$. The values of the binomial coefficients are:

$$\binom{m}{2} = .48 \ ; \quad \binom{m}{4} = .0224 \quad .$$

Eq. (108) then yields:

$$\dot{Q}_t(c) = \frac{2\pi\, L^{2+p} C_t \theta^{1.6} \sin\theta}{\cos^2\theta} \int_{\bar{x}_1}^{\bar{x}_2} \bar{x}^{1+p} \left[1 + .24\left(\frac{\alpha_e}{\theta}\right)^2 + .007\left(\frac{\alpha_e}{\theta}\right)^4 \cdots\right] d\bar{x} \tag{111}$$

Since $\left|\frac{\alpha_e}{\theta}\right| < 1$, the term involving $\left(\frac{\alpha_e}{\theta}\right)^4$ is negligibly small and will be deleted. Eq. (111) shows that the overall rate of heat transfer for the turbulent boundary layer case involves some dependence on the angle α_e unlike the laminar case as given by Eq. (109) which exhibits no such dependence.

If the following inequality holds:

$$\left|.24\left(\frac{\alpha_e}{\theta}\right)^2\right| \ll 1 \ , \text{ then}$$

$$\dot{Q}_t(c) \approx \frac{2\pi\, L^{2+p} C_t \theta^{1.6} \sin\theta}{\cos^2\theta}\ \frac{C_7}{\bar{x}_o} \tag{112}$$

and the corresponding rate of mass ablation is given by

$$\dot{M}_{w,t} \approx \frac{2\pi L^{2+p} C_t \theta^{1.6} \sin\theta}{H_{eff} \cos^2\theta} \frac{C_7}{\bar{x}_o} \quad . \tag{113}$$

5. ILLUSTRATIVE EXAMPLE

In order to illustrate the application of the foregoing analysis, a hypothetical body was chosen and the flight configuration selected was such as to reproduce the conditions typical of laminar and turbulent boundary layers successively during the re-entry phase.

The heating rate experienced during re-entry depends primarily on the time history of velocity, altitude, and attitude. For the purpose of this example, attention is focused primarily on the changes in the dynamic pitching derivatives due to ablation and a simplified approach, assuming constant missile parameters, is adopted. The flight conditions are based on some assumed but representative altitude, velocity, and oscillation conditions rather than on a calculated trajectory involving continuous changes in altitude, velocity and atmospheric conditions.

The geometric characteristics of the hypothetical re-entry body are as follows:

Length $L = 10$ feet
Cone Half-Angle $\theta = 10°$
Cone Base Radius $r_B = 1.745$ feet.

Bluntness ratios of $\xi = 0$ (pointed cone) and .2 are considered. The center of gravity location $\bar{x}_o$ is assumed to range between .3 and .8 with .1 intervals. A phase-shift angle of $\lambda = -.349$ rad. (20° lag) is assumed.

5.1 Laminar Boundary Layer Case

The typical flying conditions chosen for this case are:

Altitude $h = 150{,}000$ feet
Velocity $U_\infty = 20{,}000$ ft/sec
Free Stream Density $\rho_\infty = 3.05 \times 10^{-6}$ slug/cu. ft.
Oscillation Frequency $f = 3$ cps
Initial Angle of Oscillation $\alpha_0 = 5°$
Velocity of Sound $a_0 = 971$ ft/sec
Ratio of Specific Heats $\gamma = 1.35$.

Calculations are made for three arbitrary ablation configurations, namely, full length ablation ($\bar{x}_1 = \Gamma_1$, $\bar{x}_2 = 1$), ablation from the front half only ($\bar{x}_1 = \Gamma_1$, $\bar{x}_2 = .5$) and ablation from the rear half only ($\bar{x}_1 = .5$, $\bar{x}_2 = 1$).

The value of the pressure correction factor η for the present case as given by Eq. (2) is 1.057. The results of the calculations for the laminar boundary layer case are illustrated in the following figures.

The geometric ablation coefficients, C_3 , C_4 , C_5 , and C_6 , calculated for the three ablation configurations and different pivotal axis location are illustrated in Figures 6, 7, 8, and 9, respectively. It may be noted that C_3 and C_4 which are linear in $\bar{x}_o$ may be positive or negative whereas the parabolic coefficients C_5 and C_6 are always positive.

The geometric coefficients associated with the frictional effects are illustrated in Figures 10 and 11. Here, the linear coefficient C_7 is always positive while the parabolic coefficient C_8 may be positive or negative.

The static and dynamic derivatives due to ablation, $C_{M_\alpha}(\beta)$ and $C_{M_q}(\beta)$ are calculated from Eqs. (57) and (91), respectively, for the three ablation configurations and the results are illustrated in Figures 12 and 13. The calculations are made for a phenolic nylon ablator with the following rather arbitrary assumptions:

$$H_{eff} = 8000 \text{ BTU/lb}$$
$$a = 10$$
$$\frac{h_w}{h_s} = .2.$$

The calculated value for $K_{1\ell}$ for this case was found to be: $K_{1\ell} = .0157$.

The static and dynamic derivatives due to friction, $C_{M_\alpha}(f)$ and $C_{M_q}(f)$ calculated from Eqs. (93) and (94), respectively, are illustrated in Figures 14 and 15. For these calculations, an arbitrary constant value of .44 was used for the quantity $K_{2\ell}$; it is based on Reference 18.

The resultant static and dynamic pitching moment derivatives for the ablating cone are calculated by summation of the various contributions and the results of

the summation are illustrated in Figure 16 for the static derivative, C_{M_α} and in Figure 17 for the dynamic derivative, C_{M_q}.

The relationship between the ablating and nonablating dynamic derivatives, as given by the simplified Eq. (73), is illustrated in Figure 18. It is noteworthy that, for typical location of the pivotal axis, say, $\bar{x}_o = .65$, full length ablation on the pointed cone contributes a dynamic pitching derivative, $C_{M_q}(\beta)$ of the same sign and about the same amplitude as the aerodynamic damping derivative. Forward and aft ablation will contribute dynamic derivatives of magnitudes two to three times the nonablation value and such that forward ablation increases the dynamic damping while aft ablation destabilizes the oscillation.

The relative effect of the contribution of friction, as modified by ablation, to the dynamic pitch damping derivative, i.e., the ratio $C_{M_q}(f)/C_{M_q}(o)$ was calculated from Eq. (102) and its approximate form, Eq. (103), and the results are illustrated in Figure 19. It is apparent that these contributions have the same sign as the nonablation dynamic derivative, i.e., they are always damping. For the present example and typical pivotal axis location, the contributions range between 10 and 30 percent for the different ablation configurations.

It is instructive to examine, in turn, the effects of changes in the frequency of oscillation, f, or in the amplitude of the phase lag, λ, on the resultant dynamic derivative, C_{M_q}. Figure 20 illustrates the results of

calculations with the three chosen ablation configurations and the same phase lag of 20° but with assumed oscillation frequencies of 2, 3, 5, and 10 cycles per second. The change of frequency alters the slope of the lines for C_{M_q} versus $\bar{x}_o$ and the lower the frequency, the steeper the lines.

Figure 21 shows the effects of changing the phase lag angle while maintaining all the other factors constant. Here, again, the effect of increasing the phase lag is to steepen the slope of the lines of C_{M_q} versus $\bar{x}_o$.

Figures 20 and 21 show a striking similarity in the variation of the resultant dynamic derivative for the case of a fixed phase lag, ($\lambda = -20°$) with different frequencies (f = 2 to 10 cps) and that of a fixed frequency (f = 3 cps) and varying phase lag (λ = -5 to -40 degrees). This is due to the fact that, for the present example, the contribution of ablation to the dynamic derivative is essentially in direct proportion to $(\sin\lambda)/f$, all other factors remaining unchanged.

5.2 Turbulent Boundary Layer Case

The same geometric ablation configurations were used and the representative flying conditions selected for this case were:

Altitude $h = 100{,}000$ ft
Velocity $U_\infty = 17{,}500$ ft/sec
Free Stream Density $\rho_\infty = 3.31 \times 10^{-5}$ slug/cu. ft

Oscillation Frequency $f = 3$ cps
Initial Angle of Oscillation $\alpha_o = 5°$
Velocity of Sound $a_o = 971$ ft/sec
Ratio of Specific Heats $\gamma = 1.35$.

The same values for H_{eff}, a, h_w/h_s and K_2 were used to afford a simple comparison even though these values may not be equally realistic for both laminar and turbulent boundary layers.

The value of the pressure correction factor, η, calculated for this case was 1.063.

The geometric coefficients C_3 through C_8 will be numerically a little different from the corresponding values for the laminar case because of the different value of the exponent p being $-.2$ instead of $-.5$. The variation of these coefficients with $\bar{x}_o$ will have the same general characteristics as their laminar counterparts and will not be given in detail. The static and dynamic derivatives due to ablation, $C_{M_\alpha}(\beta)$ and $C_{M_q}(\beta)$ calculated from Eqs. (63) and (64), respectively, are illustrated in Figures 22 and 23. The calculated value for K_{1t} was found to be .0450. The dynamic derivative due to friction, $C_{M_q}(f)$ calculated from Eq. (101), is illustrated in Figure 24.

The resultant dynamic pitching derivative is illustrated in Figure 25, while Figures 26 and 27 present the variation of the ratios of $C_{M_q}(\beta)/C_{M_q}(o)$ and $C_{M_q}(f)/C_{M_q}(o)$ with $\bar{x}_o$ for all three ablation configurations. These figures

exhibit the same general characteristics as for the laminar case. There is, however, a significant difference for the case of full length ablation. The contribution of ablation to the dynamic derivative tends to destabilize the oscillation for values of $\bar{x}_o$ below .66 for the pointed case compared to .6 for the laminar case. The practical significance of this shift is discussed in the following paragraph.

Figures 28 and 29 provide a graphic comparison of the resultant static and dynamic derivatives, respectively, calculated for the three different ablation configurations on the pointed cone for the two flight cases which illustrate the laminar and turbulent boundary layer conditions. From Figure 28, it is apparent that at any specified value of $\bar{x}_o$, the differences in the value of the resultant static derivatives for the laminar and turbulent flow conditions or for different ablation configurations are quite small. Figure 29, on the other hand, illustrates very significant differences in the relationships between the resultant dynamic derivatives C_{M_q} and $\bar{x}_o$ for the laminar and turbulent boundary layer cases. Specifically, with full length ablation, the pointed cone is dynamically stable for $x_o > .56$ for the laminar case and $x_o > .61$ for the turbulent case. In this practically important range of center of gravity location, the resultant dynamic pitching moment derivatives will have different signs depending on the type of boundary layer. This feature may have far-reaching consequences for conical vehicles re-entering the atmosphere. At high altitudes of the order of 150,000 feet and flying speeds of 20,000 ft/sec, the ambient conditions will be such that the

unit Reynolds number, Re/ft , will be about 1.5×10^5 . The boundary layer is laminar and the resultant dynamic derivative will remain negative, i.e., dynamically stable. At lower altitudes of about 100,000 feet and air speeds of say, 17,500 ft/sec, the unit Reynolds number is about 2×10^6 so that the boundary layer becomes turbulent, except near the nose, and the dynamic derivative becomes positive sc that the vehicle's oscillations will diverge.

6. SUMMARY

A simple analytical method has been presented which permits the calculation of the hypersonic static and dynamic pitching moment derivatives for slender, pointed, or slightly blunted cones performing single-degree-of-freedom, small-angle oscillations about the center of gravity, taking into account the effects of ablation over arbitrary portions of the cone surface. The analysis is based on Newton's Impact Theory for hypersonic flow and is restricted to considerations of rigid body motions at low reduced frequencies. Quasi-steady conditions are postulated.

The resultant static and dynamic derivatives are obtained by adding to the nonablating derivatives, separate additional contributions due to local mass transfer effects and to changes in the local skin friction resulting from the ablation process.

The local heat transfer rates and skin friction coefficients are obtained from classical flat plate results appropriately modified to account for the local effective angle of attack and the conical flow conditions. The concept of an "effective heat of ablation" is applied to relate the local heat and mass transfer rates.

The effects of the ablation geometry are conveniently expressed in the form of geometric coefficients which have the same general characteristics but different numerical values for the laminar and turbulent cases. The differences result from different values of two

characteristic parameters p and m. The first parameter, p, controls the longitudinal distribution of the ablation intensity and appropriate values for the laminar case are -.5 and for the turbulent case, -.2. The second parameter, m, controls the variation of the ablation intensity with the effective local deflection, and it is shown that values of $m = 1$ and 1.6 are appropriate for the laminar and turbulent cases, respectively.

An arbitrary but constant phase-shift between the oscillation angle, α, and the corresponding ablation effect is assumed. The determination of the appropriate phase angle in a particular case would require a detailed analysis involving considerations of unsteady boundary layer, a fluctuating heat input, and thermal diffusivity characteristics. Such an analysis was not attempted and an arbitrary phase lag of 20 degrees was assumed for the two examples used to illustrate the application of the method to the laminar and turbulent boundary layer conditions. Some characteristic features of the effects of ablation in these two cases are pointed out and the results of a parametric study showing the individual effects of a change of phase-lag angle or oscillation frequency are illustrated.

APPENDIX A

SYMBOLS

SYMBOLS

A_B	Area of cone base
a	Proportionality factor, relating the flow deflection produced by ablation, β , to the mass injection parameter, F_e (Eq. 36)
b	Abbreviation for $\frac{\rho_\infty U_\infty}{\rho_e U_e}$
C	Coefficient relating the local rate of convective heat transfer, $\dot{q}$, to the local angle, Δ and $\bar{x}$ coordinate (Eq. 29)
C^*	Chapman-Rubesin parameter, calculated at the reference temperature
C_1, C_2	Constant coefficients, determined by the cone geometry (Eqs. 11 and 12)
C_3, C_4, C_5, C_6	Constant coefficients specified by the cone and ablation geometry (Eqs. 51, 52, 53, and 54)
C_7, C_8	Constant coefficients determined by the cone and ablation geometry (Eqs. 91 and 92)
C_f	Local skin friction coefficient
C_{f_o}	Local skin friction coefficient without ablation
C_M	Pitching moment coefficient, based on A_B and d
C_{M_α}	Static pitching moment derivative, per radian $\left(= \frac{\partial C_M}{\partial x}\right)$
C_{M_q}	Pitching derivative due to q , per radian $\left(= \frac{\partial C_M}{\partial \left(\frac{qd}{2U_\infty}\right)}\right)$

C_p	Pressure coefficient $\left(= \frac{p - p_\infty}{q_\infty}\right)$
c	Specific heat (BTU/lb-°R)
d	Cone base diameter
F_e, F_∞	Nondimensional mass injection parameters given by $\frac{\rho_w v_w}{\rho_e U_e}$ and $\frac{\rho_w v_w}{\rho_\infty U_\infty}$, respectively
f	Circular frequency, cps
H_{eff}	Effective heat of ablation (BTU/lb)
h	Enthalpy (BTU/lb)
I	Abbreviation for integral
K	Nondimensional mass transfer parameter (Eq. 75)
K_1	Abbreviation for the quantity $\frac{abCL^p}{H_{eff}\rho_\infty U_\infty}$
K_2	Nondimensional factor, appearing in Eq. 90, relating the local skin friction coefficient to the mass injection parameter, F_e
L	Length of the pointed cone
L_o, L_1, L_2	Axial distances from the cone apex to the nose, cone shoulder and center of spherical cap, respectively (Figure 1)
M	Mach number or pitching moment
$\dot{M}_w$	Rate of ablation for the entire body (lb/sec)
m	Positive real quantity, not necessarily an integer used as an exponent to the angle Δ (Eq. 29)
m_a, m_c	Molecular weight of air and coolant gas, respectively
$\dot{m}_w$	Local rate of ablation, $\dot{m}_w = \rho_w v_w$ (lb/sq ft-sec)

n	Integers, used in binomial series expansion
p	Static pressure or exponent expressing the x-wise variation of ablation or friction effects
$\dot{Q}$	Heat flux for entire body (BTU/sec)
q	Dynamic pressure $\left(= \frac{1}{2} \rho U^2\right)$, psf, or angular velocity, radian per second
$\dot{q}$	Local rate of convective heat transfer (BTU/sq ft-sec)
Re	Reynolds' number
r	Radius or cylindrical polar coordinate
r_N	Radius of spherical nose
S	Surface area
s	Distance along conical surface
T	Period of oscillation, seconds
t	Time, seconds
U	Stream velocity, ft/sec
v	Normal velocity, ft/sec
x,y,z	Cartesian coordinates with respect to body axes with origin at the cone apex
x_o	Distance from the origin to the axis of oscillation
x_1, x_2	Coordinates of the leading and trailing edges of the ablating region, respectively
y	Abbreviation for $1 - \frac{\alpha_e \sin\varphi}{\theta}$
α	Angle of attack, radians
α_o	Initial angular displacement, radians
α_e	Effective angle of attack to account for pitching velocity $\left(= \alpha + \frac{q(x - x_o)}{U_\infty}\right)$, radians
β	Local flow deflection induced by ablation, radians

γ	Ratio of specific heats
Δ	Net local deflection from the free stream direction, for the oscillating cone, radians
δ^*	Boundary layer displacement thickness
$\varkappa$	Nondimensional factor relating the change in local skin friction coefficient to the mass transfer parameter (Eq. 78)
η	Pressure correction factor to improve the Newtonian value (Eq. 2)
θ	Cone half-angle, radians
λ	Phase-shift angle, radians
ξ	Bluntness parameter $\left(= \frac{r_N}{r_B}\right)$
ρ	Fluid mass density, slugs per cubic foot
Σ	For summation
σ	Altitude density ratio
φ	Cylindrical polar coordinate
ω	Angular frequency of oscillation, radians per second

Subscripts

a	Air
B	Refers to cone base
c	Refers to coolant gas
e	At edge of boundary layer
ℓ	Laminar
N	Refers to the spherical nose of the cone
o	Without ablation
q	Indicates partial differentiation with respect to $\frac{qc}{2U_\infty}$

s	Stagnation
t	Turbulent
w	Conditions at the wall surface
α	Indicates partial differentiation with respect to angle α
∞	Free stream conditions

Superscripts

$( )'$	Value for the pointed cone
*	Value calculated at the reference temperature

Additional Symbols

--(c)	Contribution of the cone surface
--(f)	Contribution due to friction
--(F.P.)	Flat plate case
--(ℓ)	Laminar case
--(N)	Contribution of the cone's spherical nose
--(o)	Value without ablation
--(t)	Turbulent case
--(β)	Contribution due to ablation

APPENDIX B

DERIVATION OF SIMPLIFIED EXPRESSIONS FOR THE RATES OF HEAT TRANSFER TO A FLAT PLATE AT SMALL ANGLES OF ATTACK

1. Laminar Boundary Layer

The expression

$$\frac{\sin\alpha(\cos\alpha)^{.5}}{\left[.186 + .5\frac{h_w}{h_s} + .314(\sin\alpha)^2\right]^{.25}} \qquad (B1)$$

which appears in Eq. (19) may be simplified for small values of α by using the expansion

$$\sin\alpha = \alpha - \frac{\alpha^3}{3!} + \cdots$$

and

$$\cos\alpha \approx 1 - \frac{\alpha^2}{2!} + \frac{\alpha^4}{4!} - \cdots$$

and applying the binomial theorem, neglecting terms in α^4 as follows:

$$\left(\cos(\alpha)\right)^{1/2} = \left(1 - \frac{\alpha^2}{2!} \cdots\right)^{1/2} = 1 - \frac{1}{4}\alpha^2 \cdots$$

Then, the expression B1 yields

$$B1 \approx \frac{\left(\alpha - \frac{\alpha^3}{3!}\right)\left(1 - \frac{\alpha^2}{4}\right)}{\left[.186 + .5\frac{h_w}{h_s} + .314\left(\alpha - \frac{\alpha^3}{3!}\right)^2\right]^{1/4}}$$

$$B1 \approx \frac{\alpha - \frac{5}{12}\alpha^3}{\left[.186 + .5\frac{h_w}{h_s} + .314\,\alpha^2\left(1 - \frac{\alpha^2}{3!}\right)^2\right]^{1/4}}$$

$$\approx \frac{\alpha - \frac{5}{12}\alpha^3}{\left(.186 + .5\frac{h_w}{h_s}\right)^{1/4}\left[1 + \frac{.314\,\alpha^2}{.186 + .5\frac{h_w}{h_s}}\left(1 - \frac{2\alpha^2}{3!}\right)\right]^{1/4}}$$

$$\approx \frac{\left(\alpha - \frac{5}{12}\alpha^3\right)\left(1 - \frac{1}{4}\,\frac{.314\,\alpha^2}{.186 + .5\frac{h_w}{h_s}}\right)}{\left(.186 + .5\frac{h_w}{h_s}\right)^{1/4}} .$$

If one neglects terms in α^3 then

$$B1 \approx \frac{\alpha}{\left(.186 + .5\frac{h_w}{h_s}\right)^{1/4}} .$$

2. Turbulent Boundary Layer

The expression

$$\frac{(\sin\alpha)^{1.6}(\cos\alpha)^{.8}}{\left[.197 + .5\frac{h_w}{h_s} + .303(\sin\alpha)^2\right]^{.7}} \qquad (B2)$$

which appears in Eq. (24) can be simplified by a similar procedure as follows:

$$B2 \approx \frac{\left(\alpha - \frac{\alpha^3}{3!}\right)^{1.6}\left(1 - \frac{\alpha^2}{2}\right)^{.8}}{\left[.197 + .5\frac{h_w}{h_s} + .303\left(\alpha - \frac{\alpha^3}{3!}\right)^2\right]^{.7}}$$

$$\approx \frac{\alpha^{1.6}\left(1 - 1.6\frac{\alpha^2}{3!}\right)\left(1 - \frac{.8}{2}\alpha^2\right)}{\left[.197 + .5\frac{h_w}{h_s} + .303\,\alpha^2\left(1 - \frac{\alpha^2}{3!}\right)^2\right]^{.7}}$$

$$\approx \frac{\alpha^{1.6}\left(1 - \frac{1.6}{6}\alpha^2\right)\left(1 - .4\,\alpha^2\right)}{\left(.197 + .5\frac{h_w}{h_s}\right)^{.7}\left[1 + \frac{.303\,\alpha^2}{.197 + .5\frac{h_w}{h_s}}\left(1 - \frac{\alpha^2}{3}\right)\right]^{.7}} .$$

If, as before, one neglects terms of order α^3 or higher, then

$$B2 \approx \frac{\alpha^{1.6}}{\left(.197 + .5\frac{h_w}{h_s}\right)^{.7}} .$$

REFERENCES

1. "Analysis of the Effects of Phased Cyclic Blowing on the Aerodynamic Pitching Moment Derivatives of Slender Cones in Hypersonic Flow," Shukry K. Ibrahim and James S. Holdhusen, FluiDyne Engineering Corporation, Minneapolis, Minnesota, presented at a meeting of the Anti-Missile Research Advisory Council (AMRAC) in April 1966.

2. "Influence of Ablation on the Dynamics of Slender Re-Entry Configurations," J. H. Grimes, Jr. and John J. Casey, AIAA Journal of Spacecraft and Rockets, Vol. 2, No. 1, pp. 106-108 January-February 1965.

3. "Stability Investigations During Simulated Ablation in a Hypervelocity Wind Tunnel," C. J. Stalmach, Ling Temco Vought, Vought Aeronautics Division, Dallas, Texas, Transactions of the Second Technical Workshop on Dynamic Stability Testing, Arnold Air Force Station, Tennessee, Vol. 1, p. 3., April 20-22, 1965.

4. "A Linearized Analysis Concerning Boundary Layer Effects on the Static and Dynamic Behavior of Slender, Ablating and Non-Ablating Bodies," N. Thyson, Technical Memorandum RAD-TM-64-34, AVCO Corporation, July 1964.

5. "Ablation Effects on Vehicle Dynamics," Lars Eric Ericsson and J. Peter Reding, AIAA Paper 66-51, January 1966.

6. "Effects of Ablation on Hypersonic Aerodynamic Stability Characteristics," G. T. Chrusciel and S. S. Chang (Lockheed Missiles and Space Company), AIAA Paper No. 66-410, 1966.

7. "Survey on Heat Transfer at High Speeds," Ernst R. G. Eckert, (University of Minnesota), Wright Air Development Center, Wright-Patterson AFB, Ohio, WADC Technical Report 54-70, April, 1954.

8. "Survey of Boundary Layer Heat Transfer at High Velocities and High Temperatures," Ernst R. G. Eckert (University of Minnesota), Wright Air Development Center, Wright-Patterson AFB, WADC Technical Report 59-624, April 1960.

9. "Mass-Transfer Cooling in a Laminar Boundary Layer with Constant Fluid Properties," J. P. Hartnett and E.R.G. Eckert (University of Minnesota), Trans. of ASME, Paper No. 55-A-108, February 1957.

10. "Sensitivity of Skin Friction and Drag to the Distribution of Suction or Blowing," E. M. Sparrow and E.R.G. Eckert (University of Minnesota), Journal of the Aerospace Sciences, pp. 104-105, January 1962.

11. "Hypersonic Strong Viscous Interaction on a Flat Plate with Surface Mass Transfer," Ting-Yi Li (Rensselaer Polytechnic Institute) and Joseph F. Gross (The RAND Corp.), Proc. of 1961 Heat Transfer and Fluid Mechanics Institute, Stanford University Press, California, p. 146., 1961.

12. "A Review of Binary Laminar Boundary-Layer Characteristics," J. F. Gross, J. P. Hartnett, D. J. Masson, and C. Gazley, Jr., Intern. J. Heat Mass Transfer, Vol. 3, pp. 198-221, 1961.

13. "Heat Transfer, Temperature Recovery and Skin Friction on a Flat Plate with Hydrogen Release into a Laminar Boundary Layer," E.R.G. Eckert, A. A. Hayday and W. J. Minkowycz, (University of Minnesota), Int. J. Heat Mass Transfer, Vol. 4, pp. 17-29, 1961.

14. "Mass-Transfer Cooling of a Flat Plate with Various Transpiring Gases," E. M. Sparrow, W. J. Minkowycz and E.R.G. Eckert (University of Minnesota), AIAA Journal, Vol. 3, No. 7, pp. 1341-1343, July 1965.

15. "A Simplified Analysis of Skin Friction and Heat Transfer in Binary Boundary Layer Flow," Ting Y. Li, The RAND Corporation, Santa Monica, California, RM-2872-PR, September 1963.

16. "Laminar Boundary Layer with Uniform Injection," Paul A. Libby and Karl Chen (Polytechnic Institute of Brocklyn), The Physics of Fluids, Vol. 8, No. 4, pp. 568-74, April 1965.

17. "Laminar Boundary Layer on a Cone in Supersonic Flow with Uniform Mass Transfer," Paul A. Libby, NASA CR-440, April 1966.

18. "Heat and Mass Transfer in a Hypersonic Turbulent Boundary Layer," J. E. Danberg (NASA), E. M. Winkler (US Naval Ordnance Laboratory), and P. K. Chang (Catholic University of America), Proc. 1965 Heat Transfer and Fluid Mechanics Institute, pp. 87-113, 1965.

19. "Hypersonic Turbulent Transpiration Cooling Including Downstream Effects," Lawrence W. Woodruff and George C. Lorenz (The Boeing Company), AIAA Journal, Vol. 4, No. 6, pp. 969-975, June 1966.

20. "Turbulent Heat-Transfer and Skin-Friction Measurements on a Porous Cone with Air Injection at High Mach Numbers," Richard P. Fogaroli and Alan R. Saydah, (General Electric Company), AIAA Journal, Vol. 4, No. 6, pp. 1116-1117, June 1966.

21. "Stability Derivatives of Cones at Supersonic Speeds," Murray Tobak and William R. Wehrend, NACA TN 3788, September 1956.

22. "The Stability of Bodies of Revolution at Very High Mach Numbers," A.F. Charwat, Jet Propulsion, pp. 866-871, August 1957.

23. "Hypersonic Stability Derivatives of Blunted Slender Cones," Otto Walchner and James T. Clay, AIAA Journal, Vol. 3, No. 4, pp. 752-754, April 1965.

24. "Damping in Slightly Nonlinear Systems: Implications to Dynamic Stability Testing," J. M. Abel, Aerodynamics Technology Component, Data Memo No. 1:20, General Electric Company.

25. "A Generalized Approach to Dynamic-Stability Flight Analysis," Peter Jaffe, Jet Propulsion Laboratory, California Institute of Technology, JPL-TR-32-757, 1 July 1965.

26. "Determination of Factors Governing Selection and Application of Materials for Ablation Cooling of Hypervelocity Vehicles," John H. Bonin, Channon F. Price, and Donald E. Taylor, WADC Technical Report 59-87, Parts I and II, The University of Chicago, July 1959.

27. "Recent Advances in Ablation," Mac C. Adams, Avco-Everett Research Laboratory, ARS Journal, September 1959, pp. 625-632.

28 "Heat Transfer to a Vaporizing, Ablating Surface," Richard G. Fleddermann, Radio Corporation of America, J. of the Aero/Space Sciences, September 1959, pp. 604-605.

29. "Ablation of Reinforced Plastics in Supersonic Flow," George W. Sutton, General Electric Company, J. of the Aero/Space Sciences, May 1960, pp. 377-385.

30. "Analysis of the Ablation of Plastic Heat Shields that Form a Charred Surface Layer," R. J. Barriault and J. Yos, Avco Corp., ARS Journal, September 1960, pp. 823-829.

31. "Materials for Re-Entry Heat Protection of Satellites," Leo Steg, General Electric Company, ARS Journal, September 1960, pp. 815-822.

32. "A Theoretical Analysis of Effects of Ablation on Heat Transfer to an Arbitrary Axisymmetric Body," Robert T. Swann and Jerry South, NASA/Langley Research Center, NASA TN D-741, April 1961.

33. "Ablative Re-Entry Cooling," Donald L. Schmidt, Wright-Patterson AFB, Space/Aeronautics, February 1962, pp. 64-69.

34. "Thermal Degradation of a Char-Forming Plastic During Hypersonic Flight," Sinclaire M. Scala and Leon M. Gilbert, General Electric Company, ARS Journal, June 1962, pp. 917-924.

35. "Numerical Analysis of the Transient Response of Advarced Thermal Protection Systems for Atmospheric Entry," Robert T. Swann and Claud M. Pittman, NASA/Langley Research Center, NASA TN D-1370, July 1962.

36. "Ablation Over Slender Bodies," M. Trella and M. Seidman, General Applied Science Laboratories, Inc., Technical Report No. 397, 2 January 1964.

37. "Fundamental Relationships for Ablation and Hyperthermal Heat Transfer," Robert T. Achard, Wright-Patterson Air Force Base, AFFDL-TR-66-25, April 1966.

38. "Hypersonic Aerodynamics," Robert W. Truitt, The Ronald Press Company, N. Y., 1959, Ch. 6, p. 217.

39. "Equations and Charts for Determining the Hypersonic Stability Derivatives of Combinations of Cone Frustums Computed by Newtonian Impact Theory," Lewis R. Fisher, NASA/Langley Research Center, NASA TN D-149, November 1959.

40. "Design Procedures for Computing Aerodynamic Heating at Hypersonic Speeds," Wilbur L. Hankey, Jr., Richard D. Newmann, Evard H. Flinn, Flight Dynamics Laboratory, Wright Air Development Division, WADC Tech. Rep. 59-610, June 1960.

41. "Effective Displacement Thickness for Boundary Layers with Surface Mass Transfer," Wesley M. Mann, Jr., AIAA Journal, Vol. 1, No. 5, pp. 1181-1182, May 1963.

42. "Blowing Effects on Pressure Interaction Associated with Cones," N. A. Thyson and E. E. H. Schurmann, AIAA Journal, Vol. 1, No. 9, pp. 2179-2180, September 1963.

43. "Comparison of Theoretical and Experimental Induced Pressure Skin Friction Reduction, and Zero Lift Total Drag for a Pointed 7.5° Porous Cone in Presence of Turbulent Mass Addition," C. J. Studerus, General Electric Company, TIS 65SD325, 23 April 1965.

44. "Engineering Analysis of Boundary Layers and Skin Friction on Bodies of Revolution at Zero Angle of Attack," D. J. Eckstrom, Lockheed Missiles and Space Co., TM 55-2121, May 1965.

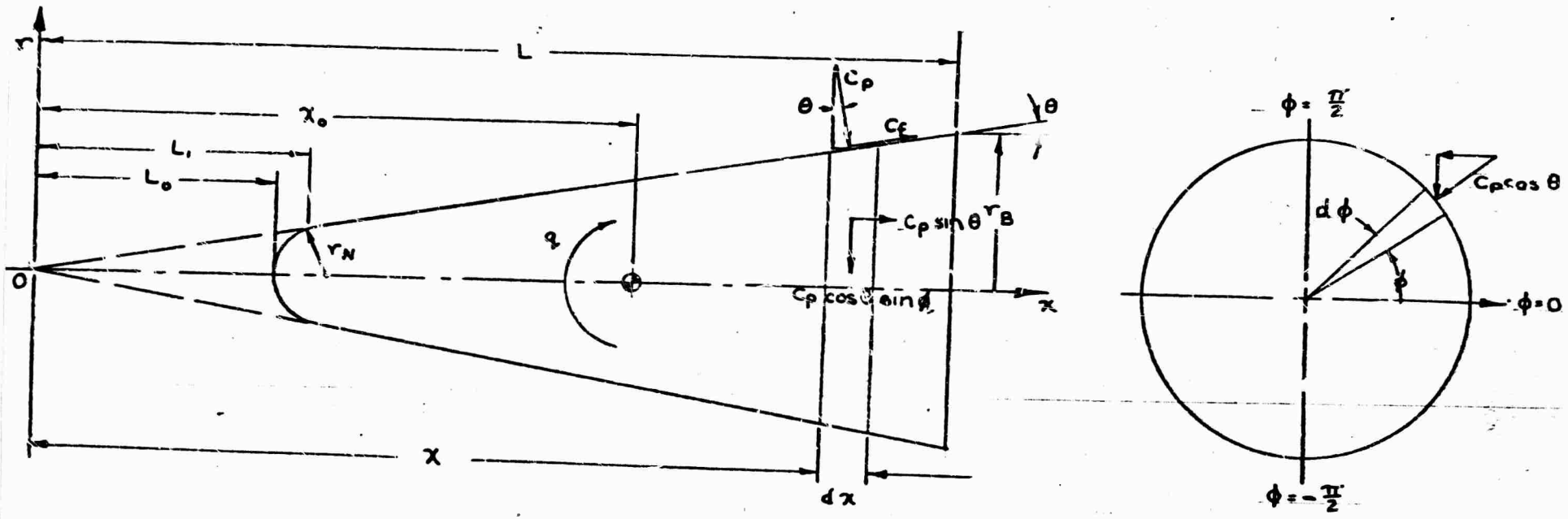

FIGURE 1 DEFINITION SKETCH FOR CONE SHOWING BODY AXES AND ELEMENTS FOR PITCHING MOMENT CALCULATIONS

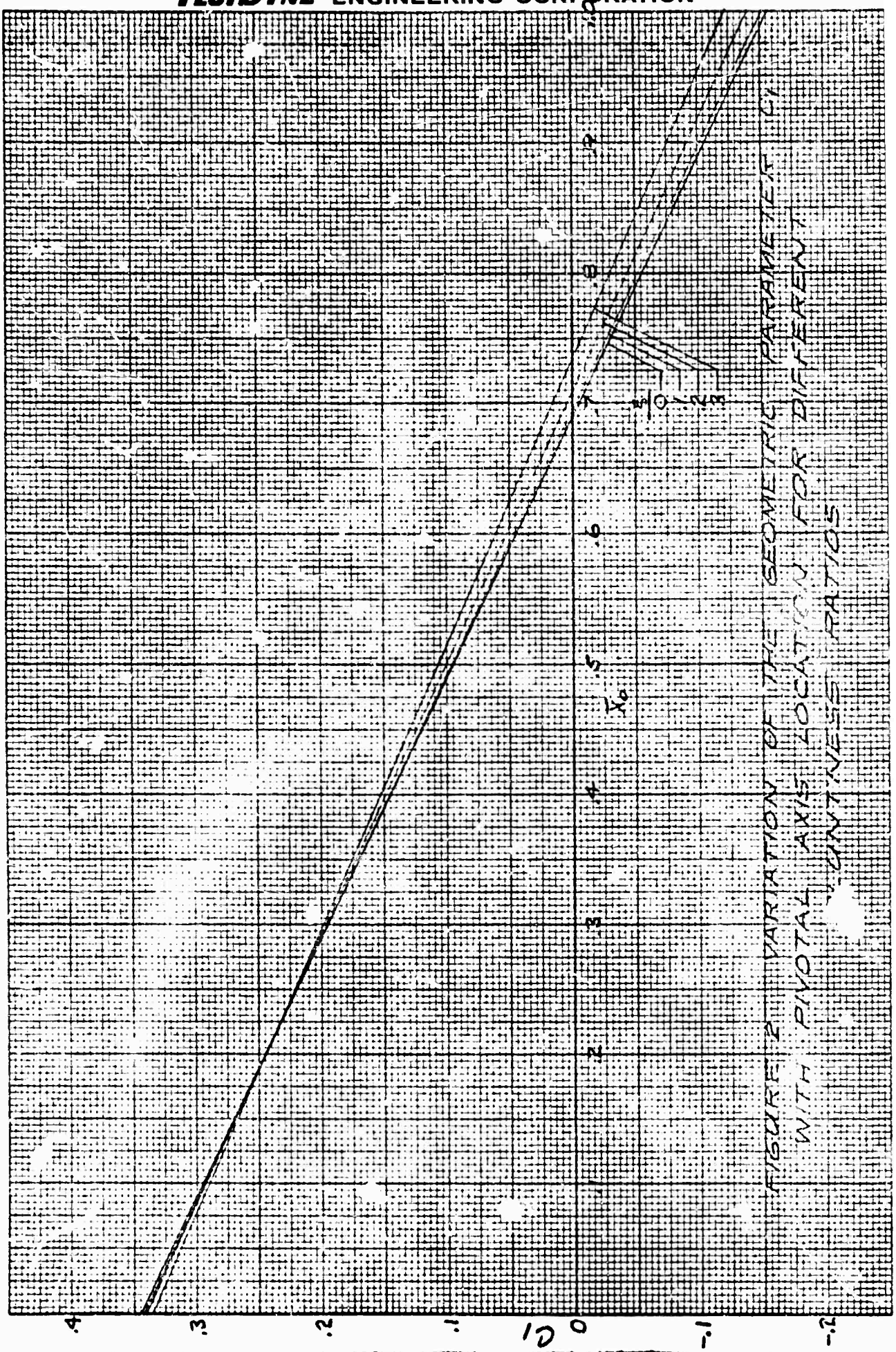

FIGURE 2 VARIATION OF THE GEOMETRIC PARAMETERS $\frac{x_0}{D}$ AND $\frac{y_0}{D}$ WITH PIVOTAL AXIS LOCATION FOR DIFFERENT UNIT VANE SECTIONS

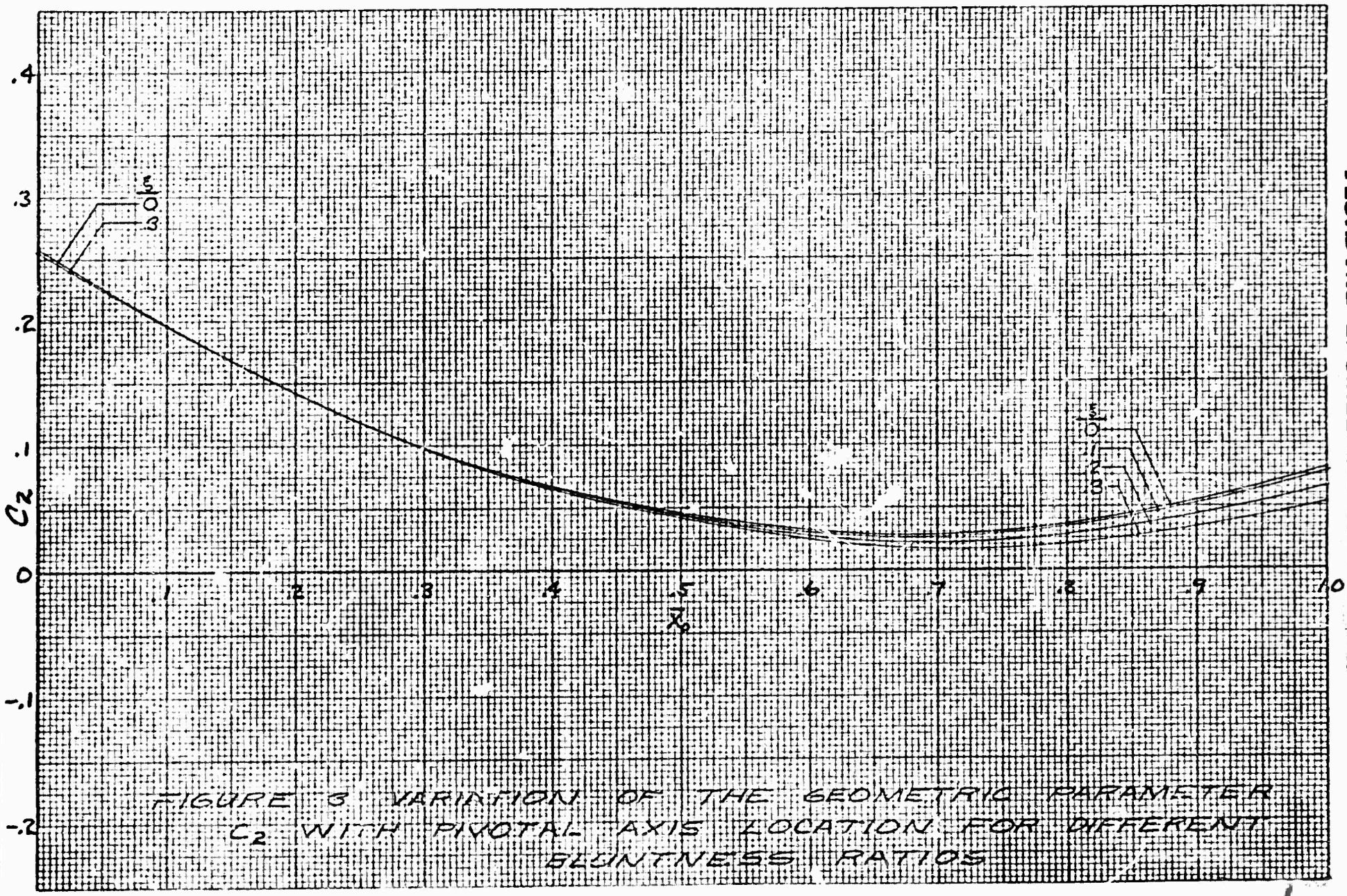

FIGURE 6 VARIATION OF THE GEOMETRIC PARAMETER C_2 WITH PIVOTAL AXIS LOCATION FOR DIFFERENT BLUNTNESS RATIOS

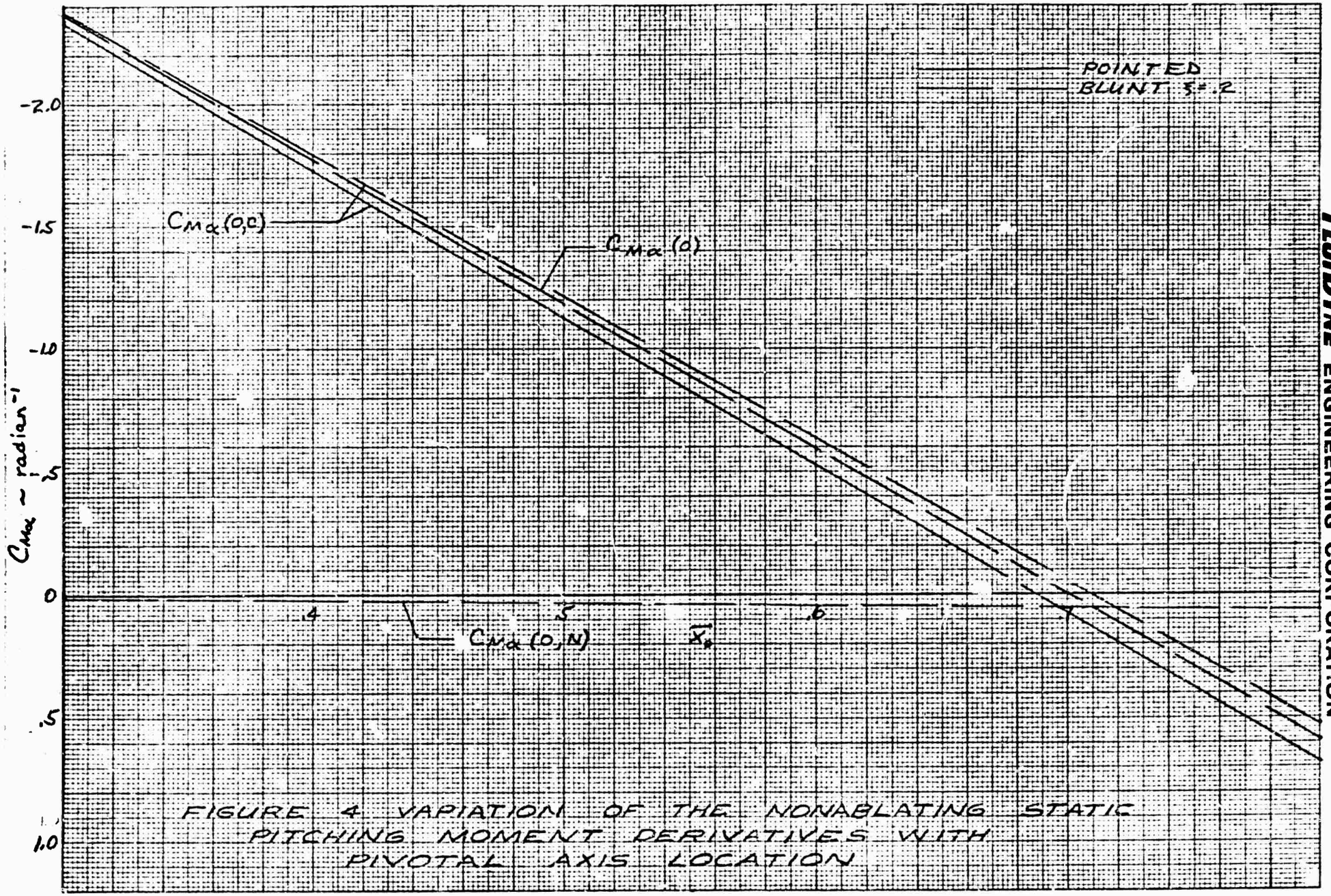

FIGURE 4 VARIATION OF THE NONABLATING STATIC PITCHING MOMENT DERIVATIVES WITH PIVOTAL AXIS LOCATION

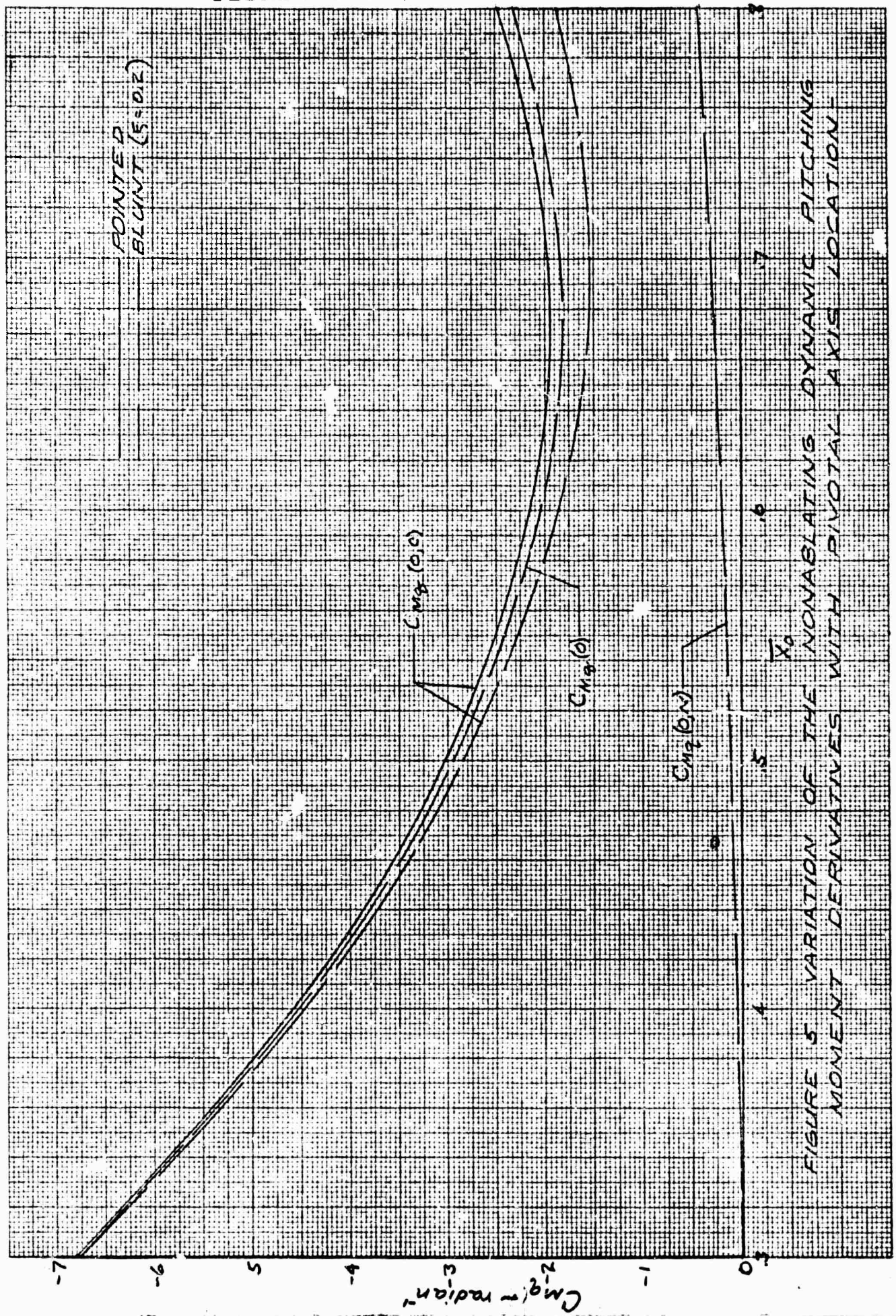

FIGURE 5 VARIATION OF THE NONABLATING DYNAMIC PITCHING MOMENT DERIVATIVES WITH PIVOTAL AXIS LOCATION

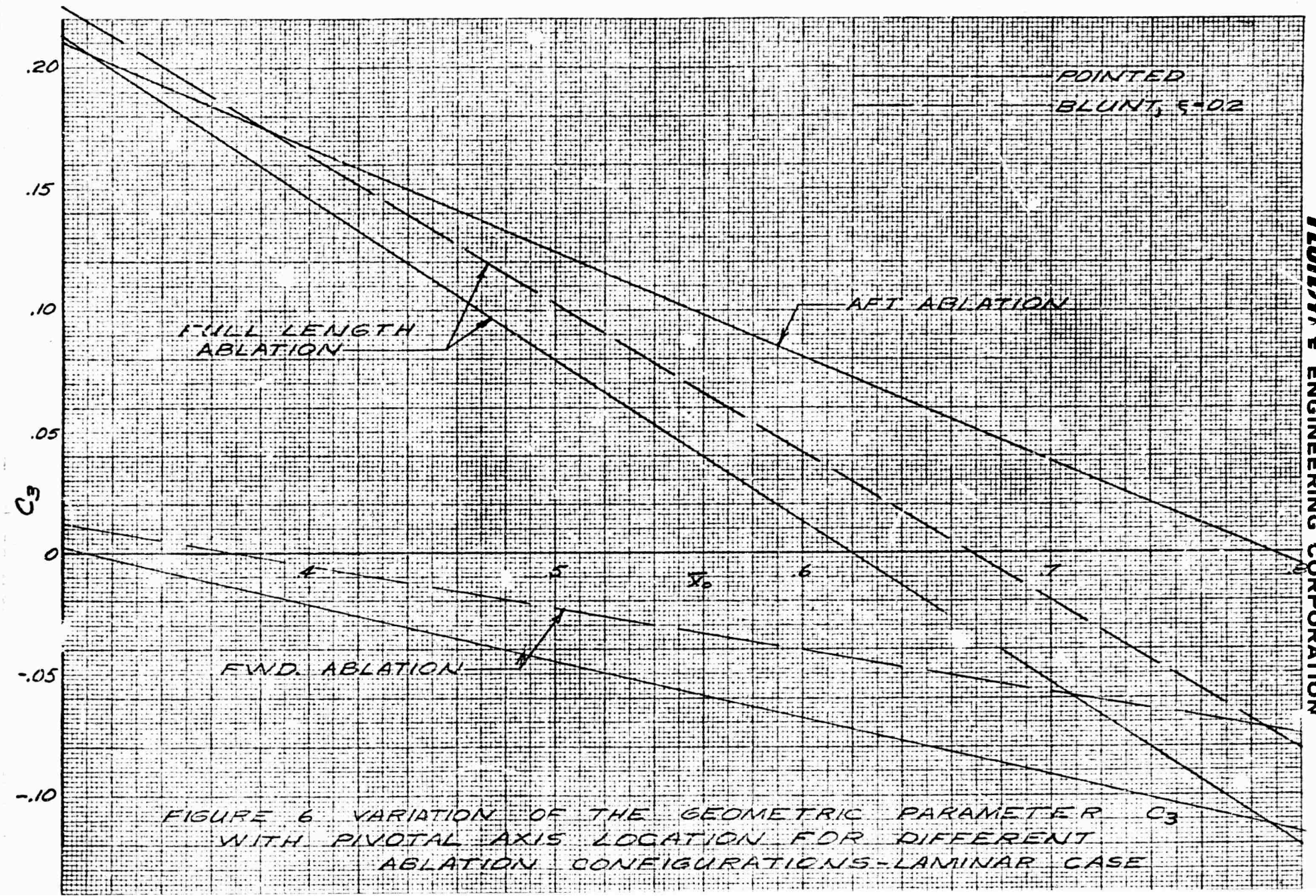

FIGURE 6 VARIATION OF THE GEOMETRIC PARAMETER C_3 WITH PIVOTAL AXIS LOCATION FOR DIFFERENT ABLATION CONFIGURATIONS - LAMINAR CASE

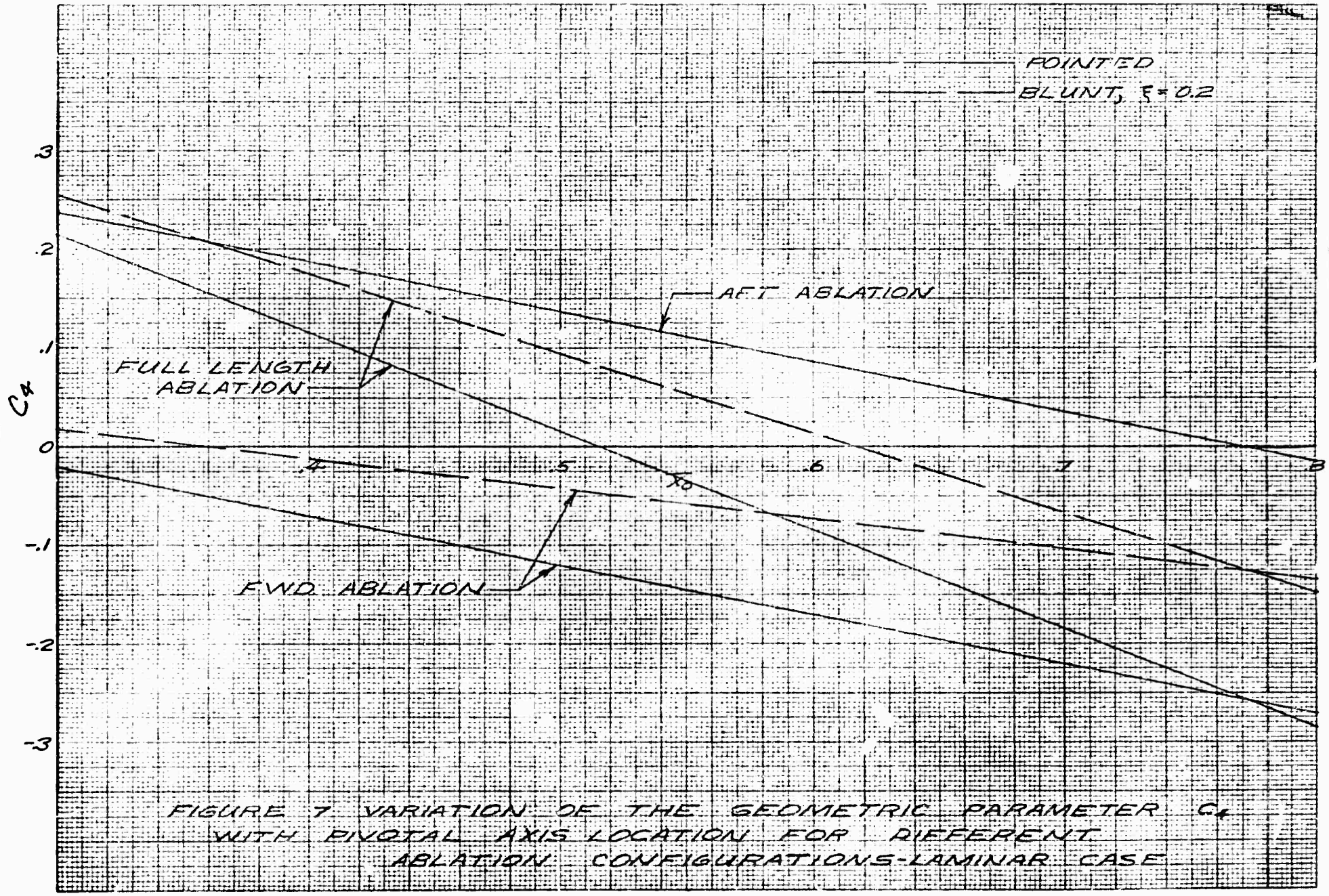

FIGURE 7 VARIATION OF THE GEOMETRIC PARAMETER C_4 WITH PIVOTAL AXIS LOCATION FOR DIFFERENT ABLATION CONFIGURATIONS-LAMINAR CASE

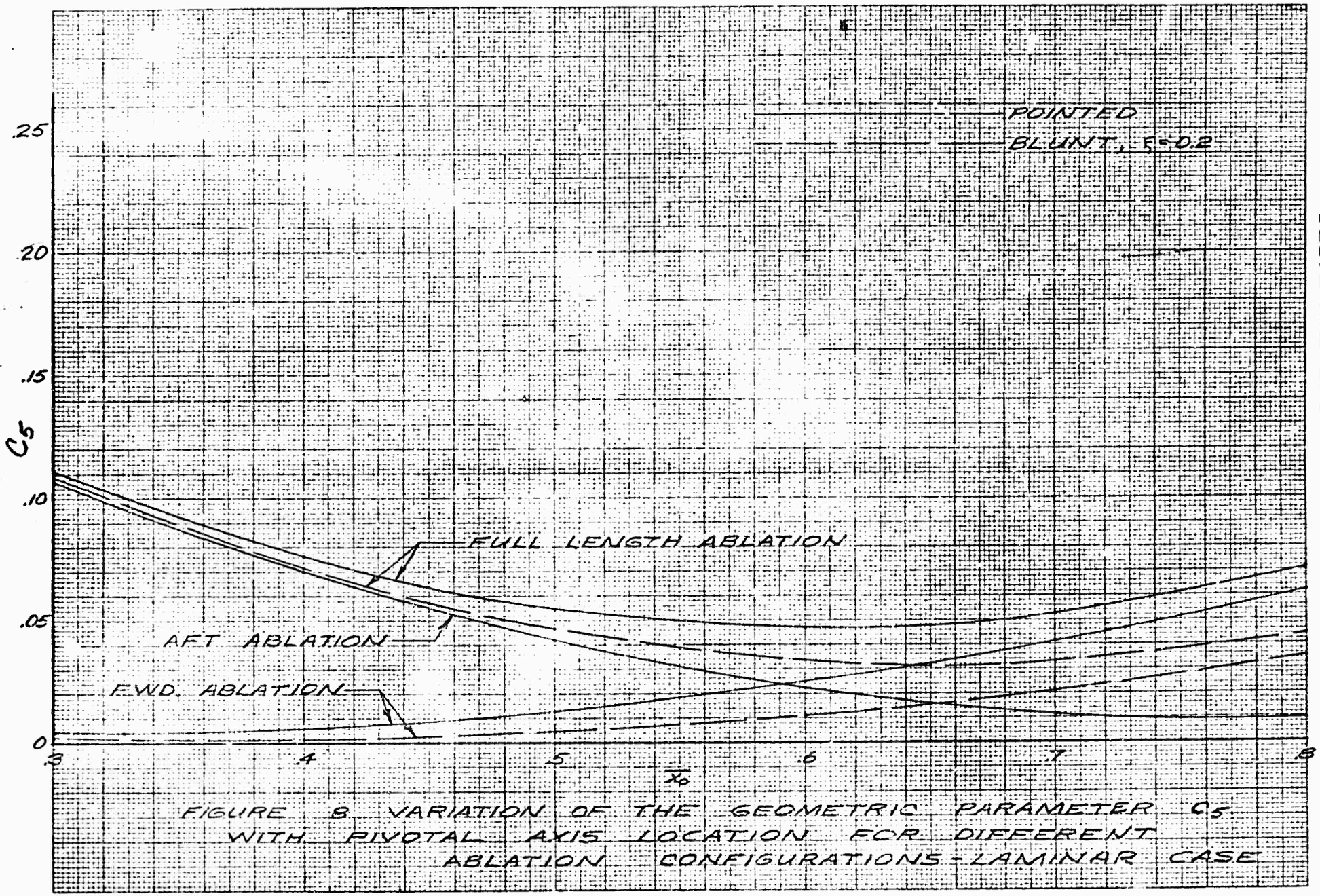

FIGURE 8 VARIATION OF THE GEOMETRIC PARAMETER C_5 WITH PIVOTAL AXIS LOCATION FOR DIFFERENT ABLATION CONFIGURATIONS - LAMINAR CASE

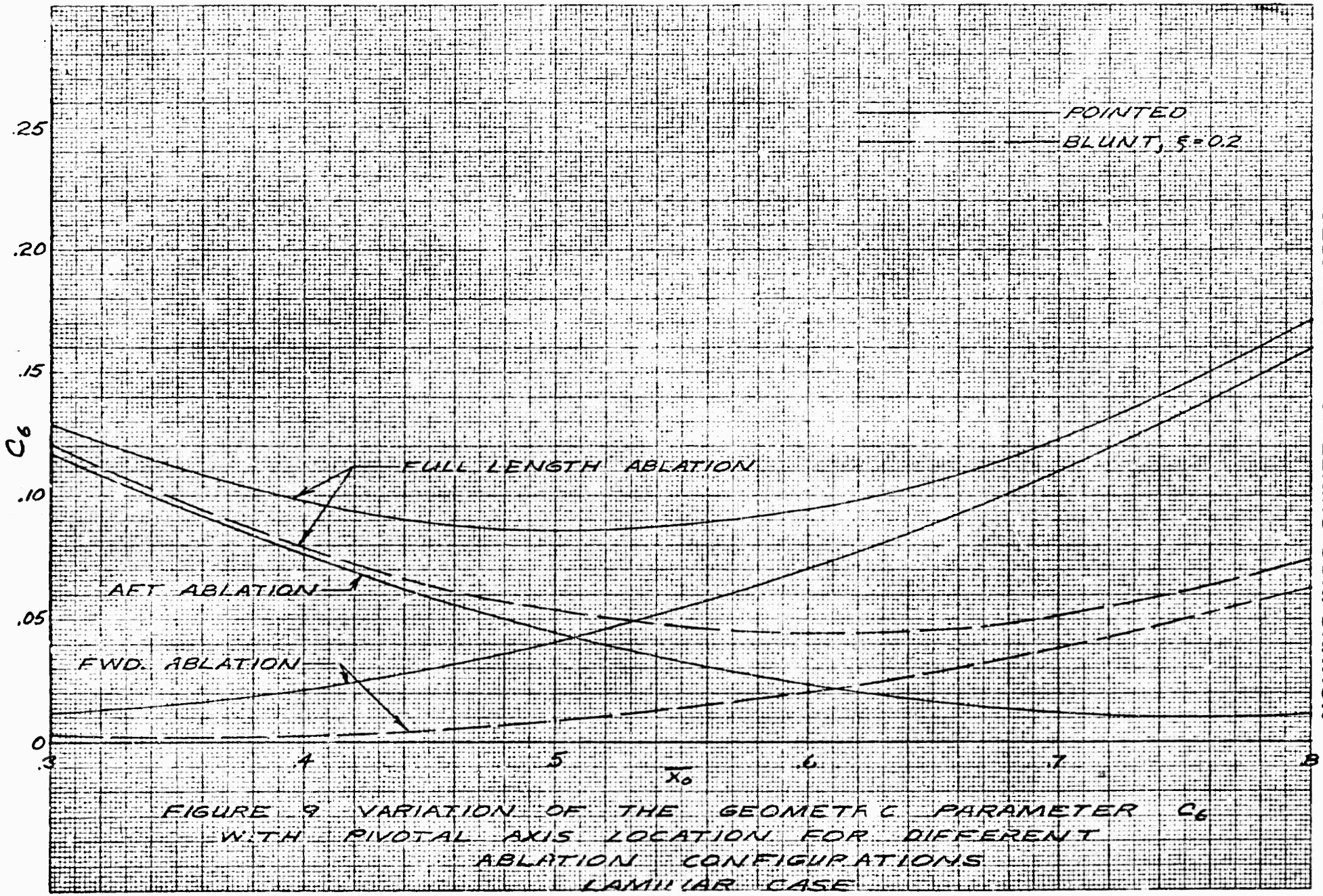

FIGURE 9 VARIATION OF THE GEOMETRIC PARAMETER C_6 WITH PIVOTAL AXIS LOCATION FOR DIFFERENT ABLATION CONFIGURATIONS LAMINAR CASE

FIGURE 10 VARIATION OF THE GEOMETRIC PARAMETER C_{Y_α} WITH PIVOTAL AXIS LOCATION FOR DIFFERENT ABLATION CONFIGURATIONS - LAMINAR CASE

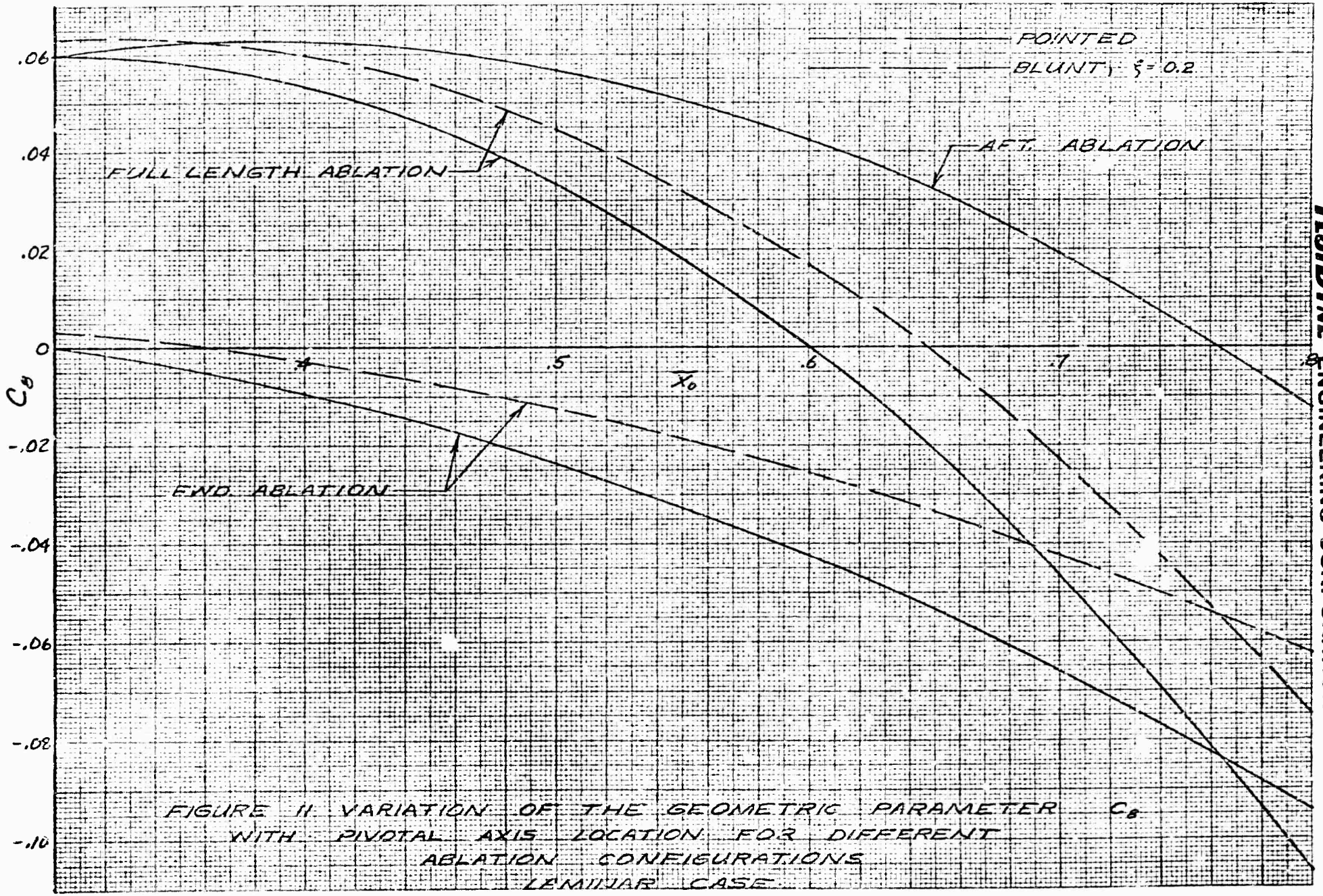

FIGURE 11 VARIATION OF THE GEOMETRIC PARAMETER C_B WITH PIVOTAL AXIS LOCATION FOR DIFFERENT ABLATION CONFIGURATIONS LEMINAR CASE

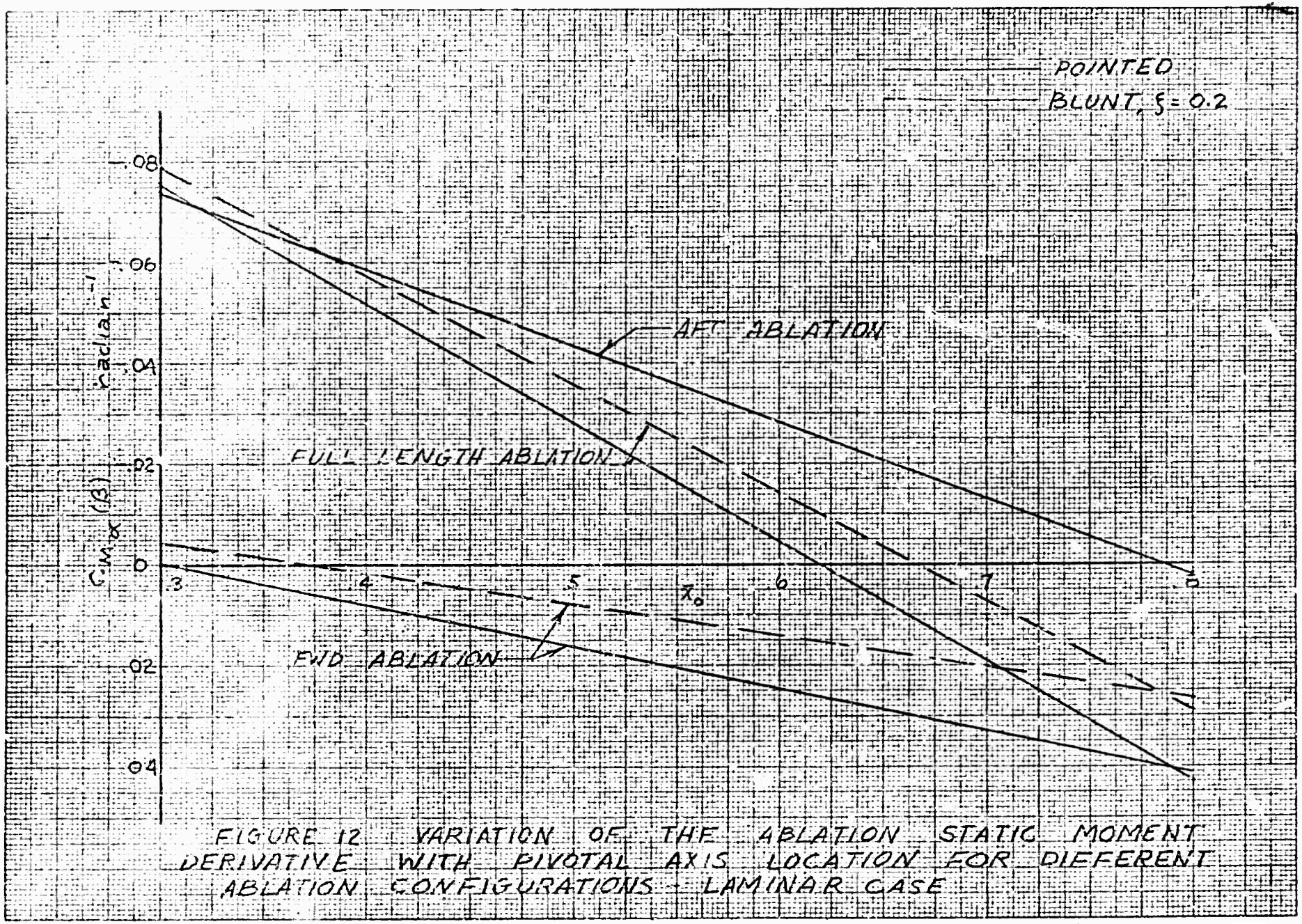

FIGURE 12 VARIATION OF THE ABLATION STATIC MOMENT DERIVATIVE WITH PIVOTAL AXIS LOCATION FOR DIEFERENT ABLATION CONFIGURATIONS - LAMINAR CASE

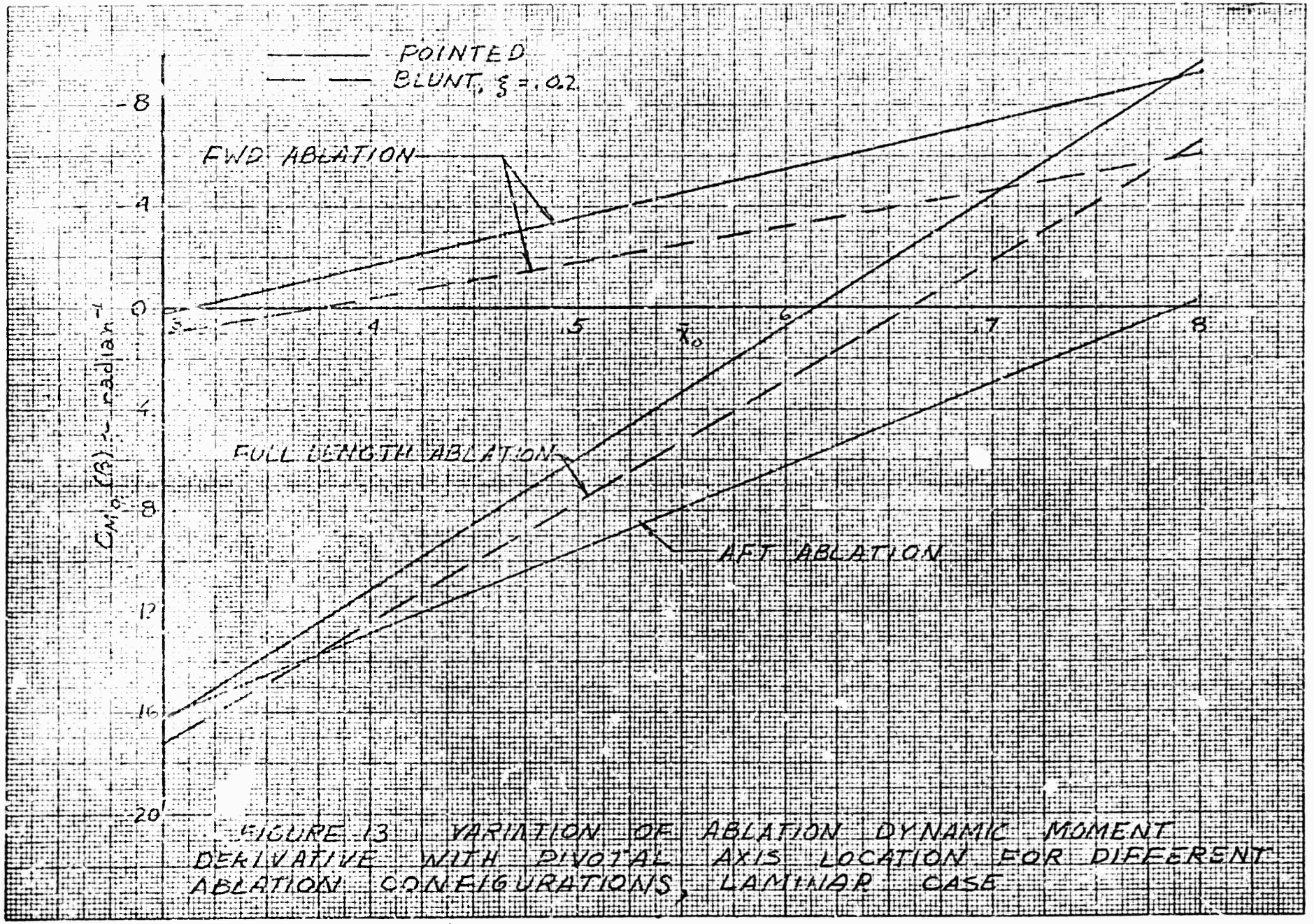

FIGURE 13 VARIATION OF ABLATION DYNAMIC MOMENT DERIVATIVE WITH PIVOTAL AXIS LOCATION FOR DIFFERENT ABLATION CONFIGURATIONS, LAMINAR CASE

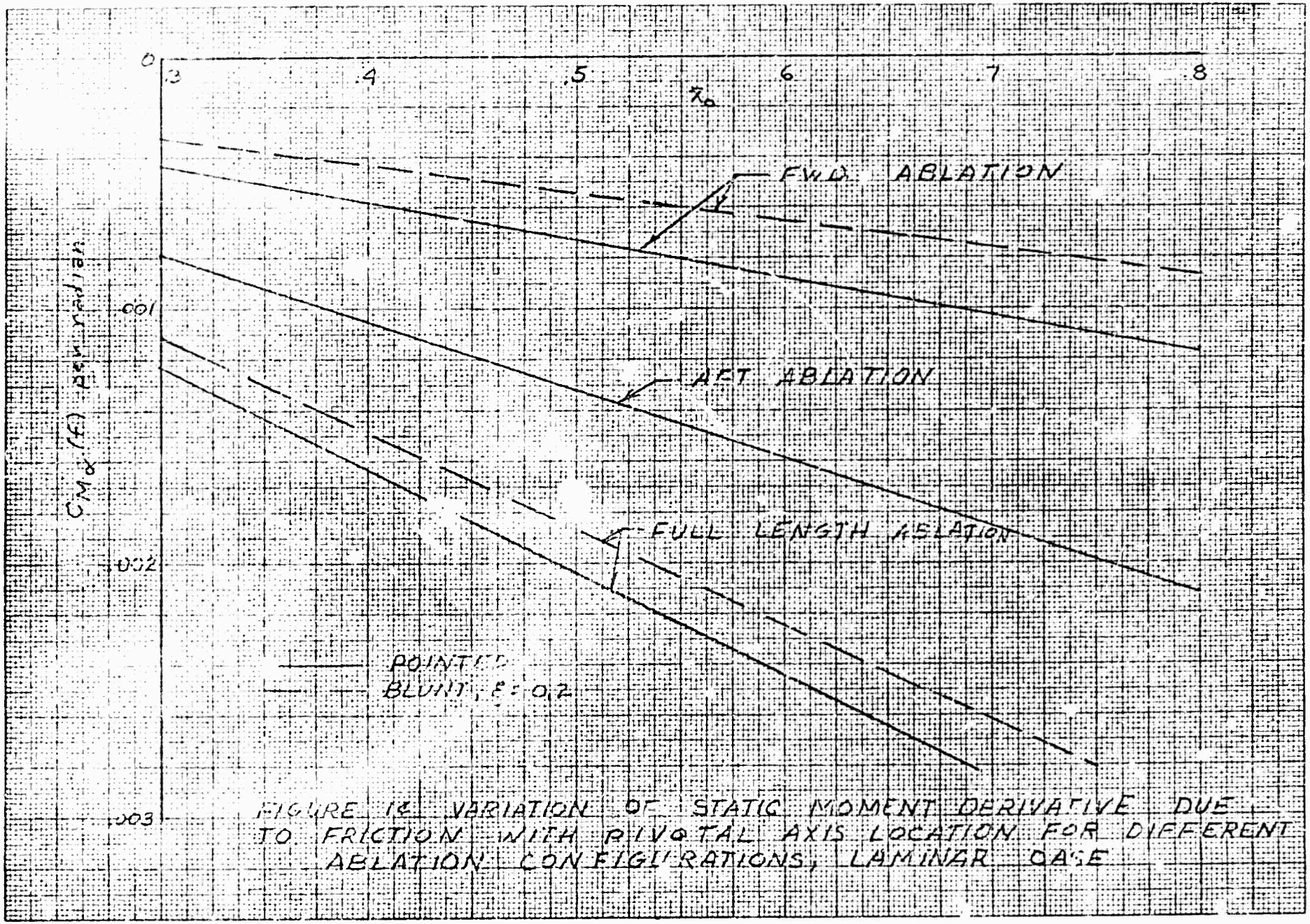

FIGURE 12. VARIATION OF STATIC MOMENT DERIVATIVE DUE TO FRICTION WITH RIVOTAL AXIS LOCATION FOR DIFFERENT ABLATION CONFIGURATIONS, LAMINAR CASE

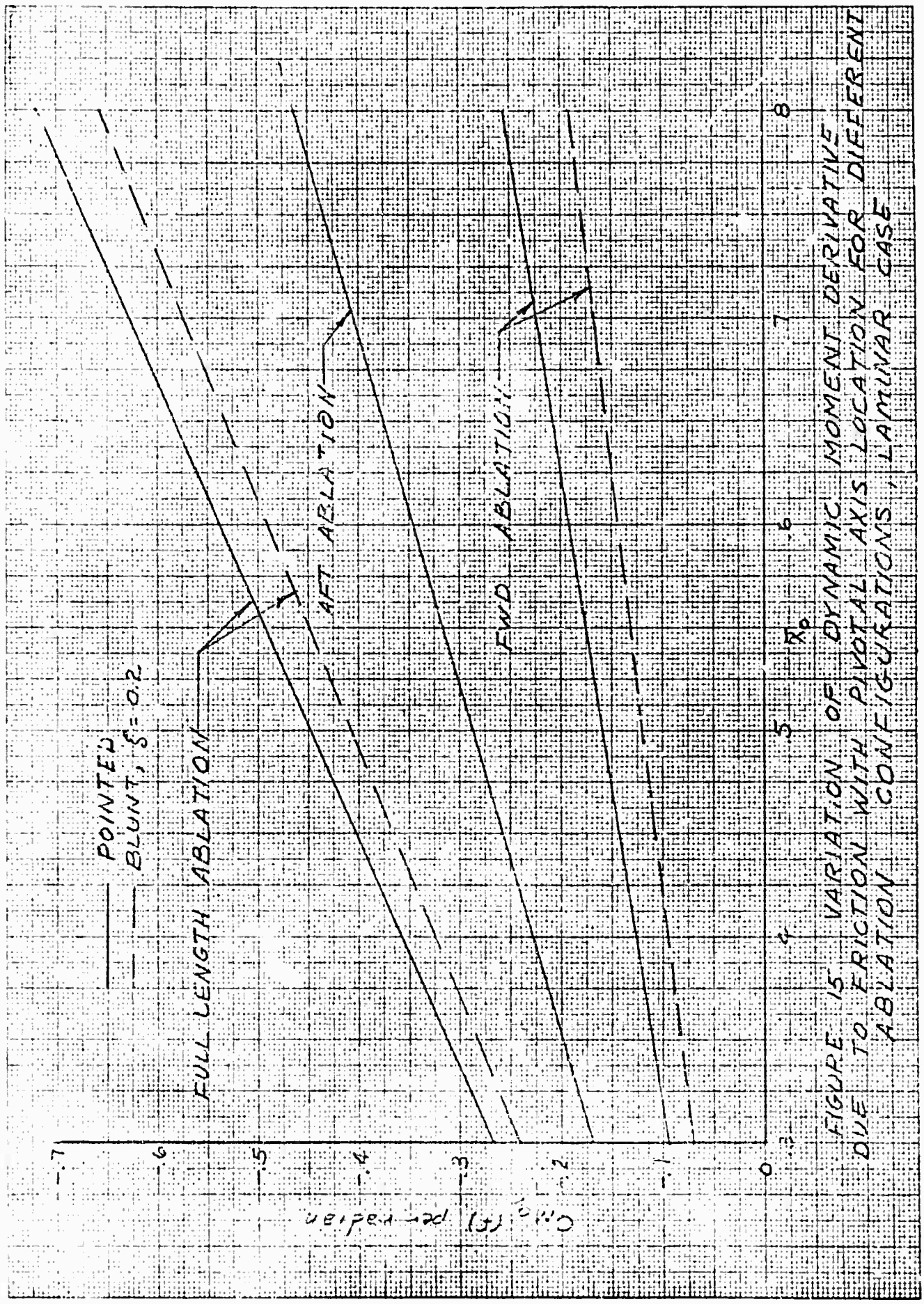

FIGURE 15 VARIATION OF DYNAMIC MOMENT DERIVATIVES DUE TO FRICTION WITH PIVOTAL AXIS LOCATION FOR DIFFERENT ABLATION CONFIGURATIONS, LAMINAR CASE

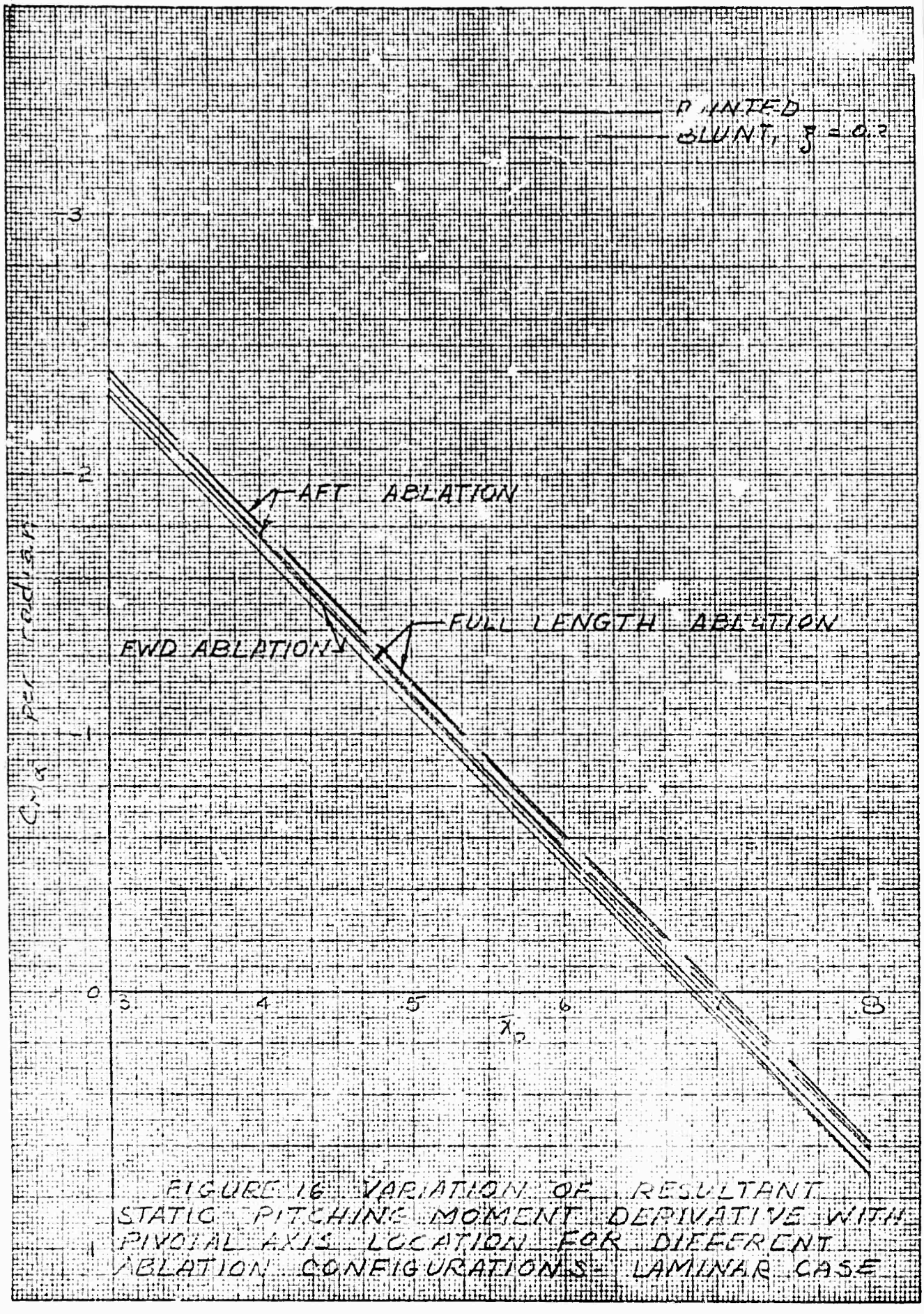

FIGURE 16 VARIATION OF RESULTANT STATIC PITCHING MOMENT DERIVATIVE WITH PIVOTAL AXIS LOCATION FOR DIFFERENT ABLATION CONFIGURATIONS - LAMINAR CASE

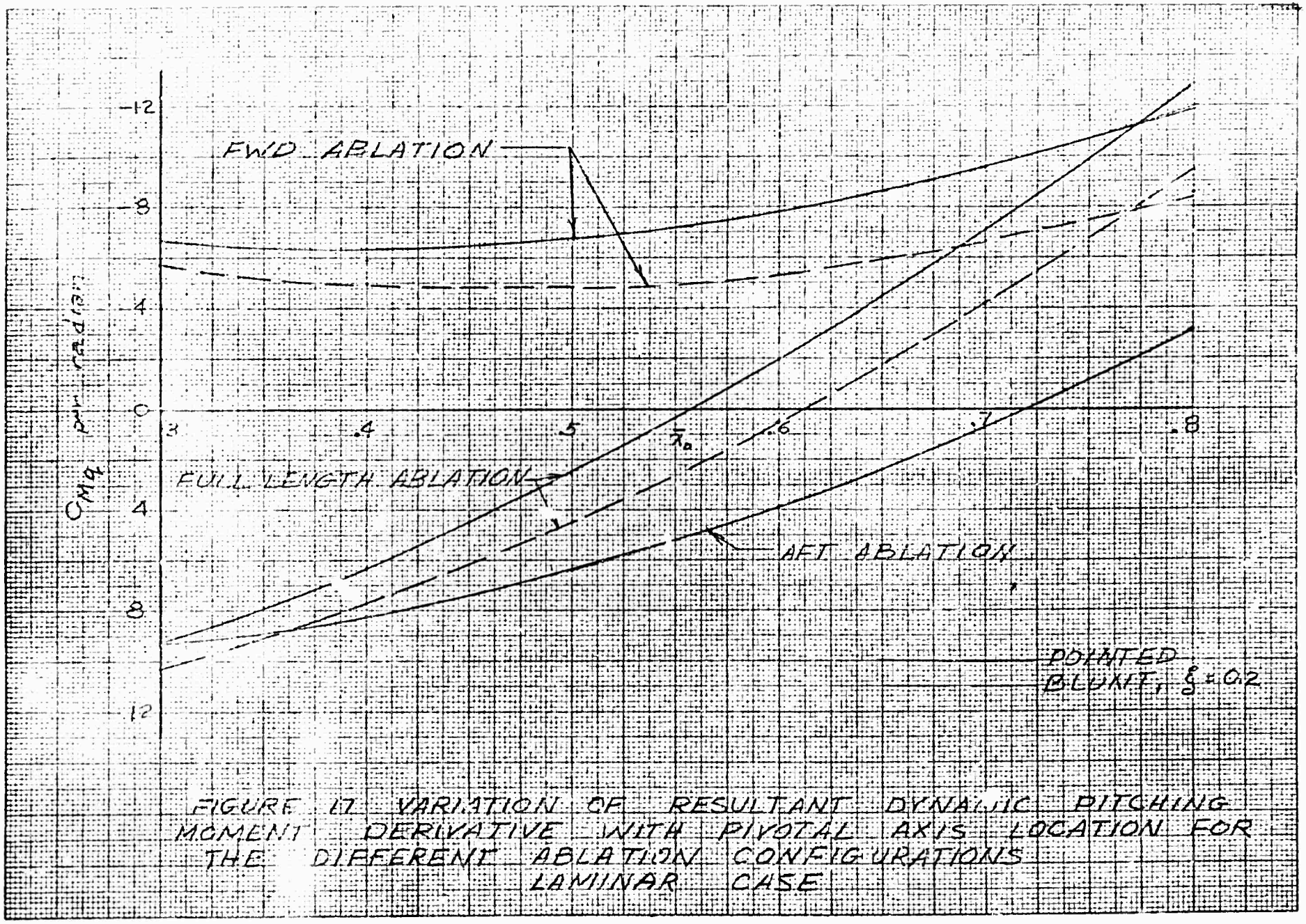

FIGURE 17 VARIATION OF RESULTANT DYNAMIC PITCHING MOMENT DERIVATIVE WITH PIVOTAL AXIS LOCATION FOR THE DIFFERENT ABLATION CONFIGURATIONS LAMINAR CASE

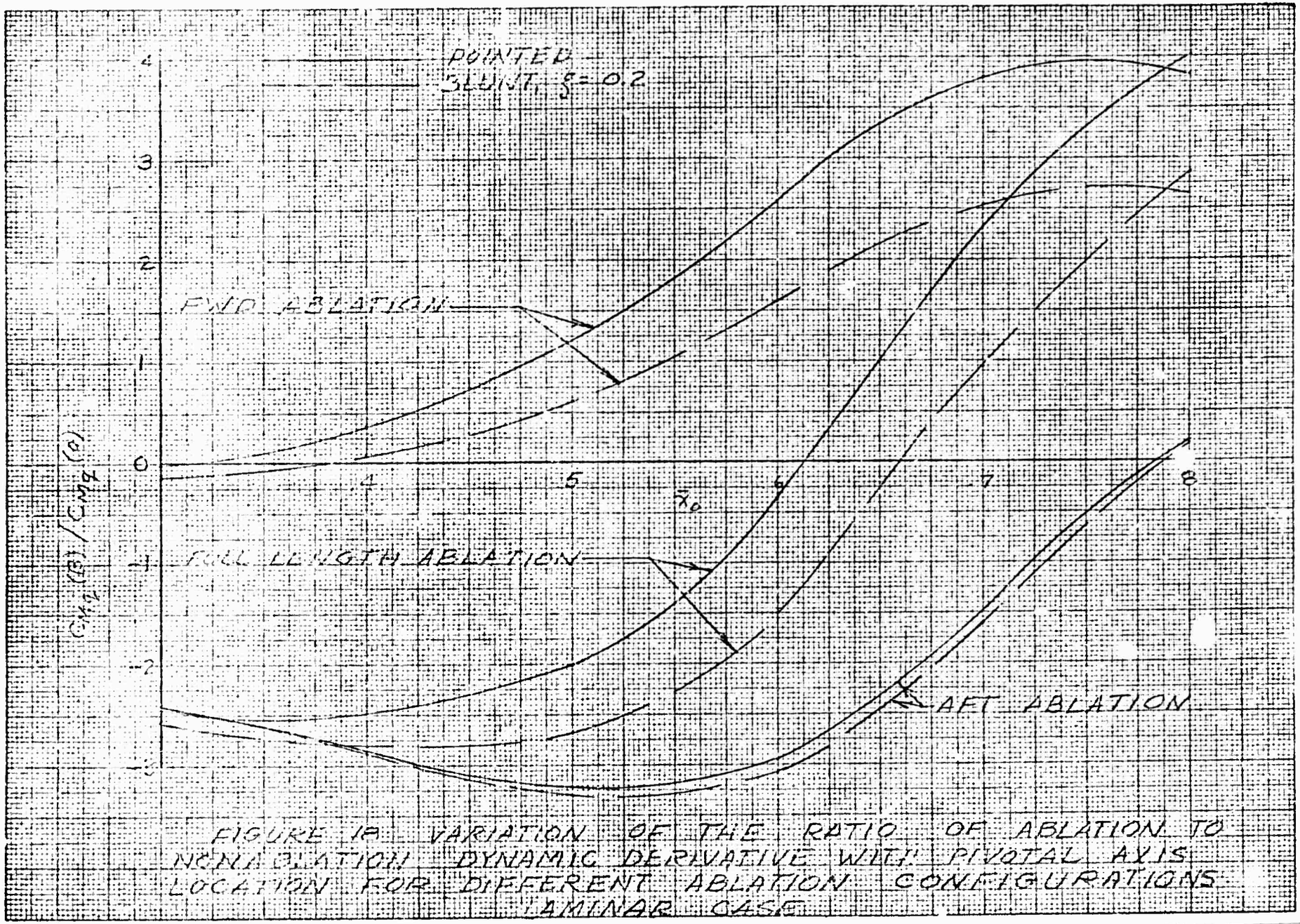

FIGURE 18 VARIATION OF THE RATIO OF ABLATION TO NON-ABLATION DYNAMIC DERIVATIVE WITH PIVOTAL AXIS LOCATION FOR DIFFERENT ABLATION CONFIGURATIONS LAMINAR CASE

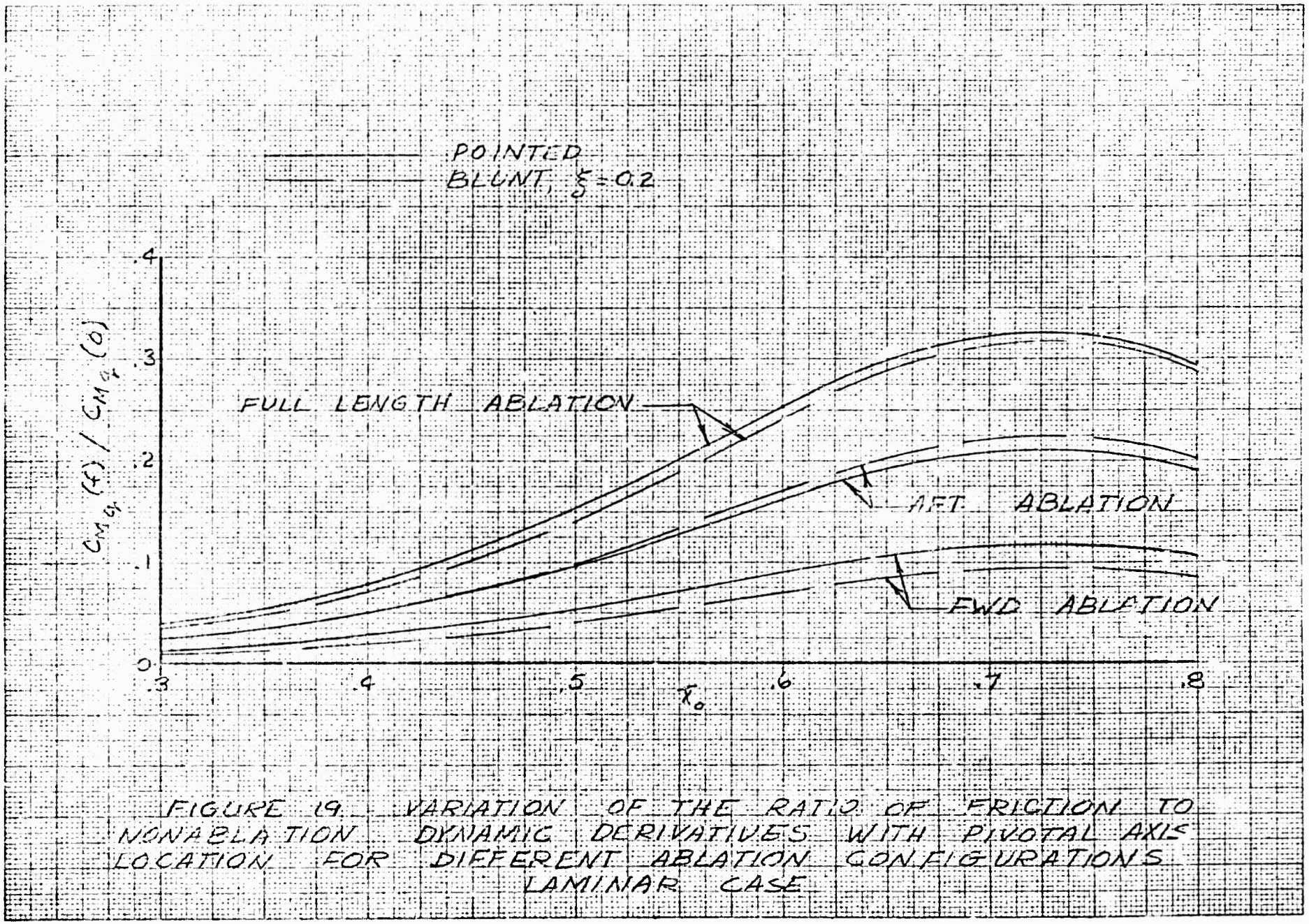

FIGURE 19 VARIATION OF THE RATIO OF FRICTION TO NONABLATION DYNAMIC DERIVATIVES WITH PIVOTAL AXIS LOCATION FOR DIFFERENT ABLATION CONFIGURATIONS LAMINAR CASE

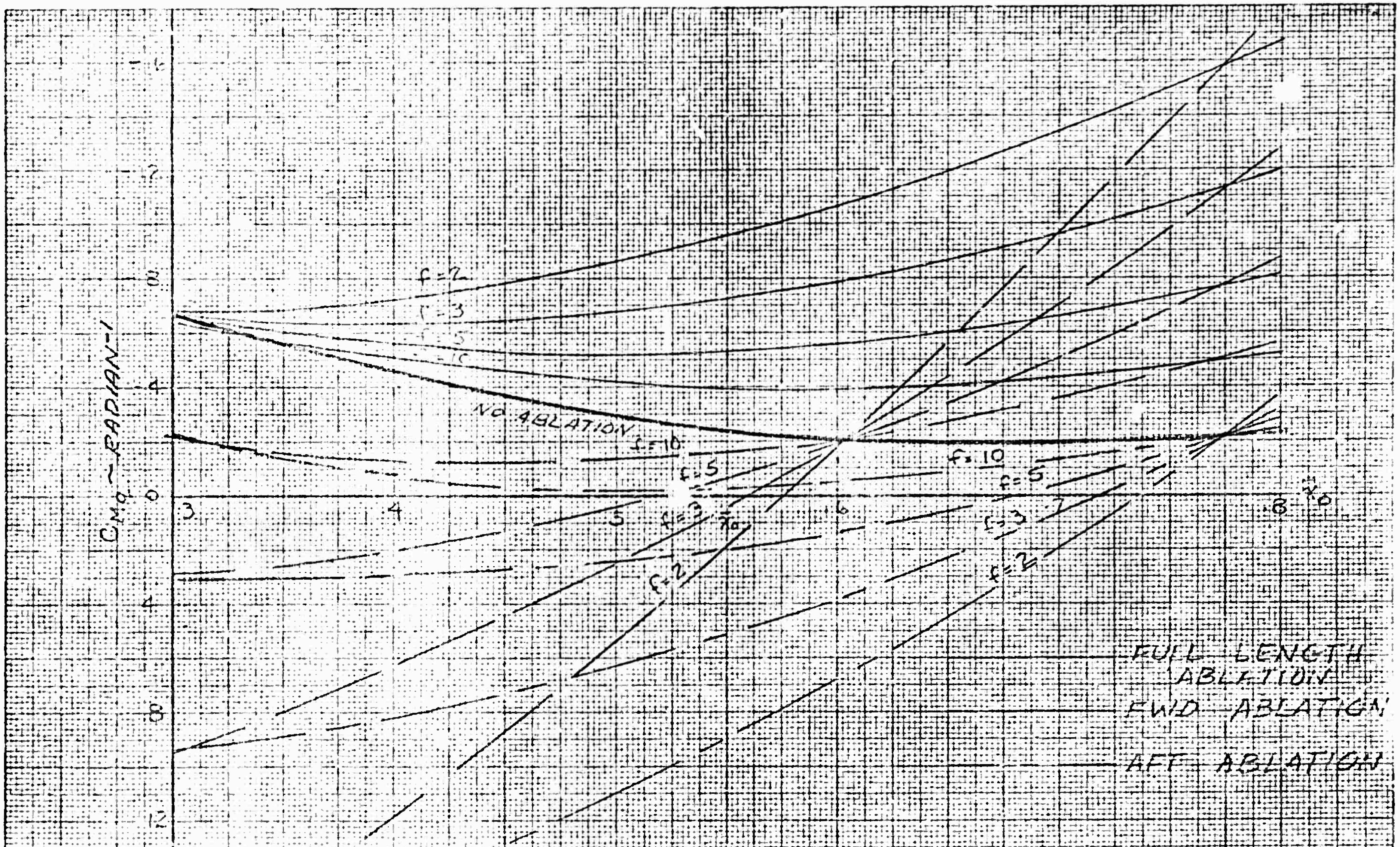

FIGURE 20 EFFECTS OF CHANGES IN OSCILLATION FREQUENCY ON THE RESULTANT DYNAMIC DERIVATIVE FOR DIFFERENT ABLATION CONFIGURATIONS FOR A POINTED CONE WITH $\theta = 10°$ AND $\lambda = 20°$ LAMINAR CASE

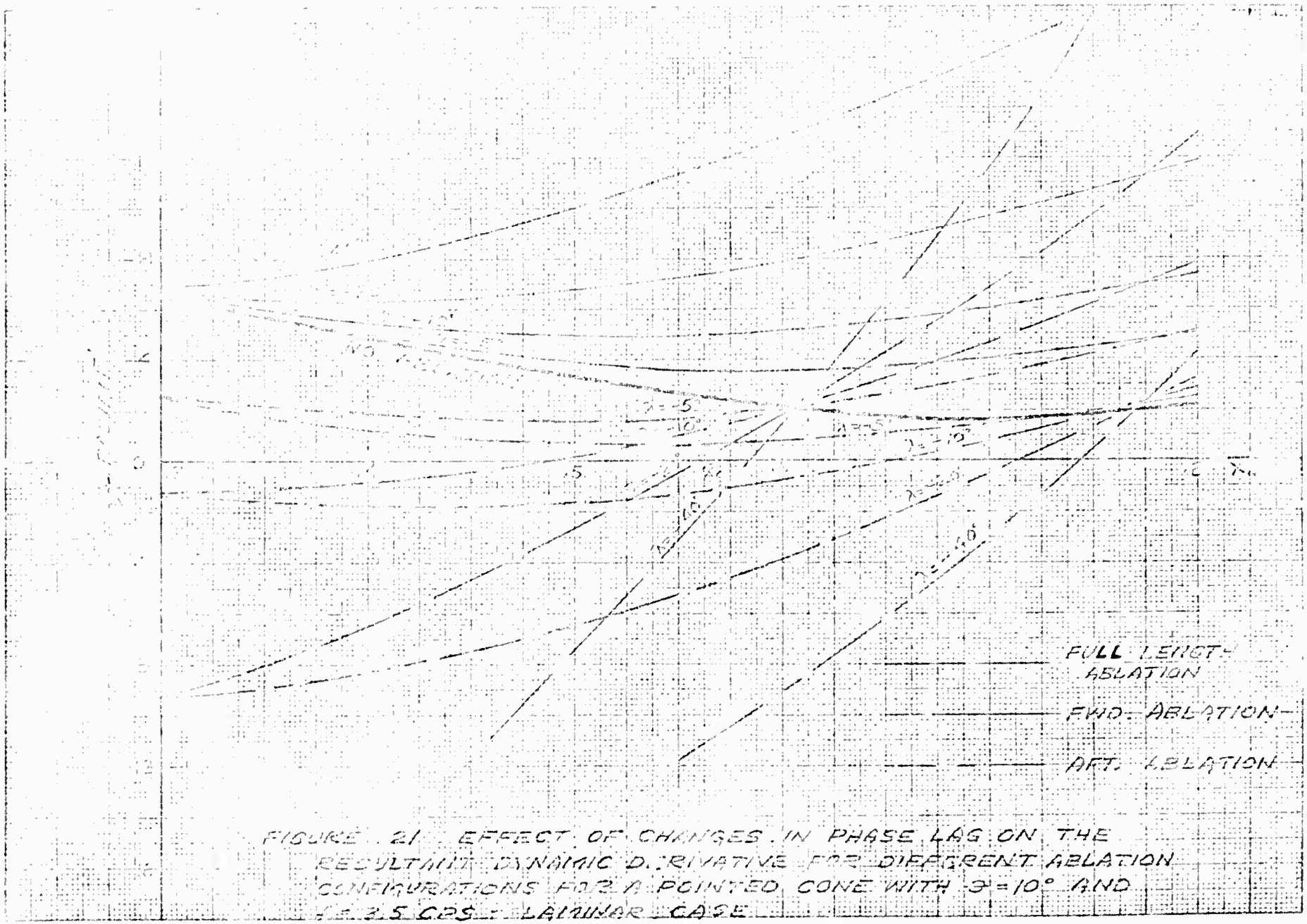

FIGURE 21 EFFECT OF CHANGES IN PHASE LAG ON THE RESULTANT DYNAMIC DERIVATIVE FOR DIFFERENT ABLATION CONFIGURATIONS FOR A POINTED CONE WITH $\vartheta = 10°$ AND $\kappa = 2.5$ CPS - LAMINAR CASE

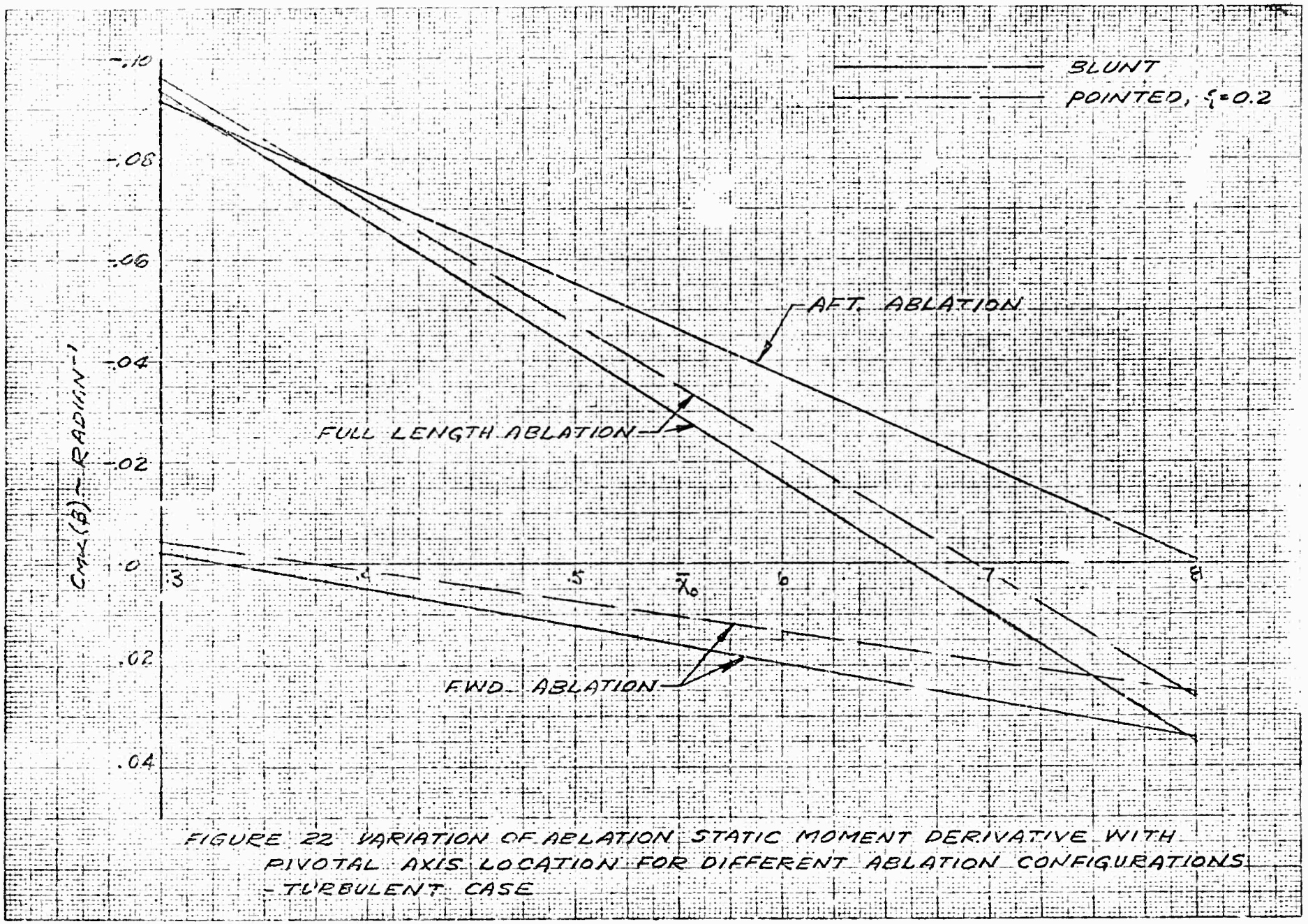

FIGURE 22 VARIATION OF ABLATION STATIC MOMENT DERIVATIVE WITH PIVOTAL AXIS LOCATION FOR DIFFERENT ABLATION CONFIGURATIONS - TURBULENT CASE

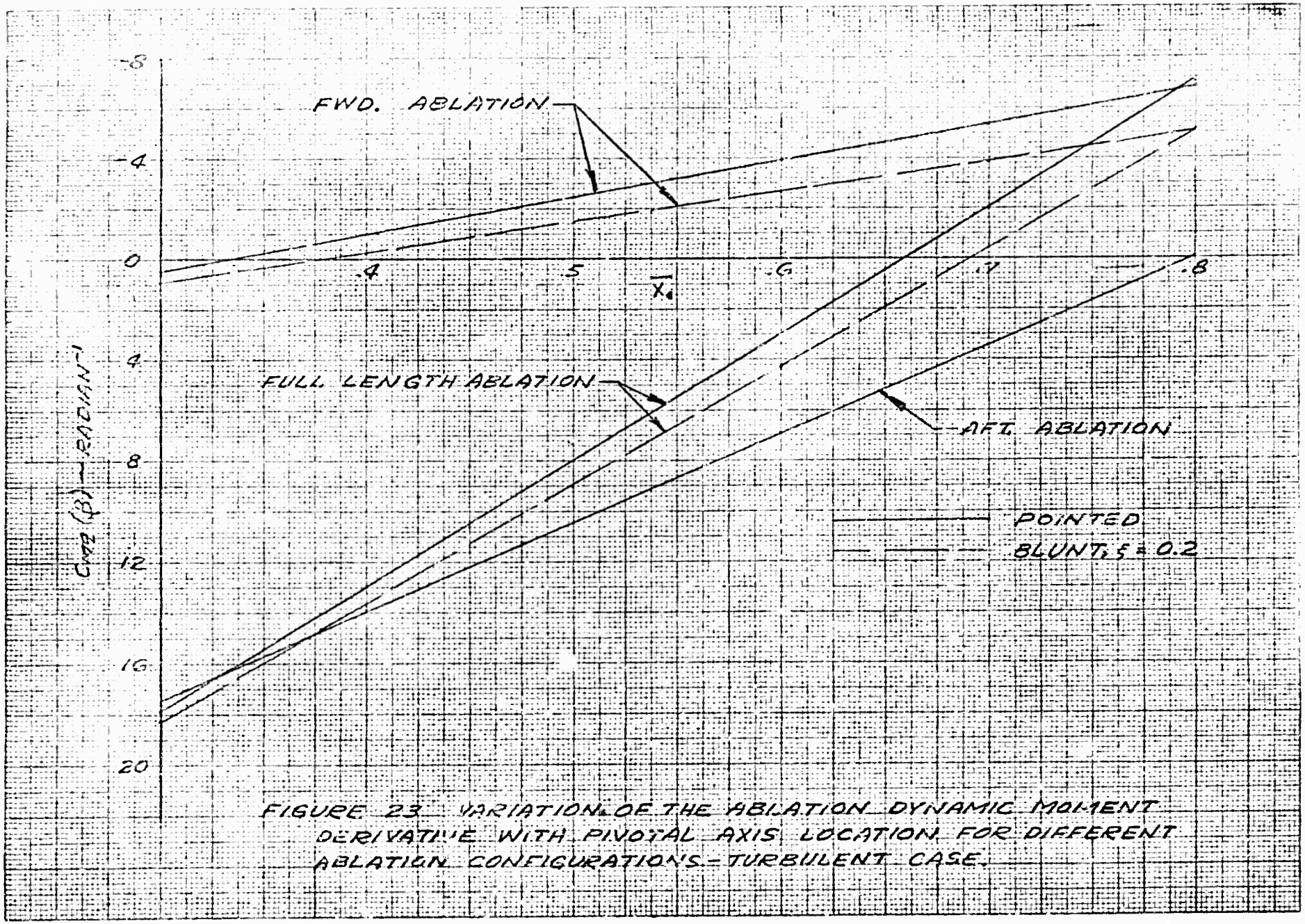

FIGURE 23 VARIATION OF THE ABLATION DYNAMIC MOMENT DERIVATIVE WITH PIVOTAL AXIS LOCATION FOR DIFFERENT ABLATION CONFIGURATIONS - TURBULENT CASE.

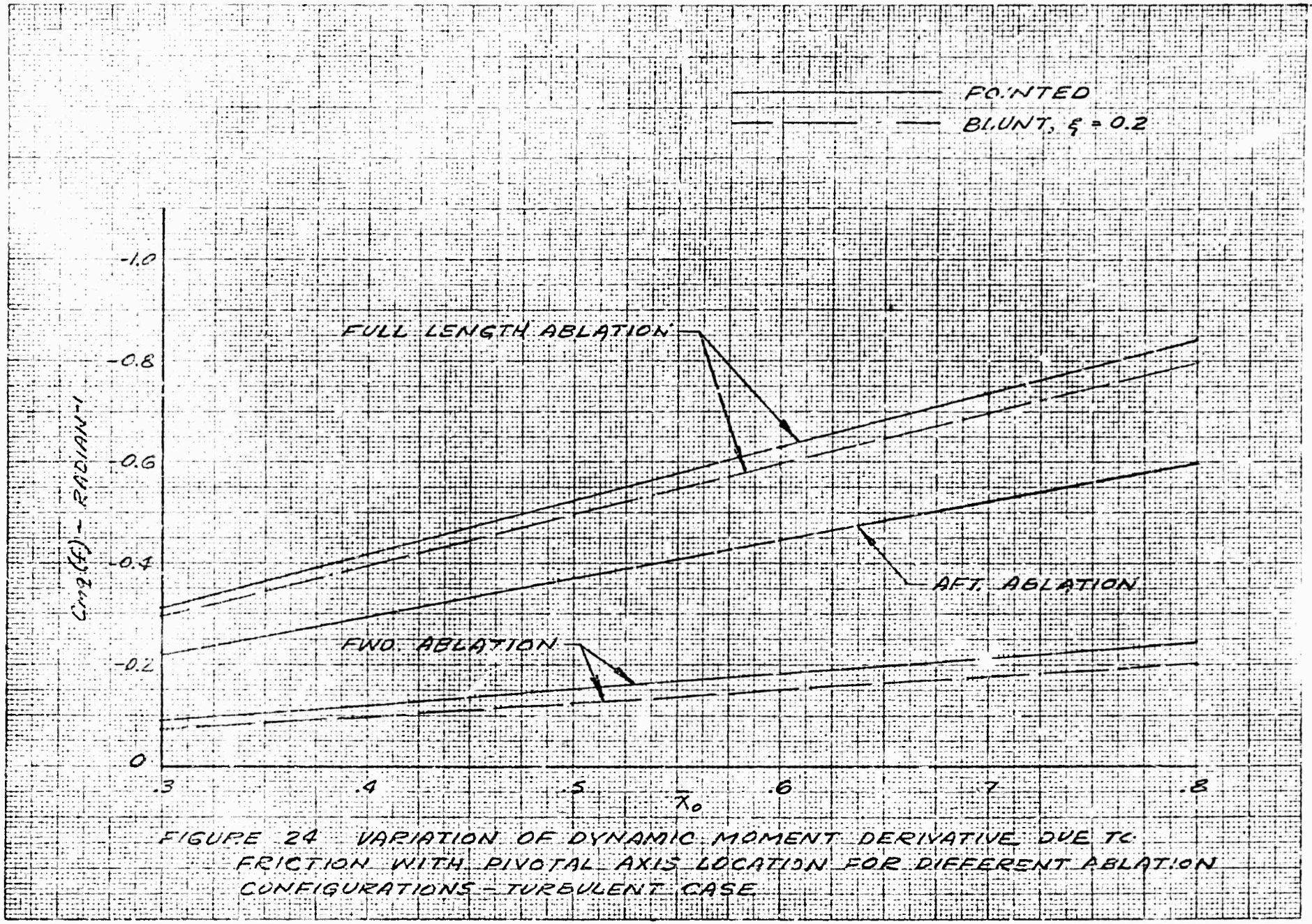

FIGURE 24 VARIATION OF DYNAMIC MOMENT DERIVATIVE DUE TO FRICTION WITH PIVOTAL AXIS LOCATION FOR DIFFERENT ABLATION CONFIGURATIONS – TURBULENT CASE

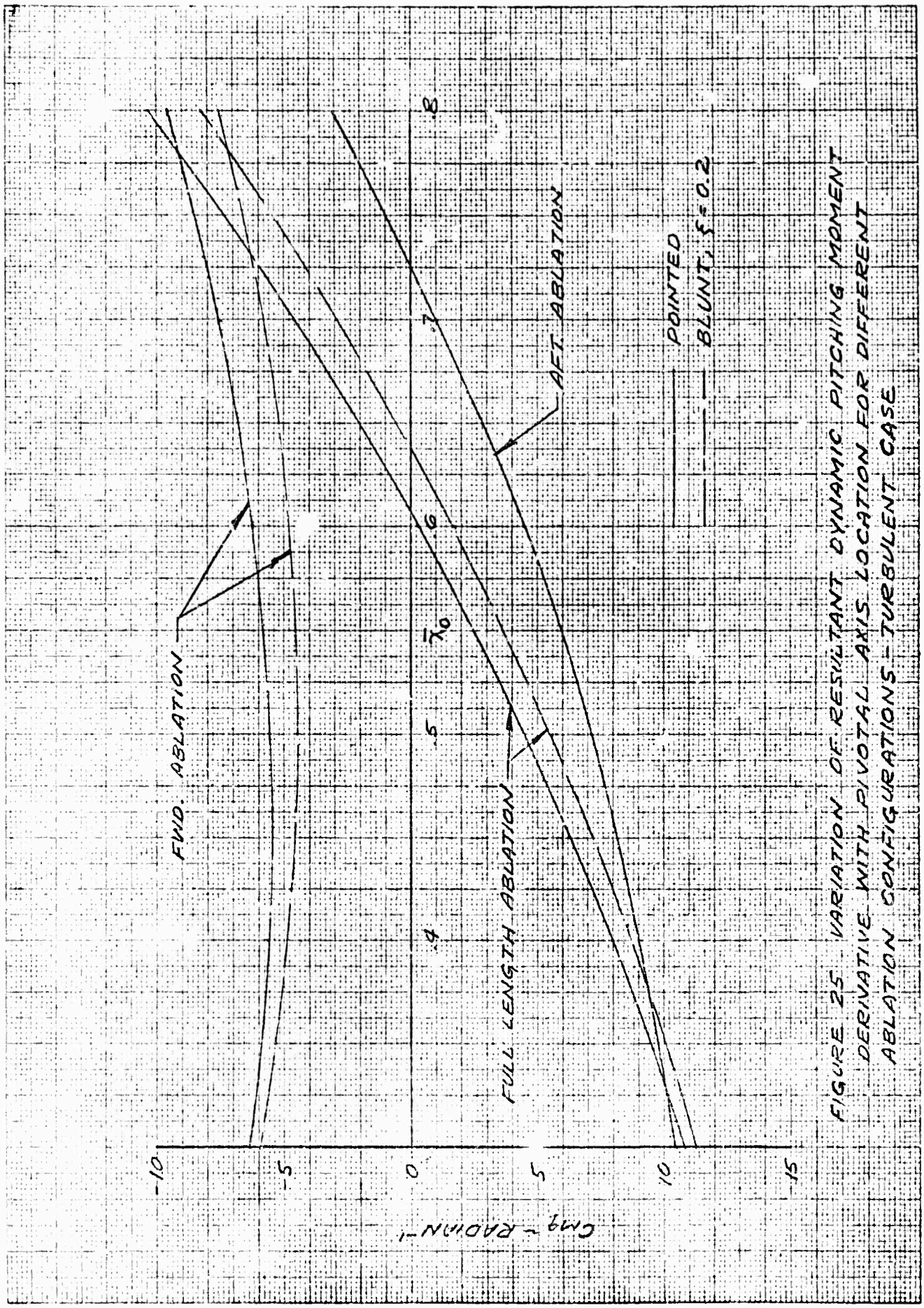

FIGURE 25 VARIATION OF RESULTANT DYNAMIC PITCHING MOMENT DERIVATIVE WITH PIVOTAL AXIS LOCATION FOR DIFFERENT ABLATION CONFIGURATIONS - TURBULENT CASE

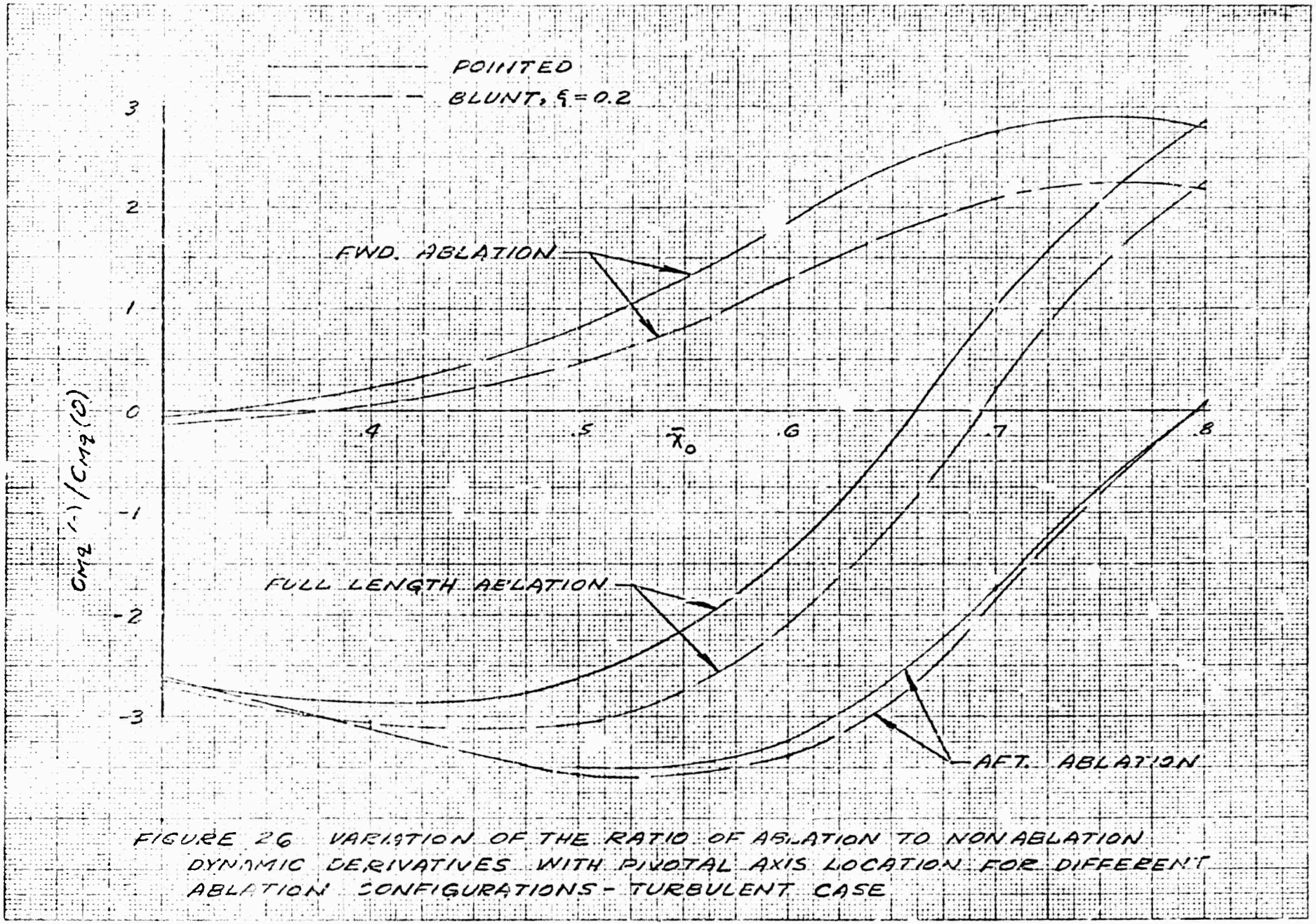

FIGURE 26 VARIATION OF THE RATIO OF ABLATION TO NON ABLATION DYNAMIC DERIVATIVES WITH PIVOTAL AXIS LOCATION FOR DIFFEERENT ABLATION CONFIGURATIONS - TURBULENT CASE

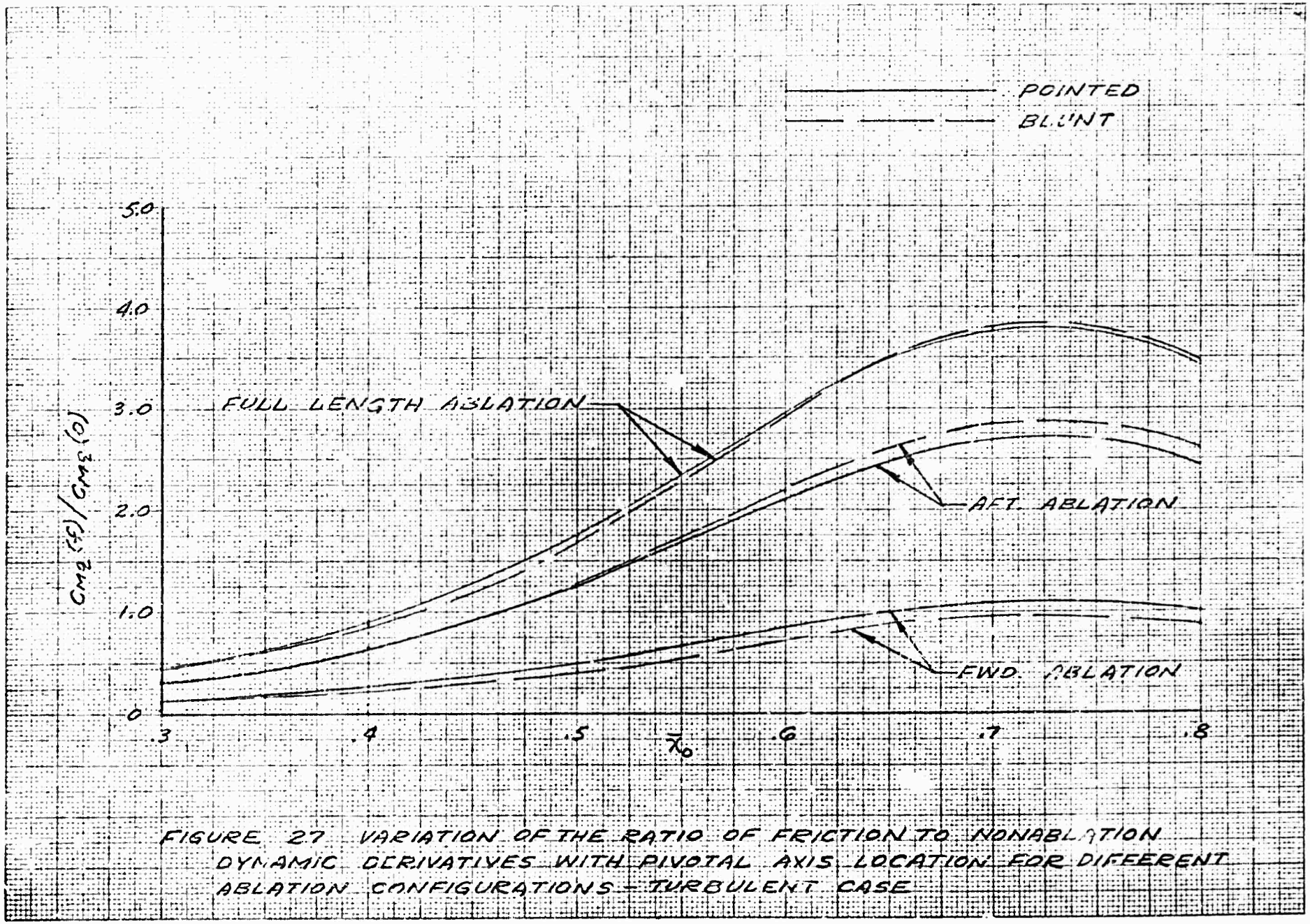

FIGURE 27 VARIATION OF THE RATIO OF FRICTION TO NONABLATION DYNAMIC DERIVATIVES WITH PIVOTAL AXIS LOCATION FOR DIFFERENT ABLATION CONFIGURATIONS – TURBULENT CASE

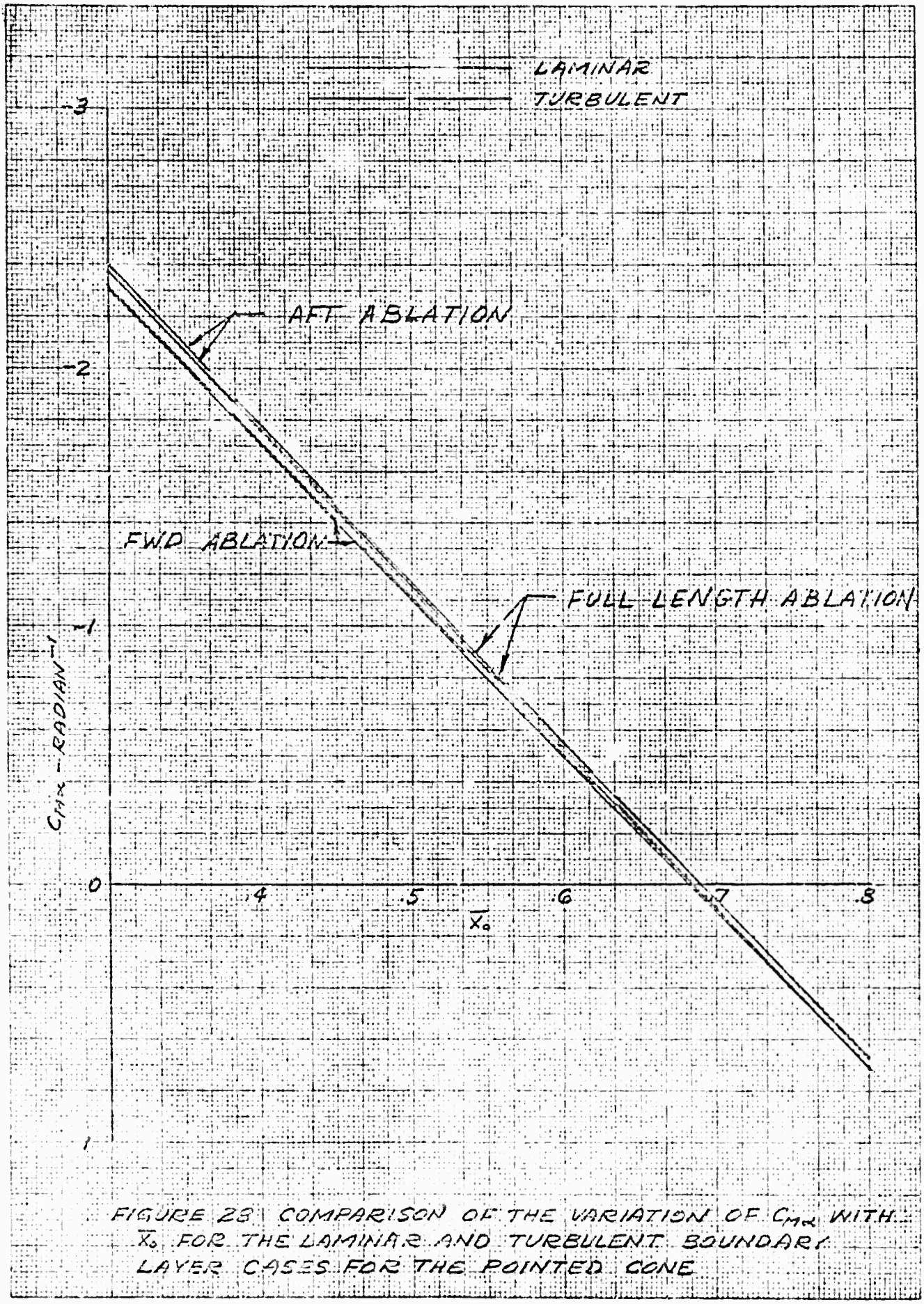

FIGURE 23 COMPARISON OF THE VARIATION OF C_{M_α} WITH $\bar{X}_o$ FOR THE LAMINAR AND TURBULENT BOUNDARY LAYER CASES FOR THE POINTED CONE

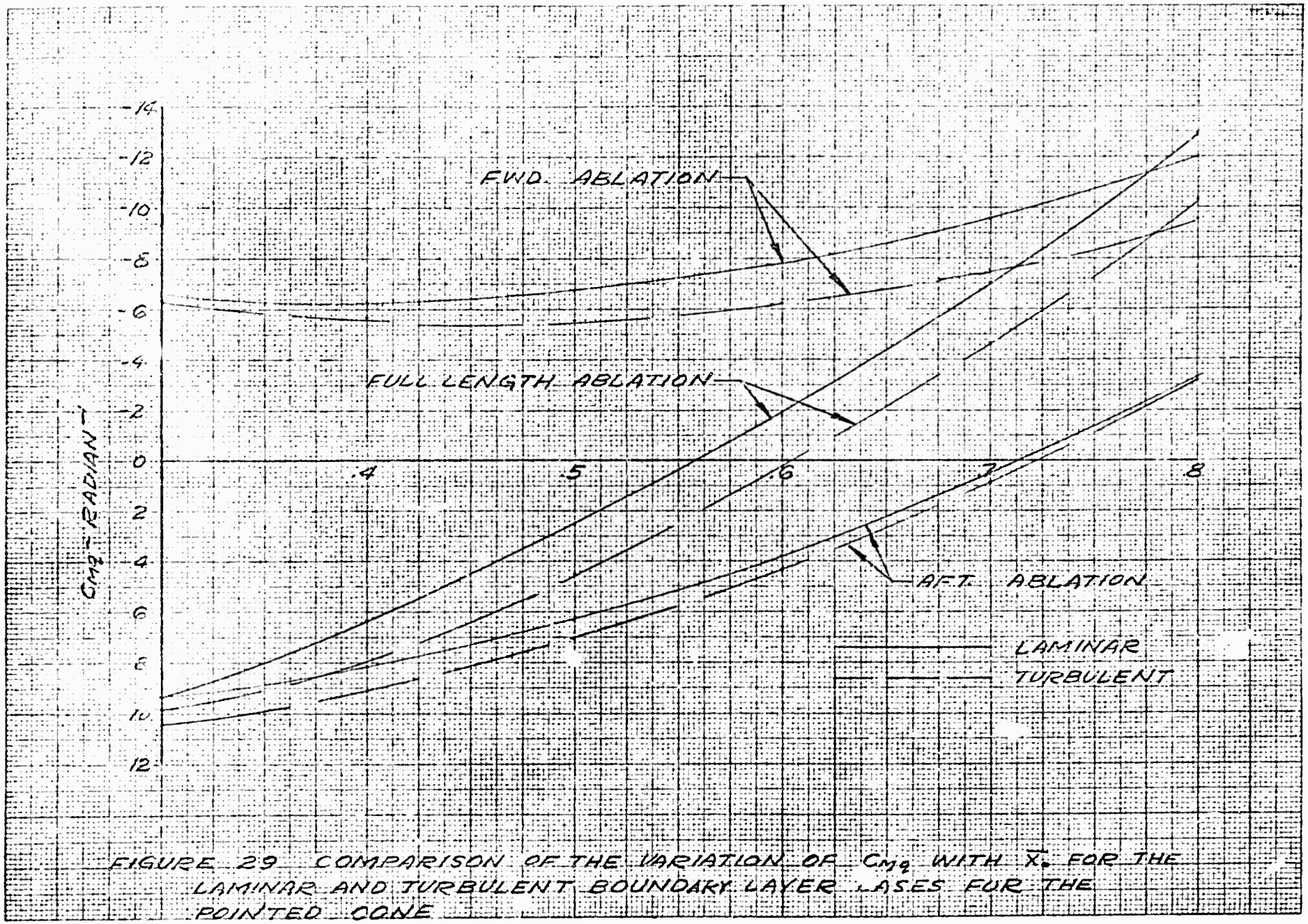

FIGURE 29 COMPARISON OF THE VARIATION OF C_{m_q} WITH $\bar{X}_{cp}$ FOR THE LAMINAR AND TURBULENT BOUNDARY LAYER CASES FOR THE POINTED CONE

Unclassified

Security Classification

DOCUMENT CONTROL DATA · R&D

(Security classification of title, body of abstract and indexing annotation must be entered when the overall report is classified)

1. ORIGINATING ACTIVITY (Corporate author)	2a. REPORT SECURITY CLASSIFICATION
FluiDyne Engineering Corporation	Unclassified
	2b. GROUP N/A

3. REPORT TITLE

Effects of Ablation on the Pitching Moment Derivatives of Cones in Hypersonic Flow

4. DESCRIPTIVE NOTES (Type of report and inclusive dates) Report of analytical work related to FluiDyne Report 0414-3-31-67 under same contract.

5. AUTHOR(S) (Last name, first name, initial)

Ibrahim, Shukry K.

6. REPORT DATE	7a. TOTAL NO. OF PAGES	7b. NO. OF REFS
4 April 1967	107	44

8a. CONTRACT OR GRANT NO.	9a. ORIGINATOR'S REPORT NUMBER(S)
Nonr 4624(00)	
b. PROJECT NO.	0414-4-4-67
c.	9b. OTHER REPORT NO(S) (Any other numbers that may be assigned this report)
d.	None

10. AVAILABILITY/LIMITATION NOTICES

11. SUPPLEMENTARY NOTES	12. SPONSORING MILITARY ACTIVITY
	ARPA Order No. 576

13 ABSTRACT A simple method is presented for calculating the hypersonic static and dynamic pitching moment derivatives for slender cones performing small-angle oscillations about the C.G. taking account of ablation effects over arbitrarily specified portions of the cone. The analysis rests on Newton's Impact Theory and is restricted to rigid body motions at low frequencies.

The nonablating pitching moment derivatives are supplemented by additional contributions due to the local ablation mass transfer and skin friction change which are derived from flat plate data modified to account for the conical flow conditions. The primary independent quantities other than the cone angle, nose bluntness and C.G. location are the ablation intensity, geometry and phase-shift w.r.t the oscillation angle. The ablation geometry is conveniently expressed by geometric coefficients of the same general type but different numerical values for the laminar and turbulent cases.

Two examples illustrate the application of the analysis to the laminar and turbulent boundary layer cases. The effect of ablation was very small on the static derivative but quite considerable on the dynamic derivative. The analysis points to significant differences in the dynamic stability characteristics of the laminar and turbulent cases with potentially serious practical consequences.

A simple parametric study illustrates the effects of a change in phase lag angle or oscillation frequency for different ablation configurations.

DD FORM 1 JAN 64 1473

Unclassified

Security Classification

14 KEY WORDS	LINK A		LINK B		LINK C	
	ROLE	WT	ROLE	WT	ROLE	WT
Re-entry						
Dynamic Stability						
Stability						
Hypersonic						
Mass Transfer						
Damping Coefficients						

INSTRUCTIONS

1. ORIGINATING ACTIVITY: Enter the name and address of the contractor, subcontractor, grantee, Department of Defense activity or other organization *(corporate author)* issuing the report.

2a. REPORT SECURITY CLASSIFICATION: Enter the overall security classification of the report. Indicate whether "Restricted Data" is included. Marking is to be in accordance with appropriate security regulations.

2b. GROUP: Automatic downgrading is specified in DoD Directive 5200.10 and Armed Forces Industrial Manual. Enter the group number. Also, when applicable, show that optional markings have been used for Group 3 and Group 4 as authorized.

3. REPORT TITLE: Enter the complete report title in all capital letters. Titles in all cases should be unclassified. If a meaningful title cannot be selected without classification, show title classification in all capitals in parenthesis immediately following the title.

4. DESCRIPTIVE NOTES: If appropriate, enter the type of report, e.g., interim, progress, summary, annual, or final. Give the inclusive dates when a specific reporting period is covered.

5. AUTHOR(S): Enter the name(s) of author(s) as shown on or in the report. Enter last name, first name, middle initial. If military, show rank and branch of service. The name of the principal author is an absolute minimum requirement.

6. REPORT DATE: Enter the date of the report as day, month, year; or month, year. If more than one date appears on the report, use date of publication.

7a. TOTAL NUMBER OF PAGES: The total page count should follow normal pagination procedures, i.e., enter the number of pages containing information.

7b. NUMBER OF REFERENCES: Enter the total number of references cited in the report.

8a. CONTRACT OR GRANT NUMBER: If appropriate, enter the applicable number of the contract or grant under which the report was written.

8b, 8c, & 8d. PROJECT NUMBER: Enter the appropriate military department identification, such as project number, subproject number, system numbers, task number, etc.

9a. ORIGINATOR'S REPORT NUMBER(S): Enter the official report number by which the document will be identified and controlled by the originating activity. This number must be unique to this report.

9b. OTHER REPORT NUMBER(S): If the report has been assigned any other report numbers *(either by the originator or by the sponsor)*, also enter this number(s).

10. AVAILABILITY/LIMITATION NOTICES: Enter any limitations on further dissemination of the report, other than those imposed by security classification, using standard statements such as:

(1) "Qualified requesters may obtain copies of this report from DDC."

(2) "Foreign announcement and dissemination of this report by DDC is not authorized."

(3) "U. S. Government agencies may obtain copies of this report directly from DDC. Other qualified DDC users shall request through _____."

(4) "U. S. military agencies may obtain copies of this report directly from DDC. Other qualified users shall request through _____."

(5) "All distribution of this report is controlled. Qualified DDC users shall request through _____."

If the report has been furnished to the Office of Technical Services, Department of Commerce, for sale to the public, indicate this fact and enter the price, if known.

11. SUPPLEMENTARY NOTES: Use for additional explanatory notes.

12 SPONSORING MILITARY ACTIVITY: Enter the name of the departmental project office or laboratory sponsoring *(paying for)* the research and development. Include address.

13. ABSTRACT: Enter an abstract giving a brief and factual summary of the document indicative of the report, even though it may also appear elsewhere in the body of the technical report. If additional space is required, a continuation sheet shall be attached.

It is highly desirable that the abstract of classified reports be unclassified. Each paragraph of the abstract shall end with an indication of the military security classification of the information in the paragraph, represented as *(TS)*, *(S)*, *(C)*, or *(U)*.

There is no limitation on the length of the abstract. However, the suggested length is from 150 to 225 words.

14. KEY WORDS: Key words are technically meaningful terms or short phrases that characterize a report and may be used as index entries for cataloging the report. Key words must be selected so that no security classification is required. Identifiers, such as equipment model designation, trade name, military project code name, geographic location, may be used as key words but will be followed by an indication of technical context. The assignment of links, rules, and weights is optional.